# Regulation of DNA replication and repair by diadenosine tetraphosphate

Thesis submitted in accordance with the requirements of the University of Liverpool for the degree of Doctor in Philosophy

**by**
**Ryan Cunningham**

**October 2010**

# ABSTRACT

**Regulation of DNA replication and repair by diadenosine tetraphosphate**
Ryan Cunningham

The dinucleotide diadenosine 5',5'''-$P^1$,$P^4$-tetraphosphate ($Ap_4A$) is present in all animal cells, typically at levels between 0.05 and 1 μM during normal growth. The level of intracellular $Ap_4A$ has previously been shown to increase several-fold in response to DNA damage, although the source and function of this increased $Ap_4A$ remains unknown. This project aimed to investigate the hypothesis that $Ap_4A$ may promote a mechanism to stall DNA replication after DNA damage, particularly in response to single strand breaks (SSBs). Using a sensitive and specific luminometric assay, a 2.1-fold increase in the level of $Ap_4A$ was detected after treatment of wild-type Chinese Hamster ovary (CHO) cells with the alkylating agent ethyl methanesulphonate (EMS), which indirectly produces single strand breaks through base excision repair (BER). A much higher (13-fold) increase was detected when cells were treated with EMS in combination with cytosine arabinoside (araC), which causes an accumulation of DNA strand breaks by inhibiting the re-synthesis stage of BER. Strikingly, an increase of up to 16-fold in the basal level of $Ap_4A$ was detected in cells deficient in XRCC1, a scaffold protein which plays a pivotal role in both the SSB repair and BER processes. XRCC1 forms a tight complex with DNA ligase IIIα (Lig3α) and targets it to DNA SSBs. Lig3α has previously been found to synthesise $Ap_4A$ *in vitro* and this reaction is specifically inhibited by the presence of DNA. The level of intracellular $Ap_4A$ was also found to be increased here by using the ligase inhibitor L67 that specifically prevents Lig3α binding to DNA. Taken together, these data suggest that Lig3α may be responsible for DNA damage-related $Ap_4A$ synthesis *in vivo* where it cannot bind its normal DNA substrate. This may be the case in the early stages of SSB repair since Lig3α would be blocked from binding SSBs by the transient binding of poly(ADP ribose) polymerase 1 (PARP-1). Interestingly, a more detailed analysis of cell extracts by HPLC found that a substantial proportion of the $Ap_4A$ accumulating in cells following DNA damage did not co-elute with an $Ap_4A$ standard, suggesting it was modified in some way. This material was found to co-elute with a sample of ADP-ribosylated $Ap_4A$ synthesised *in vitro* and was also sensitive to poly(ADP ribose) glycohydrolase (PARG) which removes ADP-ribose. Although it has already been reported to occur *in vitro*, the observations made here provide the first evidence that ADP-ribosylated $Ap_4A$ also occurs *in vivo* and is synthesised in response to DNA damage. This is particularly interesting since ADP-ribosylated $Ap_4A$ synthesised by PARP-1 has previously been shown to inhibit SV40 DNA replication *in vitro*, suggesting it may also carry out this function *in vivo*. Also within this project an $Ap_4A$-deficient cell line was engineered by transfection of wild-type CHO cells with a construct allowing inducible over-expression of NUDT2 $Ap_4A$ hydrolase. Detailed characterisation of this cell line revealed that this caused a reduction in the normal endogenous level of $Ap_4A$ and prevented the usual increase in $Ap_4A$ from occurring after treatment of the cells with EMS. Furthermore, it was found that this lack of $Ap_4A$ resulted in an increased sensitivity of cells to EMS providing a strong suggestion of a functional involvement for $Ap_4A$ in surviving DNA damage. Taken together, the observations made in this study suggest that $Ap_4A$ is synthesised by Lig3α in response to DNA damage and is subsequently ADP-ribosylated by PARP-1. This ADP-ribosylated $Ap_4A$ may have a role in stalling DNA replication in response to DNA damage and appears to be important for cell survival following such damage. In summary, this study has made significant progress in determining the function of $Ap_4A$ in animal cell signalling and has provided new insights into its proposed role in the DNA damage response.

# ACKNOWLEDGEMENTS

I would especially like to thank my supervisors, Professor Sandy McLennan and Dr. Nigel Jones, for their enormous help, support and enthusiasm for this project. Their experience and advice has been invaluable and this thesis would not have been possible without their patience, encouragement and many good ideas!

I would also like to thank my colleagues in the laboratory for their help, support and friendship, particularly Dr. Jamie Wilson who has been a constant source of encouragement and advice, Karl Xiao and Abdulaziz Aladwani.

In addition, I thank the other staff members in the School of Biological at the University of Liverpool for their assistance, particularly Dr. Mark Wilkinson for his generous support with aspects of this project.

Finally, I also thank my family and friends for all the support they have given me.

# CONTENTS

# ABBREVIATIONS AND ACRONYMS

| | |
|---|---|
| 3-AB | 3-aminobenzamide |
| ADP | adenosine diphosphate |
| AOA1 | ataxia with oculomotor apraxia type 1 |
| AP | apurinic/apyrimidinic |
| $Ap_4A$ | diadenosine 5′,5‴-$P^1$,$P^4$-tetraphosphate |
| $Ap_nA$ | diadenosine 5′,5‴-$P^1$,$P^n$-polyphosphate |
| APE1 | AP endonuclease 1 |
| APTX | aprataxin |
| araC | cytosine arabinoside |
| ATM | ataxia telangiectasia mutated |
| ATP | adenosine triphosphate |
| ATR | ATM and Rad3-related |
| BER | base excision repair |
| BRCT | breast cancer suppressor protein C-terminal |
| cDNA | complementary DNA |
| CHO | Chinese hamster ovary |
| CK2 | caesin kinase 2 |
| CS | Cockayne's syndrome |
| DEAE | diethylaminoethyl |
| DIPP | diphosphoinositol polyphosphate phosphohydrolases |
| DMEM | Dulbecco's modified Eagle's media |
| DMSO | dimethylsulphoxide |
| DNA | deoxyribose nucleic acid |
| DNA-$PK_{cs}$ | DNA-dependent protein kinase catalytic subunit |
| dRP | 5′-deoxyribose phosphate |
| DSB | double strand break |
| EDTA | ethylenediaminetetraacetic acid |
| EMS | ethyl methanesulphonate |
| FcεRI | high-affinity IgE receptor |
| FEN-1 | flap endonuclease 1 |
| FHA | forkhead-associated domain |
| GAPDH | glyceraldehyde-3-phosphate dehydrogenase |
| GGR | global genomic repair |
| HBSS | Hank's balanced salt solution |
| HEPES | N-2-hydroxyethylpiperazine-N'-2-ethanesulfonic acid |
| Hint-1 | histidine triad nucleotide binding protein 1 |
| HIT | histidine triad |
| HPLC | high performance liquid chromatography |
| HRR | homologous recombination repair |
| hTERT | human telomerase reverse transcriptase |
| IPTG | isopropyl β-D-1-thiogalactopyranoside |
| IR | ionising radiation |
| LB | Luria-Bertani |
| Lig1 | DNA ligase I |
| Lig3 | DNA ligase III |
| Lig3α | DNA ligase IIIα |
| Lig4 | DNA ligase IV |

| | |
|---|---|
| LP-BER | long-patch base excision repair |
| LysRS | lysyl-tRNA synthetase |
| MAPK | mitogen activated protein kinase |
| MEF | mouse embryonic fibroblast |
| MEM | minimum essential medium |
| MGMT | $O^6$-methylguanine-DNA methyltransferase |
| MITF | microphthalmia transcription factor |
| MMR | mismatch repair |
| MMS | methyl methanesulphonate |
| MNNG | N-methyl-N′-nitro-N-nitrosoguanidine |
| MSC | multisynthetase complex |
| NER | nucleotide excision repair |
| NHEJ | non-homologous end-joining |
| NQO | 4-Nitroquinoline 1-oxide |
| NTD | N-terminal domain |
| NUDT | Nudix-type hydrolase |
| PAR | poly(ADP-ribose) |
| PARG | poly(ADP-ribose) glycohydrolase |
| PARP-1 | poly(ADP-ribose) polymerase 1 |
| PBS | phosphate buffered saline |
| PBS | phosphate buffered saline |
| PCNA | proliferating cell nuclear antigen |
| PEP | phosphoenolpyruvate |
| PK | pyruvate kinase |
| $PP_i$ | pyrophosphate |
| pol-α | DNA polymerase α |
| pol-β | DNA polymerase β |
| pol-δ | DNA polymerase δ |
| RFC | replication factor C |
| ROS | reactive oxygen species |
| RPA | replication protein A |
| RSL1 | Rheoswitch ligand 1 |
| S.E.M. | standard error of the mean |
| SDS | sodium dodecyl sulphate |
| siRNA | small interfering RNA |
| SSB | single strand break |
| SSBR | single strand break repair |
| TAE | Tris-Acetic acid-EDTA |
| TBS | tris buffered saline |
| TCR | transcription coupled repair |
| TDP1 | tyrosyl-DNA phosphodiesterase 1 |
| TFIIH | transcription factor IIH |
| Top1 | topoisomerase 1 |
| TTD | tricothiodystrophy |
| U.V. | ultra-violet |
| WT | wild-type |
| X-Gal | 5-bromo-4-chloro-3-indolyl β-D-galactopyranoside |
| XP | *Xeroderma pigmentosum* |
| XRCC1 | x-ray cross complementing protein 1 |
| XRCC4 | x-ray cross complementing protein 4 |

# CHAPTER 1

# Introduction

## 1.1 Introduction to DNA repair

It is essential for every organism to maintain the integrity of its genome so that genetic material is transferred accurately to successive generations. DNA is constantly subject to a wide variety of damaging modifications including hydrolysis, oxidation, alkylation, bulky adduct formation and base mismatches, all of which can be induced by various substances produced naturally during cellular metabolism. In addition, DNA damage can also be induced by exogenous sources including physical agents such as ionising radiation and ultraviolet (U.V.) light, as well as chemical agents such as alkylating agents, DNA crosslinking agents and radiomimetic agents. Eukaryotic cells have evolved a number of mechanisms of DNA repair, which act on specific types of DNA damage. These DNA repair mechanisms include single strand break repair (SSBR), base excision repair (BER), nucleotide excision repair (NER), mismatch repair (MMR), homologous recombination repair (HRR) and non-homologous end-joining (NHEJ), as well as damage reversal by certain proteins such as alkyltransferases.

## 1.2 DNA repair mechanisms

### 1.2.1 DNA single strand break repair (SSBR) and base excision repair (BER)

#### 1.2.1.1 Causes and structure of DNA single strand breaks (SSBs)

A DNA single strand break (SSB) is a break in the sugar-phosphate backbone of one strand in a DNA double helix. If left unrepaired, SSBs can pose a serious threat to genetic stability and cell survival by blocking transcription or inducing DNA replication fork collapse leading to potentially lethal double strand breaks (DSBs) (Kuzminov, 2001). SSBs are typically accompanied by the loss of a single nucleotide at the damage site and the presence of DNA termini lacking the conventional 5′ phosphate and 3′ hydroxyl groups that are necessary for DNA polymerase and DNA ligase enzymes to carry out repair. These unconventional DNA ends require various forms of processing before gap-filling and ligation can take place. An overview of the SSBR process is presented in Fig. 1.1 (pg. 18).

It is estimated that several thousand SSBs occur in each human cell per day, predominantly as a result of attack by reactive oxygen species (ROS) such as hydrogen peroxide ($H_2O_2$), hydroxyl radicals ($OH^-$) and superoxide radicals ($O_2^-$) which are produced endogenously as a by-product from oxidative metabolism and are highly reactive due to their unpaired electrons. These molecules can either directly attack sugar residues, leading to their disintegration and the formation of a SSB, or can attack DNA bases causing oxidative damage which indirectly leads to SSBs by base excision repair (BER) (Lindahl, 1993). Indirect SSBs induced by BER can also be caused by exogenous agents which cause base damage, such as the DNA alkylating agents N-methyl-N′-nitro-N-nitrosoguanidine (MNNG), methyl methanesulphonate (MMS) and ethyl methanesulphonate (EMS). In addition, ionising radiation (IR) can cause SSBs, either directly through the ionisation of sugar residues or indirectly by base damage and subsequent BER. A further source of SSBs is the single strand

nicking of DNA by topoisomerase I (Top1), which normally functions to relax DNA supercoiling prior to DNA replication. Following nicking, a transient Top1/DNA cleavage complex is formed and under normal conditions, Top1 immediately re-ligates the break after the DNA has relaxed. However, under certain conditions, the ligation activity of Top1 can be uncoupled from its nicking activity resulting in a SSB with a Top1 linked 3′ terminus. The anti-cancer drug camptothecin acts by binding to the transient Top1/DNA complex and stabilising it, producing this type of break (Hsiang *et al.*, 1985).

### 1.2.1.2 Poly(ADP-ribose) polymerase 1 (PARP-1) and SSB recognition

SSBs occurring directly from the disintegration of sugar residues are primarily detected by poly(ADP-ribose) polymerase 1 (PARP-1). PARP-1 is a 113 kDa enzyme whose catalytic activity is directly stimulated by DNA SSBs. The N-terminal region of the protein contains a DNA binding domain which acts as a molecular 'nick sensor' and allows specific binding of the protein to DNA in regions containing SSBs (Kameshita *et al.*, 1984). Introduction of a SSB in a DNA duplex induces strong flexibility in the region, which results in a characteristic V-shape of the DNA molecule. Very rapidly (<15 seconds) after the break occurs, PARP-1 specifically recognises and binds to this structure, protecting approximately 7 nucleotides on each side of the nick from degradation (Ménissier-de Murcia *et al.*, 1989). The DNA binding domain of PARP-1 contains two zinc ions, each forming part of a zinc finger motif, a characteristic DNA binding domain found in numerous eukaryotic proteins (Mazen *et al.*, 1989). These zinc ions are essential for DNA binding function and are chelated by certain critical cysteine residues (C21/C56 for finger 1 and C125/C162 for finger 2) that are well conserved between species (de Murcia *et al.*, 1994). The second zinc finger motif appears to play the most important role in the binding of PARP-1 to regions of DNA containing single stranded breaks (Gradwohl *et al.*, 1990).

The C-terminal region of the molecule contains both a $NAD^+$ binding domain (Kameshita *et al.*, 1984) and a catalytic domain which is responsible for the synthesis of poly(ADP-ribose) (Simonin *et al.*, 1990). These activities are carried out at low levels by unbound PARP-1, but are increased 500-fold by activation of the enzyme through binding to a DNA SSB (de Murcia *et al.*, 1994). $NAD^+$ is used as a substrate by the enzyme in a reaction which produces both nicotinamide and ADP-ribose, the latter of which is polymerised onto an acceptor protein, most commonly PARP-1 itself (reviewed in Lindahl *et al.*, 1995). This ADP-ribosylation imparts a strong negative charge on the protein, drastically altering its properties and causing its dissociation from DNA due to electrostatic repulsion. In the case of PARP-1, this dissociation may facilitate access to the damaged region of DNA by various repair enzymes (Caldecott *et al.*, 1996). The degradation of poly(ADP-ribose) is carried out by poly(ADP-ribose) glycohydrolase (PARG), which is also required for efficient SSBR suggesting that poly(ADP-ribosylation) is a tightly controlled element of the repair process (Davidovic *et al.*, 2001).

#### 1.2.1.3 X-ray cross complementing protein 1 (XRCC1)

Following binding of PARP-1 to a DNA SSB, the DNA repair protein XRCC1 (x-ray cross complementing protein 1) is recruited from throughout the nucleus to the region of damage. This recruitment is mediated by PARP-1, which directly interacts with XRCC1, and is dependent both on binding of PARP-1 to the DNA and the subsequent auto-poly(ADP-ribosylation) of PARP-1 (Okano *et al.*, 2003).

XRCC1 is a 70 kDa scaffold protein that plays a critical role in both the SSBR and BER pathways through direct interactions with a number of important repair proteins. Cells deficient in XRCC1 are defective in re-joining SSBs and have an increased sensitivity to

agents that induce the types of DNA damage repaired by SSBR/BER. XRCC1 contains an N-terminal domain (NTD) and two BRCT (breast cancer suppressor protein C-terminal) domains which mediate multiple interactions with various enzymes involved in all stages of the SSBR and BER processes (Caldecott, 2003). The BRCT1 domain is responsible for the interaction of XRCC1 with activated PARP-1 and its accumulation at SSBs as discussed above (Masson *et al.*, 1998; Dantzer *et al.*, 2000). This domain is also involved in the interaction of XRCC1 with AP endonuclease I (APE1), which has a role in its recruitment to strand breaks created indirectly during BER (Vidal *et al.*, 2001). The NTD of XRCC1 binds to DNA polymerase-β (pol-β), which carries out small gap-filling in both SSBR and BER (Wilson, 1998) as well as some DNA end-processing activity (Sobol *et al.*, 2000). Interestingly, it has recently been shown that the NTD of XRCC1 can exist in either a reduced or oxidised form with the latter having a much greater affinity for pol-β (Cuneo & London, 2010). The DNA end processing enzymes polynucleotide kinase (PNK) and aprataxin (APTX) associate with a casein kinase 2 (CK2)-phosphorylated linker region of XRCC1 located between the two BRCT domains. These interactions are mediated by the forkhead associated (FHA) domains of PNK/APTX, which specifically target CK2-phosphorylated peptides (Whitehouse *et al.*, 2001; Luo *et al.*, 2004). In the case of PNK, this binding stimulates both the 5′ kinase and 3′ phosphatase activities of the enzyme in repairing unconventional DNA ends. A third protein, aprataxin and polynucleotide kinase-like factor (APLF), also associates with this region, again by means of a FHA domain, and may have a role in poly(ADP-ribose) signalling during SSBR (Iles *et al.*, 2007; Rulten *et al.*, 2008). Finally, the C-terminal BRCT2 domain of XRCC1 mediates the formation of a tight complex with DNA ligase IIIα (Lig3α), the DNA ligase enzyme primarily responsible for re-sealing SSBs following SSBR and BER (Caldecott *et al.*, 1994). Most cellular Lig3α is constitutively bound to XRCC1 and this interaction appears to be important for maintaining its stability *in*

*vivo*, with the level of Lig3α being reduced by up to 5-fold in XRCC1-deficient cells due to Lig3α degradation by the proteasome (Caldecott *et al.*, 1995; Moore *et al.*, 2000). XRCC1 also appears to be important in targeting Lig3α to its sites of activity (Cappelli *et al.*, 1997).

#### 1.2.1.4 Base excision repair (BER)

As mentioned above, SSBs can be induced directly by hydrolysis of the sugar-phosphate backbone of DNA, but may also be produced indirectly as part of base excision repair (BER). BER is the primary cellular mechanism for the repair of various types of DNA base damage (reviewed in Zharkov, 2008). The initial damage recognition is mediated by one of a number of DNA glycosylase enzymes, each of which is specific to either a certain type of base modification or in some cases, a number of related types. DNA glycosylases function to hydrolyse the N-glycosidic bond between the DNA base and the sugar, which causes removal of the base leaving behind an apurinic or apyrimidinic site (AP site). AP sites themselves are highly cytotoxic and mutagenic and, if left unrepaired, may re-arrange to generate SSBs. In addition to action by DNA glycosylases, endogenous molecules such as water and reactive oxygen species, produced as by-products of oxidative metabolism, may also spontaneously attack the N-glycosidic bond to directly produce an AP site. AP endonuclease 1 (APE1) is the major AP endonuclease in mammalian cells and functions to cleave the sugar-phosphate backbone of DNA to the immediate 5′ side of AP sites (Mol *et al.*, 2000). Through this endonuclease activity, APE1 is the predominant source of indirect SSBs arising through BER. The BER process and its relationship to SSBR is summarised in Fig. 1.1 (pg. 18).

### 1.2.1.5 DNA polymerase β (pol-β) and gap-filling in SSBR and BER

The incised abasic site produced by APE1 allows the recruitment of DNA polymerase-β (pol-β), a small, single-subunit DNA polymerase that primarily functions to fill in gaps during BER and SSBR (Caldecott *et al.*, 1996). Pol-β has a high affinity for the incised abasic sites produced by APE1 and efficiently binds to the substrate DNA following dissociation of APE1 (Parsons *et al.*, 2005). The 8 kDa N-terminal domain of pol-β has 5′-deoxyribose phosphate (dRP) lyase activity and catalyses the removal of the dRP from the SSB that was created by APE1. The 31 kDa C-terminal domain contains the DNA polymerase active site and is responsible for gap-filling. DNA binding of pol-β causes recruitment of the XRCC1/Lig3α complex to the site by increasing the affinity of this complex for the incised abasic site (Parsons *et al.*, 2005).

### 1.2.1.6 DNA end processing in SSBR and BER

DNA SSBs are typically characterised by the presence of DNA termini lacking the conventional 5′ phosphate and 3′ hydroxyl groups that are necessary for DNA polymerase and DNA ligase enzymes to carry out repair. These unconventional DNA ends require various forms of processing before gap-filling and ligation can take place. Although the direct SSBs caused by ROS and IR do commonly have conventional phosphate groups at the 5′ termini, the 3′ termini are normally 'damaged' by the presence of either phosphate or phosphoglycolate groups (Ward, 1998). The former is a major substrate for PNK (Whitehouse *et al.*, 2001), while the latter is primarily removed by APE1 (Winters *et al.*, 1992; Winters *et al.*, 1994). In contrast, where the break is created indirectly by APE1 incision, the 5′ termini normally possess a deoxyribose phosphate (dRP) group, which is removed by the dRP lyase activity of pol-β (Sobol *et al.*, 2000). It is worth noting that if this dRP residue becomes oxidised then it is no longer a substrate for pol-β and as a result, BER

then normally proceeds by the long patch pathway (discussed on pg. 16). Where BER is initiated by bifunctional DNA glycosylase enzymes which also possess AP lyase activity, the 3′ end of the SSB produced can possess either a phosphate group (removed by PNK) or an α,β unsaturated aldehyde group (removed by APE1), depending on the mechanism of AP lyase action (Chen *et al.*, 1991; Izumi *et al.*, 2000; Wiederhold *et al.*, 2004). Finally, TOP1 linked termini are processed by tyrosyl-DNA phosphodiesterase 1 (TDP1) which removes the covalently linked peptide to allow subsequent repair (Pouliot *et al.*, 1999).

#### 1.2.1.7 Aprataxin (APTX) and its role in DNA end processing

Aprataxin (APTX) was originally identified as a protein defective in the neurodegenerative disorder ataxia with oculomotor apraxia type 1 (AOA1) (Date *et al.*, 2001; Moreira *et al.*, 2001). It is encoded by the *APTX* gene and exists in either a short 19 kDa form or a long 39 kDa form. The N-terminal region of the protein contains a phosphoprotein-binding FHA domain while the C-terminal contains a zinc finger DNA binding domain (Gueven *et al.*, 2004). APTX plays an important role in DNA SSBR and cells deficient in APTX have been shown to have an increased sensitivity to agents that specifically induce DNA SSBs (Luo *et al.*, 2004; Mosesso *et al.*, 2005). The FHA domain of APTX directly interacts with the C-terminal region of XRCC1, as well as the double strand break (DSB) repair protein XRCC4. Specific phosphorylation of XRCC1 by CK2 is required for APTX binding. It appears that APTX forms part of a SSB repair complex including both XRCC1 and Lig3α (Luo *et al.*, 2004).

A specific function of APTX appears to be the removal of DNA adenylates that arise from the abortive ligation of unconventional SSBs that have been modified by oxidative damage. APTX is the only protein known to be capable of repairing this type of lesion, and does so by

catalysing the removal of AMP from the 5′ terminus of the break site, which then allows the strand to act as a substrate for DNA ligases to repair the break (Ahel *et al.*, 2006; Rass *et al.*, 2007). The C-terminal zinc finger domain is required for efficient binding to DNA-adenylate complexes and disruption of this motif reduces the DNA-adenylate hydrolase activity. The catalytic activity of APTX is mediated by a central histidine triad (HIT) domain, a characteristic motif for a superfamily of proteins with nucleotide hydrolase and transferase activity (Brenner, 2002).

#### 1.2.1.8 Long patch BER (LP-BER)

Under certain conditions where the 5′ terminus of a strand break cannot be processed, an alternative BER pathway termed long patch BER (LP-BER) is used which results in the excision of more than one nucleotide (Frosina *et al.*, 1996; Klungland & Lindahl, 1997). This involves the continuation of DNA polymerase gap-filling by progressive displacement of the strand containing the damaged 5′ residue. This mechanism is dependent on a complex which comprises both proliferating cell nuclear antigen (PCNA), a sliding clamp protein which primarily functions during DNA replication, and the clamp loader replication factor C (RFC). Pol-β itself can carry out strand displacement synthesis when stimulated by PARP-1 and flap endonuclease-1 (FEN-1) or alternatively, a polymerase switch can occur with DNA polymerase δ (pol-δ) and/or DNA polymerase ε (pol-ε) continuing strand synthesis (Prasad *et al.*, 2000). The flap structure formed is nicked by FEN-1 and the displaced section of DNA containing the damaged terminus is then excised. Unlike short-patch BER, the XRCC1/Lig3α complex does not carry out ligation; instead this function is completed by Lig1, which directly interacts with PCNA (Levin *et al.*, 1997). PCNA also directly interacts with XRCC1 (Fan *et al.*, 2004; Uchiyama *et al.*, 2008) and this may be responsible for the recruitment of the RFC-PCNA complex to sites of LP-BER (Hashiguchi *et al.*, 2007).

### 1.2.1.9 Ligation of DNA breaks in SSBR and BER

DNA ligases function to link together DNA strands by catalysing the formation of a phosphodiester bond to seal the gap. Mammalian DNA ligase enzymes are encoded by three separate genes, *LIG1*, *LIG3* and *LIG4* (reviewed by Tomkinson *et al.*, 2006). The *LIG1* gene encodes DNA ligase I (Lig1), which is the primary ligase involved in DNA replication. It directly interacts with PCNA and functions to ligate Okazaki fragments during discontinuous lagging strand synthesis, as well as having an additional role in LP-BER. *LIG4* encodes DNA ligase IV (Lig4), which forms a constitutive complex with XRCC4 that is essential for Lig4 stability *in vivo*. Its primary function is to ligate DNA DSBs during non-homologous end-joining (NHEJ). The third gene, *LIG3* encodes three isoforms of DNA ligase III (Lig3). The main form, Lig3α forms a tight complex with XRCC1 and functions to ligate DNA strand breaks following SSBR and BER. The second isoform Lig3β is similar to Lig3α, apart from the fact that it lacks the C-terminal region required for XRCC1 interaction. It is expressed only in the testis and is presumed to have a role in genetic recombination during meiosis. The final isoform, mtLig3, is exclusively involved in maintaining the integrity of the mitochondrial genome.

The primary role of Lig3α appears to be in the repair of damage-induced DNA breaks. An N-terminal zinc finger domain has been identified which shares homology with the two zinc finger domains present in PARP-1 that are responsible for detection and binding to DNA SSBs (Wei *et al.*, 1995; Molinete *et al.*, 1993). This is not present in any other ligase enzymes, and is not required for ligation itself, but has been found to facilitate specific recognition and binding of the enzyme to SSBs, possibly displacing PARP-1. This allows ligation of the break, and therefore removal of the damage (Caldecott *et al.*, 1996).

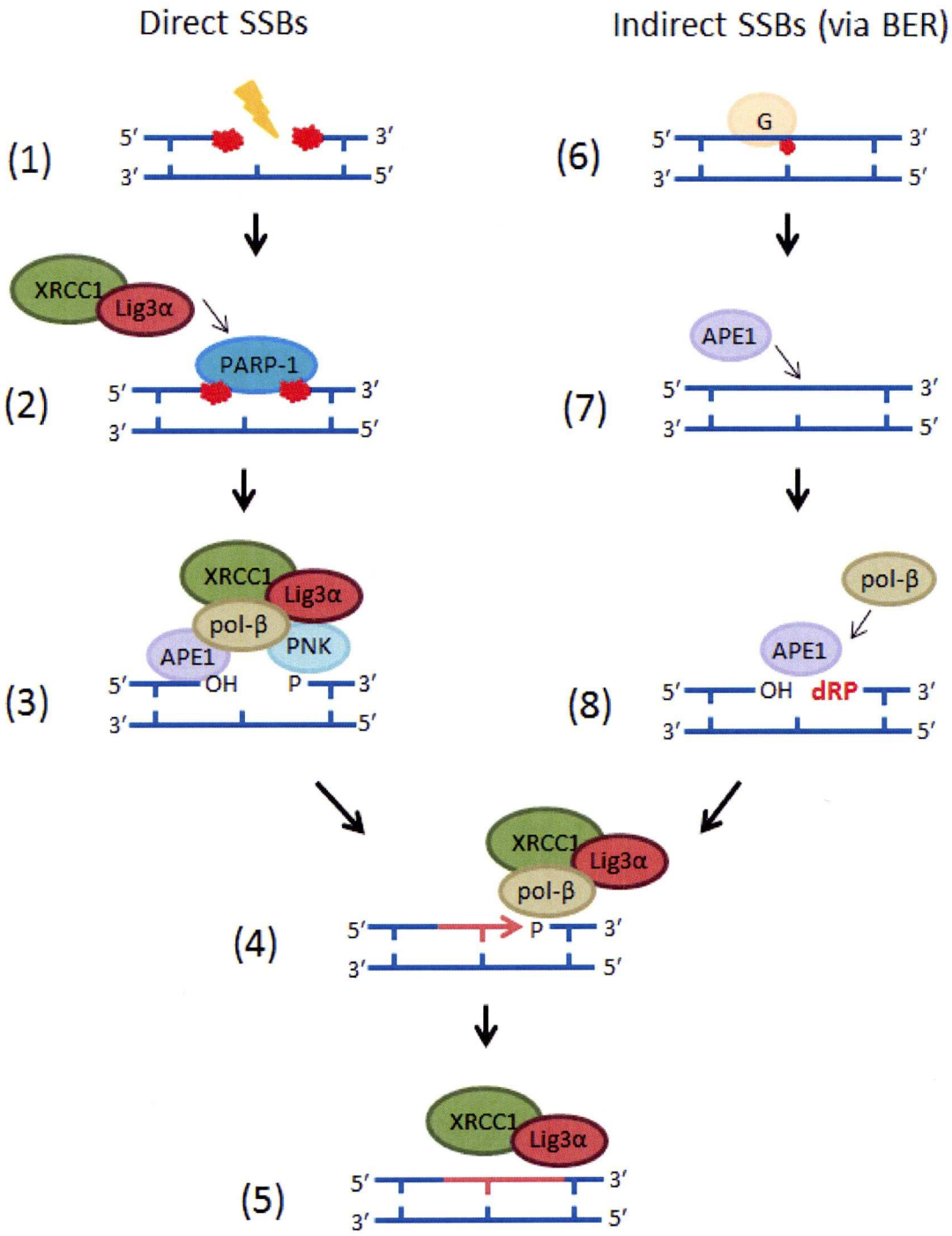


**Figure 1.1** Repair of single strand breaks (SSBs) created either directly or indirectly by base excision repair (BER). (1) A DNA single strand break (SSB) with damaged ends is created by hydrolysis of the sugar-phosphate backbone. (2) Poly(ADP-ribose) polymerase 1 (PARP-1) recognises the SSB, binds to it and recruits the XRCC1-DNA ligase IIIα (Lig3α) complex. (3) The end-processing enzymes AP endonuclease 1 (APE1) and polynucleotide kinase (PNK) are recruited to repair the damaged ends, producing conventional 5′ phosphate and 3′ hydroxyl groups. (4) DNA polymerase β (pol-β) carries out gap-filling by inserting a single nucleotide into the gap. (5) The nick is sealed by Lig3α, thus completing repair. (6) A damaged nucleoside is recognised by a specific DNA glycosylase enzyme (G), which cleaves it to produce an apurinic or apyrimidinic (AP) site. (7) APE1 binds to the AP site and cleaves the sugar-phosphate backbone, leaving a 5′ deoxyribose phosphate (dRP) group. (8) APE1 recruits pol-β, which fills in the gap and removes the 5′ dRP group to allow ligation.

### 1.2.2 Alkyl transferases

Although the BER pathway has an important role in the repair of various types of DNA base alkylation and other damage, some alkylation lesions can be directly repaired by damage reversal. $O^6$-methylguanine generally accounts for less than 8% of total DNA alkylation (Beranek, 1990) but is particularly relevant since it has the strongest mutagenic potential. If left unrepaired, $O^6$-methylguanine may mispair with thymine during the DNA replication phase of the cell cycle. In the following DNA replication cycle this then pairs with adenine, thus producing a GC→AT transition mutation. $O^6$-alkylation lesions such as $O^6$-methylguanine and $O^6$-ethylguanine can be directly repaired in a one-step transfer reaction carried out by $O^6$-methylguanine-DNA methyltransferase (MGMT) (Tano *et al.*, 1990) . This is a 24 kDa protein which removes $O^6$-alkyl groups by stoichiometric transfer to an internal cysteine residue in the protein, thus restoring the DNA base to its original unmodified form. Certain other alkyl groups can also be transferred to MGMT including those from $O^4$-methylthymine. Unlike a true enzymic reaction, transfer of an alkyl group to MGMT results in its irreversible inactivation and targets it for ubiquitination and subsequent degradation by the proteasome (reviewed in Pegg *et al.*, 1995; Pegg, 2000).

### 1.2.3 Nucleotide excision repair (NER)

Nucleotide excision repair (NER) is a DNA excision repair mechanism that functions to remove large lesions, which distort the DNA double helix, such as U.V.-induced 6,4-photoproducts, pyrimidine dimers and bulky chemical adducts. In mammalian cells there are two distinct NER pathways termed global genomic repair (GGR) and transcription coupled repair (TCR). GGR acts on the entire genome, while TCR acts exclusively on transcribed DNA strands and is closely associated with RNA polymerase II. NER involves many repair proteins (Wood *et al.*, 2001) and defects in specific components can cause either *Xeroderma*

*pigmentosum* (XP), Cockayne's syndrome (CS) or Tricothiodystrophy (TTD). XP patients suffer from extreme photosensitivity of the skin and a high incidence of skin cancer due to defects in the NER pathway, which normally functions to remove various types of U.V.-induced DNA damage. CS patients have defects specifically in the TCR pathway of NER and suffer from various symptoms including physical and mental retardation, neurological dysfunction and skeletal abnormalities due to an increased level of damage in transcribed DNA. TTD has some similarities to CS and patients suffer from brittle hair and nails, with some also showing photosensitivity. The precise mechanism of NER damage recognition and complex assembly remains unclear, but it is likely to involve the sequential recruitment of various repair proteins and factors at the site of damage as part of a co-ordinated repair process to excise a section of ssDNA containing the damage and re-synthesise it using the complementary strand as a template.

In GGR, most lesions are recognised by a complex of XPC and hHR23B (Sugasawa *et al.*, 2001), although some types of U.V.-induced lesions may alternatively be recognised by a second damage recognition complex comprising DDB1 and DDB2/XPE. In TCR, the CS proteins CSA and CSB have a role in damage recognition where it causes RNA polymerase II stalling during transcription. XPA is also thought to be involved in GGR damage recognition and although its exact role in this is unclear, it is essential for the formation of the core incision complex in both pathways (Mu *et al.*, 1997). Following damage recognition, XPB and XPD, both subunits of transcription factor IIH (TFIIH), carry out DNA unwinding by 5′-3′ and 3′-5′ helicase activities respectively, which allows access to the damage site (Evans *et al.*, 1997). Next, XPG makes an incision 3-9 nucleotides away from the damage site in the 3′ direction (Habraken *et al.*, 1994) and XPF/ERCC1 makes a second incision 15-25 nucleotides away in the 5′ direction (Sijbers *et al.*, 1996). This allows the excision of a 24-32 nucleotide

fragment of single stranded DNA containing the damage. The remaining strand is transiently protected by replication protein A (RPA) while gap-filling is carried out by pol δ/ε in a process that also involves the RFC-PCNA complex. Since the complementary strand is used as a template, this is an example of error-free repair. Finally, the gap is sealed by Lig1, thus completing the repair process.

### 1.2.4 Photoreactivation

Photoreactivation is a mechanism to repair pyrimidine dimers, which occur when two consecutive thymine or cytosine bases on the same DNA strand become covalently linked. These lesions are induced by exposure to U.V. light and result in a distortion to the DNA double helix. Removal of pyrimidine dimers can be carried out by photolyase enzymes, which bind to these sites and carry out direct repair. Photolyases contain two non-covalently linked flavin adenine dinucleotide (FAD) light harvesting co-factors and require visible light to complete their reaction mechanism. This involves reduced FADH acting as an electron donor to break the pyrimine dimer and restore the bases to their unmodified state (reviewed by Sancar, 1994). Since all known photolyases are found only in bacteria and fungi, they are unlikely to be relevant to DNA repair in mammalian cells.

### 1.2.5 Mismatch repair (MMR)

The DNA mismatch repair pathway functions to remove base mismatches that can occur as a result of DNA polymerase errors during replication. Such mismatches can also occur as a result of base deamination, oxidation or methylation. The repair mechanism involves initial recognition of the mismatch by the heterodimeric MutSα complex consisting of the MSH2 and MSH6 proteins (Fishel *et al.*, 1993; Palombo *et al.*, 1995). Upon binding the lesion, MutSα associates with MutLα, a second heterodimeric complex comprising the MLH1 and

PMS2 proteins (Li & Modrich, 1995). In the case of mismatches caused by DNA polymerase error, the nascent strand is identified by the presence of an un-ligated nick which is bound by the RFC-PCNA complex (Kadyrov *et al.*, 2006). PMS2 then introduces a second nick on the opposite side of the damage site and excision of the strand containing the incorrect base is carried out by exonuclease I (Genschel *et al.*, 2002). Finally, the strand is re-synthesised by pol- δ and the break is sealed by Lig1 (Longley *et al.*, 1997).

### 1.2.6 Double strand break repair

DNA double strand breaks (DSBs) are far more cytotoxic to cells than SSBs and can lead to dangerous genetic re-arrangements and/or cell death. The two primary pathways for the removal of DSBs include non-homologous end-joining (NHEJ) and homologous recombination repair (HRR).

NHEJ ligates two ends of a DNA DSB together without the need for substantial sequence homology. Since it can sometimes lead to the loss of nucleotides at the site of repair, it is considered an error-prone mechanism. The first stage of NHEJ involves the binding of the Ku70/Ku80 heterodimer to both ends of the DSB, which protects them from exonuclease digestion (Jeggo *et al.*, 1992). This heterodimer then associates with DNA-dependent protein kinase catalytic subunit (DNA-$PK_{cs}$) to form a holoenzyme, which is activated upon contact with the DNA break (Gottlieb & Jackson, 1993). Activated DNA-$PK_{cs}$ phosphorylates a number of proteins including various factors involved in DSB end-processing, such as the MRN complex (consisting of MRE11-Rad50-NBS1) (Maser *et al.*, 1997). The break is ligated by Lig4 (Lee *et al.*, 2003), which forms a constitutive complex with the scaffold protein XRCC4, essential for the stability of Lig4 *in vivo* (Bryans *et al.*, 1999).

The second major method of DNA DSB repair is homologous recombination repair (HRR). Unlike NHEJ, the damaged DNA molecule must enter into physical contact with a homologous, undamaged double strand DNA molecule, which is used as a template for repair. This makes HRR an important means of error-free DBS repair, but restricts it to the late S and G2 phases of the cell cycle (Johnson & Jasin, 2000). The mechanism involves an initial processing stage carried out by the MRN complex (consisting of MRE11, Rad50 and NBS1) to produce 3′ single strand overhangs, which become bound by Rad52 (Trujillo *et al.*, 1998; Stasiak *et al.*, 2000). Interaction of Rad52 with Rad51 induces strand exchange with the homologous, undamaged DNA molecule and allows subsequent DNA synthesis using the complementary strand of the other molecule as a template (Shen *et al.*, 1996; Gupta *et al.*, 1998). The structure formed is called a Holliday junction and is later resolved to separate the two homologous DNA molecules (Holliday *et al.*, 1964; Constaninou *et al.*, 2001). A number of other proteins are involved in the process of HRR, namely Rad51B, Rad51C, Rad51D, XRCC2 and XRCC3 (Schild *et al.*, 2000; Masson *et al.*, 2001; Liu *et al.*, 2002; Wiese *et al.*, 2002).

## 1.3 Cell division and the DNA damage checkpoint

The cell cycle is the process by which cell division takes place and has a four distinct phases. During the $G_1$ (gap 1) phase, cells increase in size and prepare for DNA replication, which then occurs during the S (DNA synthesis) phase. The $G_2$ (gap 2) phase is another period of cell growth and preparation involving the synthesis of various cellular components that are required for division. Cell division itself then takes place in the M (mitosis) phase, when the cell separates its chromosomes into two separate nuclei and divides to produce two identical daughter cells.

It is essential that cell division is tightly controlled and does not occur if the cell has not received the appropriate growth signals, has no space to grow into, has not reached an adequate size or if its DNA is damaged. Checkpoints are control mechanisms by which cell cycle progression can be restricted by preventing certain events from occurring until various pre-requisites have been satisfied. One such checkpoint is the DNA damage checkpoint, which prevents or halts the cell division cycle in the presence of DNA damage. This is extremely important since if replication occurs using a damaged DNA template, a mutation is likely to occur and a daughter cell will inherit an altered copy of the genome. Such mutations are often lethal to individual cells and are a particular problem in multicellular organisms, where mutation of certain genes can lead to a susceptibility to cancer. The DNA damage checkpoint has a number of components including the G1/S component, which can prevent the cell from entering the S-phase and the G2/M component, which can stop the cell entering mitosis. The third part of the DNA damage checkpoint is the intra-S phase component, which can interrupt DNA replication when damage is detected, thus allowing repair to occur before replication continues. Considerable evidence has accumulated which suggests that the dinucleoside polyphosphate diadenosine 5′,5‴-$P^1$,$P^4$-tetraphosphate ($Ap_4A$) may play a role in this replication stalling, particularly where DNA SSBs are detected.

## 1.4 Diadenosine 5′,5‴-$P^1$,$P^4$-tetraphosphate ($Ap_4A$)

### 1.4.1 Introduction to $Ap_4A$ and other dinucleotides

Diadenosine 5′,5‴-$P^1$,$P^4$-tetraphosphate ($Ap_4A$) was first discovered in 1966 as a product of the back reaction of amino acid activation during protein synthesis (Zamecnik *et al.*, 1966; Randerath *et al.*, 1966). It is one member of a family of dinucleoside polyphosphates, all of which consist of two nucleosides linked together by a polyphosphate bridge attached to the 5′ carbon of each (reviewed in McLennan, 2000). In the case of $Ap_4A$, the structure consists of two adenosine nucleosides, linked 5′-5′ by four phosphate groups (Fig. 1.2). Other dinucleotides have similar structures to $Ap_4A$ and include both homodinucleotides (eg. $Ap_4A$, $Gp_5G$) and heterodinucleotides (eg. $Ap_4G$, $Ap_5C$), varying both in terms of the number of phosphate groups present (from 2 to 7) and the nature of the nucleosides. The most abundant examples have at least one adenosine moiety in the structure and $Ap_4A$ is thought to be the most common.

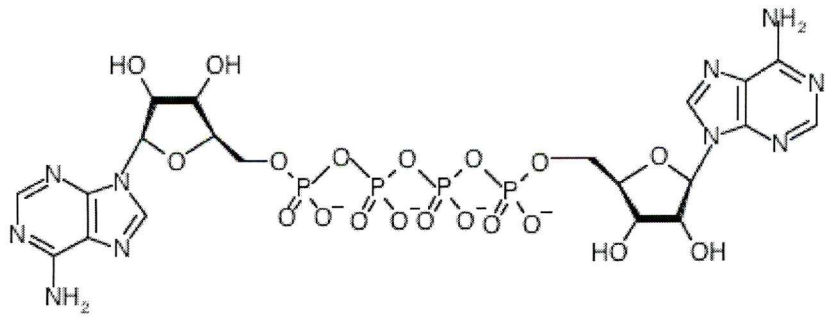


**Figure 1.2** Chemical structure of diadenosine 5′,5‴-$P^1$,$P^4$-tetraphosphate ($Ap_4A$).

In mammalian cells, the intracellular concentration of $Ap_4A$ is typically 0.05-1 μM during normal cellular growth (Garrison & Barnes, 1992). There have been conflicting reports on how these levels may change during the cell cycle with one piece of evidence claiming a

transient 1000-fold increase in $Ap_4A$ at the G1/S boundary (Weinmann-Dorsch *et al.*, 1984) and another claiming a 50-fold decrease just prior to S-phase (Morioka & Shimada, 1985). However, other investigations have found no significant change in $Ap_4A$ levels throughout the cell cycle in mammalian cells (Moris *et al.*, 1987; Perret *et al.*, 1990).

### 1.4.2 Synthesis of $Ap_4A$

Several sources of intracellular $Ap_4A$ have been identified, the principal one of which is thought to be synthesis by aminoacyl-tRNA synthetases (Plateau & Blanquet, 1992). These enzymes normally catalyse the aminoacylation of tRNA molecules, which functions to couple them to their corresponding amino acids, therefore activating the amino acid for use in protein synthesis. This process proceeds by the following 2 step reaction

(1) Enzyme + amino acid + ATP $\leftrightarrow$ Enzyme-aminoacyl-AMP + Pyrophosphate ($PP_i$)

(2) Enzyme-aminoacyl-AMP + tRNA $\rightarrow$ Enzyme + AMP + aminoacyl tRNA

Reaction (1) is freely reversible. However, in the presence of pyrophosphatase (PPase), which degrades pyrophosphate and prevents the reversal of the reaction (1), and in the absence of tRNA, some aminoacyl-tRNA synthetases catalyse the synthesis of $Ap_4A$ (Zamecnik *et al.*, 1966). This occurs through the addition of adenylate to an ATP molecule instead of $PP_i$ or a tRNA -:

Enzyme-aminoacyl-AMP + ATP $\rightarrow$ Enzyme + amino acid + **$Ap_4A$**

Further studies have since determined that the synthesis of $Ap_4A$ is actually a more general process that is carried out by various ligases and transferases (Sillero & Günther Sillero,

2000). In each case, this involves the enzyme catalysing the transfer of one nucleotidyl moiety to another, via the formation of an enzyme- or acyl- nucleotidyl intermediate and with the release of pyrophosphate -:

(1) Enzyme + ATP $\rightarrow$ Enzyme-AMP + Pyrophosphate ($PP_i$)

(2) Enzyme-AMP + ATP $\rightarrow$ Enzyme + **$Ap_4A$**

Various other dinucleoside polyphosphates are produced in similar mechanisms that involve the addition of adenylate to other acceptor nucleotides besides ATP. Two common examples are the production of $Ap_3A$ and $Ap_4G$ through the addition of an AMP moiety to ADP and GTP respectively (Sillero & Günther Sillero, 2000). Some specific enzymes found to produce $Ap_4A$ are firefly luciferase, which synthesises $Ap_4A$ *in vitro* and also *in vivo* when the luciferase gene is transfected into mammalian cells (Murphy & McLennan, 2004), acyl-CoA synthetases (Fontes *et al.*, 1998) and DNA ligases such as T4 DNA ligase (Madrid *et al.*, 1998). One specific mammalian DNA ligase enzyme found to produce $Ap_4A$ is human Lig3α (McLennan, 2000), which has an important role in the repair of DNA SSBs following damage (Caldecott *et al.*, 1996).

### 1.4.3 Degradation of $Ap_4A$

In addition to the rate of synthesis, the intracellular concentration of $Ap_4A$ is also determined by its rate of degradation (Guranowski, 2000). As it is effectively an ATP analogue, if the level of $Ap_4A$ became excessive, it could inhibit various essential enzyme activities including protein kinases (Levy *et al.* 1983), potentially even becoming lethal to the cell. Therefore, it is important that $Ap_4A$ is not allowed to accumulate and that its synthesis by various enzymes is balanced by hydrolysis. While it is likely that some $Ap_4A$ is degraded through the non-

specific hydrolytic activity of various nucleotide pyrophosphate family enzymes, there are also several specific hydrolytic enzymes that are presumed to play a key role in the regulation of intracellular $Ap_4A$ (Guranowski, 2000). One such enzyme is human Nudix-type hydrolase 2 (NUDT2), a 17 kDa enzyme which is a member of the Nudix superfamily of proteins (Thorne *et al.*, 1995) and which hydrolyses $Ap_4A$ asymmetrically to produce AMP and ATP. The Nudix superfamily is widespread among eukaryotes, bacteria, archaea and viruses and consists mainly of pyrophosphohydrolases that act upon substrates of the general structure **nu**cleoside **di**phosphate linked to another moiety, **X** (NDPX), to yield NMP plus P-X (McLennan, 2006). $Ap_4A$ hydrolase has also been found to be active on $Ap_5A$ and $Ap_6A$, but shows no hydrolytic activity towards $Ap_3A$ (Lazewska *et al.*, 1993). Other members of the Nudix protein family that display a level of specificity for $Ap_4A$ are the diphosphoinositol polyphosphate phosphohydrolases (DIPPs, e.g. NUDT3, NUDT4, NUDT10 and NUDT11) (McLennan, 2006). These 19 kDa enzymes have a relatively low level of hydrolytic activity on $Ap_4A$ as a substrate, but a considerably higher activity towards $Ap_5A$ and $Ap_6A$, possibly due to the greater negative charge of these molecules (Safrany *et al.*, 1999; Leslie *et al.*, 2002). As their name suggests they also hydrolyse the unrelated diphosphoinositol polyphosphates. In addition to Nudix family proteins, another enzyme that hydrolyses $Ap_4A$ *in vitro* is Fragile histidine triad protein (Fhit), a member of the HIT superfamily encoded by the *FHIT* tumour suppressor gene. However, its preferred substrate is $Ap_3A$ and it appears that its hydrolytic activity is limited to this *in vivo* (Murphy *et al.*, 2000).

### 1.4.4 Proposed and known functions of $Ap_4A$

The precise role of $Ap_4A$ and its relative importance to cellular function remains uncertain but based on a number of observations, several potential functions have been suggested.

One possible role for $Ap_4A$ could be to induce apoptosis under certain conditions in response to cellular stresses. The level of $Ap_4A$ has been found to increase in response to various cellular stresses including hypothermia and heat shock (Baker & Jacobson, 1986) and in some cases accumulation of $Ap_4A$ has been reported to correlate with an accumulation of apoptotic cells (Vartanian *et al.*, 1997). Furthermore when certain cell types were permeabilised and treated with 10 μM $Ap_4A$, apoptosis was induced, although this was not the case in all cell types examined (Vartanian *et al.*, 1999). When a hydrolysis resistant $Ap_4A$ analogue was used instead of $Ap_4A$ itself, apoptosis did not occur suggesting that $Ap_4A$ is hydrolysed at some point in the pathway. One suggestion for a protein that may carry out this function is glyceraldehyde-3-phosphate dehydrogenase (GAPDH) (McLennan, 2000), since it is already known to bind $Ap_4A$ (Baxi & Vishwanatha, 1995) and also has a known involvement in the apoptotic process (Sawa *et al.*, 1997; Tajima *et al.*, 1999; Sen *et al.*, 2008).

An alternative role proposed for $Ap_4A$ is as a second messenger to mediate the release of insulin from pancreatic β cells in response to an increase in extracellular glucose (Ripoll *et al.*, 1996). This study found that a 70-fold increase in the concentration of intracellular $Ap_4A$ occurs in β cells following incubation in concentrations of glucose that induce insulin release. In addition, this level of $Ap_4A$ was found to be an effective inhibitor of the ATP-regulated $K^+$ channels when applied to the intracellular side of membrane patches excised from β cells. Since these $K^+$ channels regulate the release of insulin, it could be the case that $Ap_4A$ has a role in mediating insulin release from β cells in response to increased glucose outside the cell.

As an analogue of ATP, it has been reported that $Ap_4A$ may also be involved in inhibiting various enzymes *in vivo* including adenylate kinase (Purich & Fromm, 1972) or various protein kinases (Levy *et al.*, 1983), thus playing a role in the regulation of their activity.

One of the most recent and most interesting suggestions for a function for intracellular $Ap_4A$ is as a transcriptional activator with a role in regulating gene expression in response to various stimuli (Yannay-Cohen *et al.*, 2009). The high-affinity IgE receptor (FcεRI) is a tetrameric receptor complex constitutively expressed on the surface of immune system mast cells. Following FcεRI-mediated aggregation of these cells, the MAPK (mitogen activated protein kinase) signalling cascade is activated which ultimately leads to an allergic response. It has been found that the level of intracellular $Ap_4A$ is increased during mast cell activation and this appears to be specifically synthesised by lysyl-tRNA synthetase (LysRS), an aminoacyl-tRNA synthetase that forms part of the multisynthetase complex (MSC) (Lee & Razin, 2005). Specific phosphorylation of LysRS at serine 207 is required for $Ap_4A$ synthesis, and this also causes it to be released from the MSC (Yannay-Cohen *et al.*, 2009). In addition, this study also found that LysRS is translocated into the nucleus upon mast cell activation and this is dependent on the MAPK signalling cascade. It has also been shown that LysRS can bind to microphthalmia transcription factor (MITF) which normally exists in complex with histidine triad nucleotide binding protein 1 (Hint-1) which negatively regulates its activity (Lee *et al.*, 2004). Interestingly, Hint-1 has been found to bind $Ap_4A$ and this binding has the effect of releasing it from the complex and enabling MITF to transcribe its target genes. Based on this, a model has been proposed which suggests that mast cell activation activates the MAPK signalling cascade, resulting in the phosphorylation of LysRS. This would release it from the MSC and induce its translocation into the nucleus where it would bind to MITF while producing $Ap_4A$ in high amounts. This excess $Ap_4A$ would

function as a transcriptional activator by binding to Hint-1 and therefore inducing MITF-dependent gene expression.

$Ap_4A$ can also arise extracellularly as a result of its release from the secretory granules of certain specialised cell types including blood platelets and adrenal chromaffin cells. $Ap_4A$ stored in platelet granules is released under certain physiological conditions and has an antithrombotic role in the cardiovascular system as a potent competitive inhibitor of ADP-induced platelet aggregation (Lüthje *et al.*, 1985; Chan *et al.*, 1997). The $Ap_4A$ released from adrenal chromaffin cells has a role in the nervous system as a neurotransmitter and can activate specific purinoreceptors that control certain $Ca^{2+}$ channels in the brain (reviewed in Pintor *et al.*, 2000).

However, of all the various functions proposed for $Ap_4A$, the one that is of particular relevance to the proposed study is an involvement in the stalling of DNA replication following DNA damage and there appears to be considerable evidence to support this hypothesis.

## 1.5 $Ap_4A$ and the DNA damage response

### 1.5.1 Increases in $Ap_4A$ in response to DNA damage

The first piece of evidence suggesting a role for $Ap_4A$ in the DNA damage response came from observations that the intracellular level of $Ap_4A$ in mammalian cells is increased by up to 8-fold under various conditions that induce DNA strand breaks (Baker & Ames, 1988). This study found that treatment of cells with several DNA damaging agents results in an accumulation of $Ap_4A$, and that the level of this accumulation is generally higher where there

is a greater incidence of DNA strand breaks. A small increase in $Ap_4A$ (<2-fold) was also detected after cells were treated with 4-Nitroquinoline 1-oxide (NQO) and U.V., which do not generally produce strand breaks directly, but are primarily bulky lesions repaired by the nucleotide excision repair (NER) pathway. This increase in $Ap_4A$ was higher (4-6-fold) when cells were pre-treated with cytosine arabinoside (araC), a potent inhibitor of DNA repair that results in an accumulation of DNA strand breaks. Interestingly, $Ap_4A$ accumulation was not detected in *Xeroderma pigmentosum* XP-A cells after the same treatments, and these cells also did not accumulate strand breaks rapidly following DNA damage due to a defect in NER, which normally creates SSBs by incision in order to excise various bulky lesions. In XP variant (XP-V) cells, which are incision repair proficient, the same increases in $Ap_4A$ were detected as in wild-type cells. This suggests that the short single strand gaps produced as NER intermediates result in increased $Ap_4A$ to a certain extent, although the largest increases occurred following treatment with agents which cause strand breaks directly and alkylated base damage which leads indirectly to SSBs during BER. Together, these findings suggested that intracellular $Ap_4A$ accumulation occurred as a cellular response particularly to the presence of DNA SSBs.

Similar findings were observed in a later study, in which an increase in $Ap_4A$ was detected following treatment of mammalian cells with the alkylating agent MNNG (Gilson *et al.*, 1988). The maximum $Ap_4A$ level occurred one hour after the end of MNNG treatment and returned to normal levels after approximately 7 hours, suggesting that the $Ap_4A$ produced in response to damage may possibly be used, either directly or indirectly, during subsequent DNA repair. Interestingly, it was reported that where the cells were treated with 3-aminobenzamide (3-AB), which is an inhibitor of PARP-1, the increase in $Ap_4A$ occurred normally, but then the levels remained continuously stable for the duration of the 3-AB

incubation. Once PARP-1 inhibition was relieved, the levels of $Ap_4A$ declined, probably reflecting repair of SSBs and possibly suggesting that PARP-1 has some role in the process responsible for the removal of $Ap_4A$ from the cell. PARP-1 is well characterised and has a known role in the recognition and repair of DNA SSBs (see pg. 10), providing a further suggestion that $Ap_4A$ is in some way involved with the cellular response to SSBs.

### 1.5.2 ADP-ribosylation of $Ap_4A$ by PARP-1

A further link between $Ap_4A$ and the activity of PARP-1 in SSB recognition and processing comes from the finding that, in addition to various proteins, $Ap_4A$ can actually act as an acceptor for ADP-ribose in a poly(ADP-ribose) polymerase reaction (Yoshihara & Tanaka, 1981). The product of this reaction was found to be both mono and poly(ADP-ribosylated) $Ap_4A$, the bound poly(ADP-ribose) elongating at one end of the product during the reaction (Fig. 1.3). Furthermore, it has been reported that poly(ADP-ribosylated) $Ap_4A$ acts as an efficient inhibitor of *in vitro* replication of simian virus 40 (SV40) DNA, which has been extensively studied as a model system for eukaryotic DNA replication (Baker *et al.*, 1987). The inhibitory effect is eliminated either by the addition of enzymes that degrade $Ap_4A$, or those that degrade poly(ADP-ribose), suggesting both components must be intact for inhibition to occur. It also appears to be specific to $Ap_4A$, with no inhibition of DNA replication occurring when $Gp_4G$ was used in its place. These findings suggest that $Ap_4A$ and its ADP-ribosylated derivatives may be part of a novel and as yet uninvestigated mechanism to stall DNA replication *in vivo* in the presence of DNA strand breaks.

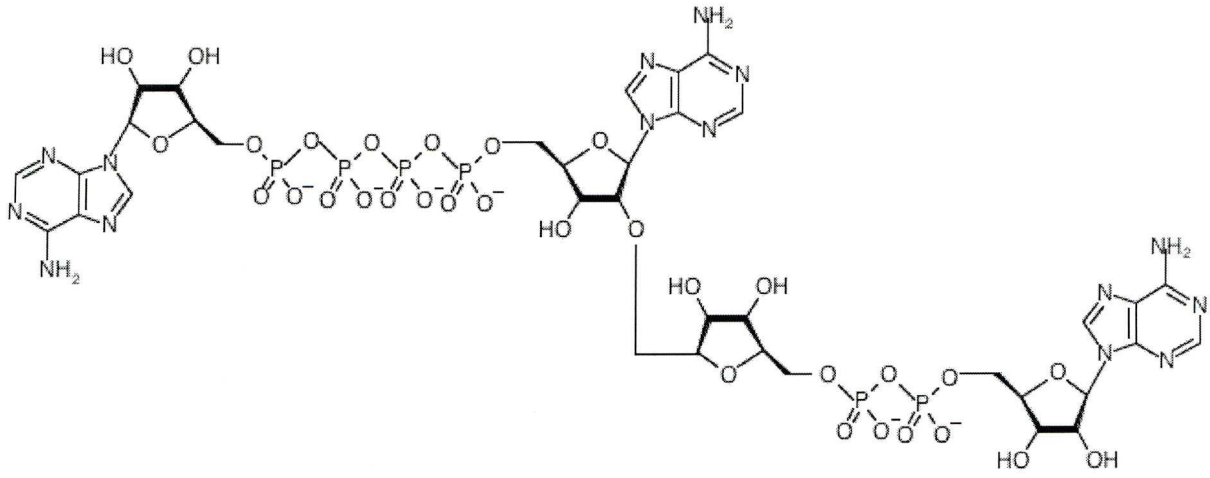

**Figure 1.3** Chemical structure of mono ADP-ribosylated $Ap_4A$, adapted from Yoshihara & Tanaka, 1981. This structure assumes a 1'-2' linkage between $Ap_4A$ and ADP-ribose, as is the case between the individual ADP-ribose units of a poly(ADP-ribose) chain. However, as yet, this has not been proven.

### 1.5.3 Synthesis of $Ap_4A$ by DNA ligase IIIα (Lig3α)

In addition to its role in the ligation of DNA strands following DNA damage, Lig3α also has the ability to synthesise $Ap_4A$. This synthesis is inhibited by both ligatable and non-ligatable DNA (McLennan, 2000). Based on this evidence, it has been suggested that following recruitment of the XRCC1/pol-β/Lig3α complex to a DNA SSB by PARP-1, Lig3α may be unable to bind the site of damage immediately due to prior binding of PARP-1, as both molecules have the same recognition sites and DNA binding domains (Mackey *et al.*, 1999). In the absence of DNA inhibition, Lig3α may produce $Ap_4A$ at the site of DNA damage (McLennan, 2000). This would account for the increase in cellular $Ap_4A$ following exposure to DNA damage (Baker & Ames, 1988).

### 1.5.4 Hydrolysis of $Ap_4A$ by APTX

The most recent piece of evidence implicating a role for $Ap_4A$ in DNA repair comes from the finding that the catalytic HIT domain of APTX is also able to bind and hydrolyse $Ap_4A$

(Kijas *et al.*, 2006). Through its $Ap_4A$ hydrolase activity, APTX may be involved in the regulation of DNA damage related $Ap_4A$ and may be the factor responsible for the return of $Ap_4A$ levels to normal following the initial sharp rise in response to DNA damage (Gilson *et al.*, 1988).

### 1.5.5 Possible mechanism of $Ap_4A$ action through DNA polymerase α (pol-α)

Since $Ap_4A$ can act as a primer for PARP-1 *in vitro*, and is indeed preferred over some protein targets (Yoshihara & Tanaka, 1981), it is entirely possible that it would also be poly(ADP-ribosylated) by the enzyme *in vivo*. Poly(ADP-ribosylated) $Ap_4A$ has already been shown to be an efficient inhibitor of SV40 DNA replication (Baker *et al.*, 1987) so its production *in vivo* may function to stall DNA replication, allowing time for the break to be repaired.

There are many possibilities for the mechanism of action of poly(ADP-ribosylated) $Ap_4A$ in stalling DNA replication and one such mechanism could be the binding of poly(ADP-ribosylated) $Ap_4A$ to a protein target required for DNA replication. This is likely to have the same effect as direct poly(ADP-ribosylation), imparting a large negative charge on the protein and inducing its dissociation from DNA. A possible advantage of this over direct ADP-ribosylation of the protein would be that poly(ADP-ribosylated) $Ap_4A$ could diffuse beyond the initial region of its production and inhibit replicon activity elsewhere in the nucleus as part of a more global response to DNA damage. One potential target for poly(ADP-ribosylated) $Ap_4A$ could be DNA polymerase-α/primase, since a number of studies have reported links between $Ap_4A$ and this complex (Grummt *et al.*, 1979; Baril *et al.*, 1983; Rapaport & Feldman, 1984; Baxi *et al.*, 1994).

DNA polymerase-α/primase (pol-α) plays a pivotal role in the initiation of DNA replication in eukaryotic cells and is an essential component of the cellular replicative apparatus. Inhibitors of pol-α have been shown to inhibit DNA synthesis both *in vitro* and *in vivo* (Loeb *et al.*, 1986) and pol-α/primase activity is essential for initiation of DNA synthesis on single-stranded DNA templates. Due to the discontinuous nature of lagging strand DNA replication, continued pol-α/primase activity at the replication fork is required for replication fork progression along the DNA template. In addition to the core structure of 4 subunits, various co-factors of DNA pol-α have been purified, some of which have been found to improve the efficiency of the complex.

In HeLa cells, an $Ap_4A$ binding protein has been characterised which appears to partially regulate the activity of a multiprotein form of pol-α (Baril *et al.*, 1983). It has been determined that this protein is a heterodimer consisting of 45 kDa and 22 kDa subunits, designated as A1 and A2 respectively (Baxi *et al.*, 1994). The binding activity is localised to the A1 subunit and appears to be specific to $Ap_4A$, although some other dinucleoside polyphosphates do compete for binding with $Ap_4A$ to a certain degree. This binding appears to require the presence of at least one adenosine nucleotide since $Ap_4G$ is able to compete with $Ap_4A$ for binding, whereas $Gp_4G$ is not (Baxi *et al.*, 1994). The identity of this pol-α associated $Ap_4A$ binding protein remains unknown, but it could be the target via which $Ap_4A$ and/or ADP-ribosylated $Ap_4A$ contributes to the stalling of DNA replication in response to DNA damage (McLennan, 2000).

## 1.6 Proposed model for $Ap_4A$ involvement in the DNA damage response

Based on the various observations reported so far, a model has been proposed for the mechanism by which $Ap_4A$ might contribute to the slowing of DNA replication during S-phase in response to the presence of certain types of DNA damage (McLennan, 2000). In this model (Fig. 1.4), the transient binding of PARP-1 to SSBs prevents Lig3α from binding to the damage site when it is initially recruited by the interaction of activated PARP-1 with the XRCC1-Lig3α complex. Under these conditions, Lig3α would rapidly produce $Ap_4A$, which would then be ADP-ribosylated by PARP-1. This ADP-ribosylated $Ap_4A$ could diffuse throughout the nucleus and bind to pol-α complexes, inhibiting pol-α activity by preventing it from properly binding to DNA due to the negative charge it imparts. This would slow DNA replication by stopping the initiation of new replication forks and by preventing lagging strand priming events during ongoing DNA replication. This mechanism would form a novel part of the intra-S phase DNA damage checkpoint to slow DNA replication to allow time for DNA repair to occur.

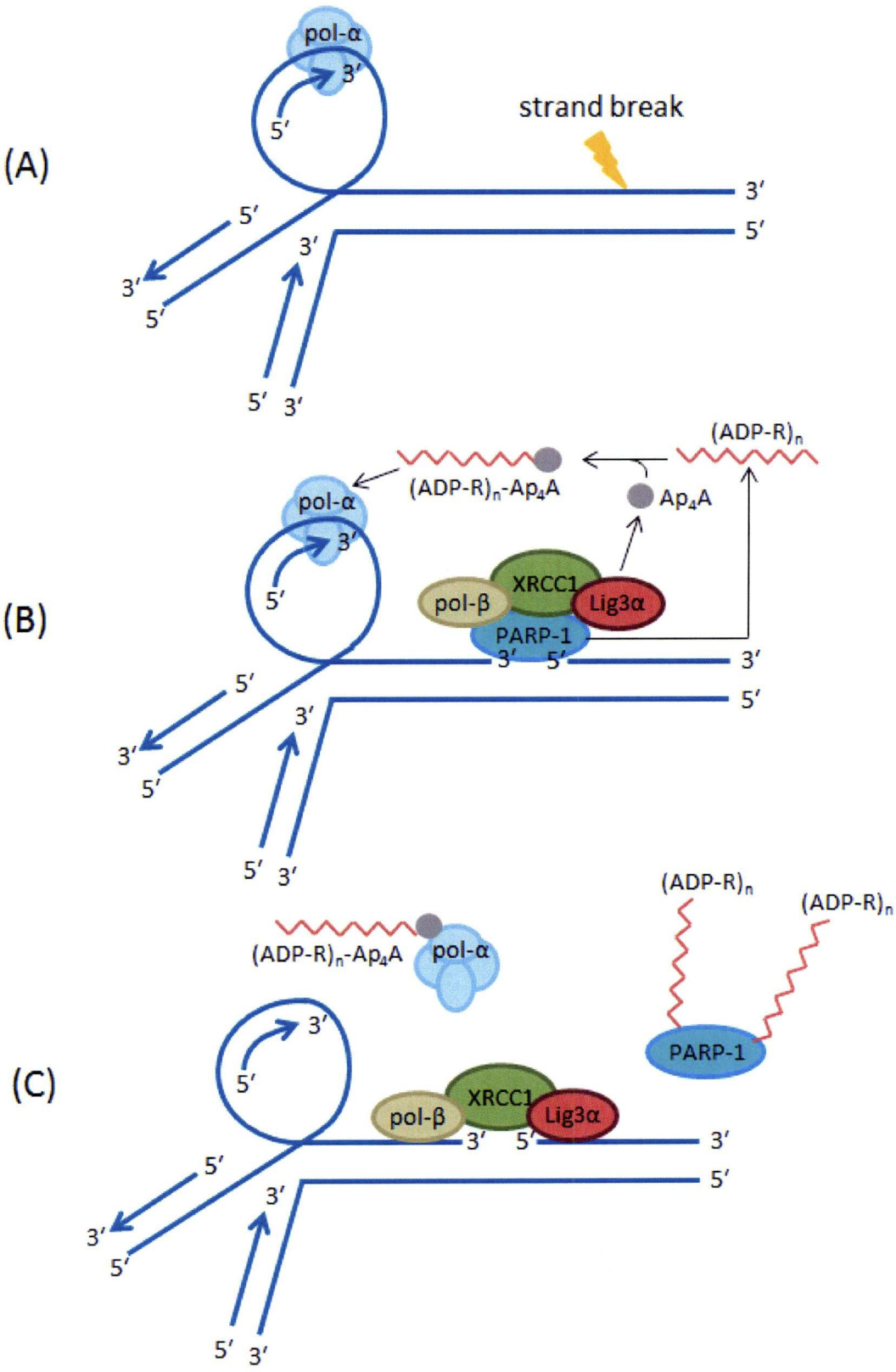


**Figure 1.4** Proposed model for $Ap_4A$ involvement in intra-S phase checkpoint control from McLennan, 2000. (A) A simplified replication fork with DNA polymerase-α/primase (pol-α) initiating a lagging strand DNA fragment while a single strand break (SSB) is generated ahead of the fork. (B) Poly(ADP ribose) polymerase 1 (PARP-1) binds to the SSB and forms a complex with DNA polymerase-β (pol-β), XRCC1 and DNA ligase III (Lig3α). Unable to bind DNA immediately, Lig3α synthesises $Ap_4A$, which acts as a primer for ADP-ribosylation by PARP-1. The ADP-ribosylated $Ap_4A$ then binds to the $Ap_4A$-binding site on the protein associated with pol-α and inhibits it, possibly by reducing its interaction with DNA. ADP ribosylated $Ap_4A$ also diffuses throughout the nucleus and inhibits other replication forks in the same way. (C) Auto-ADP-ribosylation of PARP-1 reduces its affinity for DNA and allows pol-β and Lig3α to bind to the DNA and carry out the repair process.

## 1.7 Project aims

The aim of this project is to further investigate the possible role of $Ap_4A$ in the DNA damage response. As discussed above, there are various pieces of evidence that taken together provide a strong suggestion that $Ap_4A$ is in some way involved in DNA repair. The model above provides an initial hypothesis which will be tested in various ways using a range of cells and techniques. This project aims to conclusively determine whether or not $Ap_4A$ does have a role in the DNA damage response and to probe the exact molecular details of this involvement.

# CHAPTER 2

# Materials and Methods

## 2.1 Materials

### 2.1.1 Cell lines

**AA8** is a parental wild-type cell line derived from Chinese hamster ovary (Thompson *et al.*, 1980a).

**EM9** is an AA8-derived *XRCC1* mutant, originally isolated by its hypersensitivity to ethylmethanesulphonate (EMS). It carries the premature termination mutation Q221X in the *XRCC1* gene and as a result, fails to express functional XRCC1 (Thompson *et al.*, 1980b; Thompson *et al.*, 1990; Shen *et al.*, 1998).

**EM7** is an AA8-derived *XRCC1* mutant, originally isolated by its hypersensitivity to ethylmethanesulphonate (EMS). It carries a point mutation in the first intron of the *XRCC1* gene which prevents normal splicing from occurring. As a result, the cells fail to express functional XRCC1 (Thompson *et al.*, 1980; Thompson *et al.*, 1990; Shen *et al.*, 1998).

**H9T3-7-1** is derived from the XRCC1-deficient CHO cell line EM9 (see above) by transfection with the pH9T3-7 cosmid containing *XRCC1* cDNA. As a result, expression of XRCC1 is restored (Thompson *et al.*, 1990).

**CHO-K1** is a parental wild-type cell line derived from Chinese hamster ovary (Kao & Puck, 1968).

**XR-1** is a CHO-K1-derived *XRCC4* mutant, originally isolated by its hypersensitivity to X-rays (Stamato *et al.*, 1983; Li *et al.*, 1995)

**A549-pS1** is a strain of the human lung epithelial cell line A549 which has been transfected with an empty copy of the constitutive pS expression vector (Iles *et al.*, 2007).

**A549-pSC5** is a strain of the human lung epithelial cell line A549 which has been stably transfected with the constitutive pS expression vector containing a sequence which produces human APLF-targeting siRNA molecules. As a result, these cells are constitutively depleted of cellular APLF (Iles *et al.*, 2007).

**FD105 M20** is a human skin fibroblastic cell line cell line derived from a patient with ataxia with oculomotor apraxia type 1 (AOA1) and immortalised by constitutive over-expression of human telomerase reverse transcriptase (hTERT). These cells carry the premature termination mutation W279X in the *APTX* gene and as a result, fail to express APTX protein (Clements *et al.*, 2004).

**FD105 M21** is derived from the APTX-deficient cell line FD105 M20 (see above) by transfection with full length human *APTX* cDNA under the control of a constitutive expression promoter. As a result, stable expression of APTX has been restored (El-Khamisy *et al.*, 2009).

**HeLa** is an immortal human cell line derived from cervical adenocarcinoma cells (Scherer *et al.*, 1951).

**HEK-293** is derived from human embryonic kidney cells which have been immortalised by adenovirus transformation (Graham & Smiley, 1977).

***Xrcc1***$^{-/-}$ mouse embryonic fibroblast (MEF) cells are derived from homozygous *Xrcc1*$^{-/-}$ mouse embryos, in which both copies of the *Xrcc1* gene have been disrupted by targeted insertion of a DNA fragment containing a premature stop codon. As a result, these cells fail to express functional XRCC1 (Tebbs *et al.*, 1999).

***Xrcc1***$^{+/+}$ MEF cells are derived from homozygous *Xrcc1*$^{+/+}$ mouse embryos, in which both copies of the *Xrcc1* gene are functional. These cells express XRCC1 normally (Tebbs *et al.*, 1999).

Cell lines were kindly provided as follows -:

AA8, EM9, CHO-K1, XR-1 and HeLa from Dr. N.J. Jones, University of Liverpool, UK.

HEK-293 from Prof. A.G. McLennan, University of Liverpool, UK.

EM7 and H9T3-7-1 from Dr. L.H. Thompson, Lawrence Livermore National Laboratory, CA, USA.

A549-pS1, A549-pSC5, FD105 M20, FD105 M21, *Xrcc1*$^{+/+}$ MEFs and *Xrcc1*$^{-/-}$ MEFs from Prof. K.W. Caldecott, University of Sussex, UK.

### 2.1.2 Recombinant proteins

**APTX** and **XRCC1** were provided by Prof. K.W. Caldecott, University of Sussex, UK.

**NUDT2** was provided by Prof. A.G. McLennan, University of Liverpool, UK (Swarbrick *et al.*, 2005).

### 2.1.3 Primary antibodies

**Anti-NUDT2** rabbit polyclonal antibody (Hankin *et al.*, 1995) was provided by Prof. A.G. McLennan, University of Liverpool, UK.

**Anti-XRCC1** rabbit polyclonal antibody was obtained from Abcam (ID: ab9147)

### 2.1.4 Constructs

**Human *NUDT2* cDNA**, cloned into the pOTB7 vector, was obtained from the I.M.A.G.E. consortium (ID: 3623134).

## 2.2 Methods

### 2.2.1 Cell culture and maintenance

**Cell growth conditions:** With the exception of human AOA1 fibroblasts, all cells were routinely maintained in Dulbecco's modified Eagle's media (DMEM, Lonza), supplemented with 10% (v/v) foetal calf serum (Autogene-Bioclear), 1% (v/v) non-essential amino acids (Lonza) and 100 µg/mL penicillin-streptomycin (Lonza). Human AOA1 fibroblasts were maintained in minimum essential medium (MEM, Lonza), supplemented with 15% (v/v) foetal calf serum, 1% (v/v) non-essential amino acids and 0.3 µg/mL puromycin (Lonza). All cells were grown in an incubator at 37 °C under a 5% (v/v) $CO_2$/air mix.

**Subculturing:** Trypsinisation was performed as cells approached confluence using 0.12% (w/v) trypsin with 0.008% (w/v) EDTA, following a brief wash with Hank's Balanced Salt Solution (HBSS, Lonza). The trypsin was quenched by addition of an equal volume of culture medium, after which the cells were centrifuged for 5 min at 500 x *g* to form a pellet and then re-suspended in fresh culture medium. Approximately 1 x $10^6$ cells were returned to the flask each time.

**Cell storage:** Stocks of all cell lines were stored in 1 mL aliquots at -196 °C under liquid nitrogen. To freeze down, approximately 1 x $10^6$ cells were re-suspended in 1 mL HBSS containing 10% (v/v) dimethylsulphoxide (DMSO, Sigma-Aldrich) and transferred to a 2 mL cryogenic tube. This was then cooled gradually to -80 °C in a cell freezer containing isopropanol and transferred to liquid nitrogen the following day. To recover frozen cells, the cryogenic tube was removed from liquid nitrogen and thawed in a water bath at 37 °C. The contents were then added to 5 mL culture medium and centrifuged for 5 min at 500 x *g*, after which the pellet was re-suspended in fresh medium and transferred to a flask.

### 2.2.2 Treatment of cells with DNA damaging agents

Cells were treated with ethyl methanesulphonate (EMS, Sigma-Aldrich) by direct addition of the liquid to serum-free growth medium. Cell monolayers were extracted for analysis 4 h after the addition of EMS. Cells treated with cytosine arabinoside (araC, Sigma-Aldrich) were pre-incubated in 200 μM of the nucleoside for 1 h prior to EMS treatment by addition of concentrated stock solution (20 mM) to the medium. In these cases, araC remained in the medium until monolayers were extracted.

### 2.2.3 Nucleotide extraction and assay

Nucleotide extraction and $Ap_3A/Ap_4A$ assays were carried out using a technique based on the procedure previously published by Fisher & McLennan, 2008. For each determination, six 90 mm dishes of cells were grown to about 80% confluence. Cells were counted in two dishes, while the remaining four were used for nucleotide extraction and subsequent $Ap_4A$ or $Ap_3A$ assay as described below.

**Nucleotide extraction:** Cell layers were washed briefly with 4 mL of warm (37 °C) PBS, which was rapidly removed and the dishes were placed on an ice-cold tray. Three mL of ice-cold 0.4 M trichloroacetic acid (TCA) was added to each of the dishes and cells were scraped into a chilled glass tube on ice. Each dish was rinsed with two 1 mL portions of TCA, and the combined 5 mL extract was left at 4 °C for 15 min. Five mL of 0.6 M tri-*n*-octylamine in 1,1,2-trichlorotrifluoroethane was added, the tube was shaken for 5 min to neutralise the TCA and then centrifuged at 500 x *g* for 5 min. A 4.4 mL portion of the upper aqueous layer was removed, mixed with 110 μL of 2 M Tris-HCl, pH8.5, 0.2 M magnesium acetate, and 10 units shrimp alkaline phosphatase (Roche) and incubated for 1 h at 37 °C to hydrolyse mono-nucleotides. Next, 100 μL of a 50% (v/v) DEAE-Sephacel (Sigma-Aldrich) suspension in 20

mM Tris-HCl, pH7.6 was added to adsorb the remaining nucleotides. Following 10 min of intermittent shaking, the suspension was centrifuged for 1 min at 12,000 x *g* and the supernatant was discarded. The pellet was washed with three 1.5 mL portions of water and then shaken for 5 min with 0.5 mL of 1.0 M triethylammonium bicarbonate (pH7.5) to elute the dinucleotides. After centrifugation for 1 min, the supernatant was removed, the elution was repeated in the same manner, and the combined supernatants were vacuum-dried at 70 °C for 2 h.

**$Ap_4A$ assay:** Nucleotide extracts were prepared as described above and the vacuum-dried samples were re-dissolved in 100 µL assay buffer (25 mM HEPES-NaOH, pH7.8, 5 mM magnesium acetate). Ten units of alkaline phosphatase were added and the tubes were incubated for 30 min at 37 °C to hydrolyse any residual ATP, followed by 15 min at 65 °C to inactivate the alkaline phosphatase. Two 50 µL samples were assayed from each tube by first placing in a 3 mL tube along with 21 µL water and adding 50 µL BacTiter-Glo reagent (Promega), which contains a mixture of luciferase enzyme and its substrate luciferin. Luciferase hydrolyses luciferin in an ATP-dependent reaction, forming oxyluciferin and producing luminescence proportional to the amount of ATP in the reaction. The tube was placed in a luminometer at 25 °C (BioOrbit 1250) attached to a chart recorder and the initial luminescence recorded as a measure of the background level of ATP. Finally 225 ng of recombinant human NUDT2 enzyme was added, which hydrolyses $Ap_4A$ asymmetrically producing one molecule of ATP for each molecule of $Ap_4A$. Luminescence was measured a second time, giving a measure of the combined level of ATP and $Ap_4A$. For each experiment, three standards containing a known amount of $Ap_4A$ were also measured and used to convert the level of luminescence to the amount of $Ap_4A$ in the samples.

**$Ap_3A$ assay:** Nucleotide extracts were prepared as described above and the vacuum-dried samples were re-dissolved in 100 µL assay buffer (25 mM HEPES-NaOH, pH7.8, 5 mM magnesium acetate). Ten units of alkaline phosphatase and 225 ng of recombinant human NUDT2 were added and then the tubes were incubated for 30 min at 37 °C to eliminate residual ATP and $Ap_4A$, followed by 15 min at 65 °C to inactivate the alkaline phosphatase and NUDT2. Two 50 µL samples were assayed from each tube by first placing in a 3 mL tube along with 18 µL of 25 mM phosphoenolpyruvate (PEP, Sigma-Aldrich) and 5 µg pyruvate kinase (Roche) and adding 50 µL BacTiter-Glo reagent. Pyruvate kinase catalyses the formation of a single ATP molecule from each molecule of ADP in the reaction mix by the transfer of a phosphate group from PEP. The tube was placed in a luminometer at 25 °C (BioOrbit 1250) attached to a chart recorder and the level of luminescence was recorded as a measure of the background level of ATP and ADP. Two hundred ng of recombinant human NUDT2 enzyme was then added and luminescence measured a second time, to ensure that all $Ap_4A$ had been removed in the pre-incubation. Finally, recombinant human Fhit protein, a specific $Ap_3A$ hydrolase (Fisher & McLennan, 2008), was added, which hydrolyses $Ap_3A$ asymmetrically, producing a single molecule each of ADP and AMP for each molecule of $Ap_3A$. Neither of these two products are directly detected by the luciferase reaction, but the presence of PEP and pyruvate kinase in the reaction converts ADP to ATP which is detected by the assay. Luminescence was measured a final time, giving a measure of the combined level of both the background ATP/ADP/$Ap_4A$ and $Ap_3A$. For each experiment, three standards containing a known amount of $Ap_3A$ were also measured and used to convert the measure of luminescence to the amount of $Ap_3A$ in the samples.

### 2.2.4 siRNA knockdown of XRCC1 in HeLa cells

Human XRCC1-targetting siRNA (ID:17841, Table 2.1) was purchased from Ambion and the lyophilised RNA was re-suspended in RNase-free water to a concentration of 10 pmol/μL and stored at -80 °C until use. For siRNA knockdown, HeLa cells were seeded into a 6-well plate with 2 mL antibiotic-free growth medium in each well and then incubated until achieving 50% confluence. Prior to transfection, 300 pmol of siRNA and 5 μl of lipofectamine (Invitrogen) were each added to separate 250 μL aliquots of OptiMEM-1 medium (Invitrogen), mixed and left at room temperature for 5 min. The two aliquots were then combined, mixed and left at room temperature for a further 20 min to allow siRNA/lipofectamine complex formation. Five hundred μL of the mixture was then added to each well and cells were incubated overnight, after which the medium was replaced with normal growth medium. When cells became confluent, they were trypsinised and transferred to 90 mm tissue culture dishes. Cells were extracted for the analysis of XRCC1 expression or $Ap_4A$ level on reaching 70% confluency, normally 3-4 days following the original transfection with siRNA.

**Table 2.1** Sequence of annealed siRNA molecule with 3′ overhanging TT dinucleotides (tt) used for knockdown of XRCC1 expression in human cells. siRNA was purchased from Ambion.

| siRNA | Sequence |
|---|---|
| Anti-XRCC1<br>ID: 17841 | 5′-GGAAGAUAUAGACAUUGAGtt-3′ – sense sequence<br>3′-ttCCUUCUAUAUCUGUAACUC-5′ – antisense sequence |

### 2.2.5 $Ap_4A$ hydrolase enzyme activity assay of recombinant proteins

Purified recombinant proteins (100 ng NUDT2, 100 ng XRCC1 or 150 ng APTX) were incubated at 25 °C in a total reaction volume of 100 µL containing 70 mM HEPES-NaOH, pH7.8, 10 mM $MgCl_2$ and either 10 µM $Ap_4A$ substrate (for NUDT2 and XRCC1) or 100 µM $Ap_4A$ substrate (for APTX). The tube was immediately placed in a luminometer at 25 °C (BioOrbit 1250) attached to a chart recorder and the linear increase in luminescence over an initial time period of approximately 10 min was recorded as a measure of the rate of ATP production by hydrolysis of the substrate. To measure $Ap_4A$ phosphorylase activity, phosphate was also present in the reaction at a final concentration of 5 mM. To measure possible symmetrical hydrolysis of $Ap_4A$, phosphoenolpyruvate (PEP) was added to a final concentration of 5 mM along with pyruvate kinase (Roche) to a final concentration of 50 ng/mL in order to convert any ADP product to ATP, which is detected by the assay. At least two determinations were made in all cases.

### 2.2.6 Treatment of cells with DNA ligase inhibitors

The DNA ligase inhibitors L67 and L82 were obtained from ChemDiv (San Diego, CA, USA). Concentrated stock solutions (5 mM) were prepared in DMSO and stored at -20 °C. Cells were treated with 50 µM of either L67 or L82 by direct addition of the stock solution to the growth medium. An equal volume of DMSO was added to untreated cells as a control. Cell monolayers were extracted for $Ap_4A$ analysis 18 h after addition.

### 2.2.7 Analysis of cell extracts by high performance liquid chromatography (HPLC)

For chromatographic analysis, eight 90 mm dishes of cells were grown to 70% confluence and nucleotides were extracted as described previously (pg. 45-46). Following extraction, the vacuum-dried samples were re-suspended in 30 µL of 1.0 M triethylammonium bicarbonate

(pH7.5), combined into a single tube and vacuum-dried again at 70 °C for 2 h. The sample was then re-suspended in 21 mM ammonium bicarbonate, pH9.6, and applied to a MonoQ column (GE Healthcare), equilibrated with 21 mM ammonium bicarbonate, pH9.6. Nucleotides were eluted with a linear gradient of ionic strength achieved by increasing concentration of ammonium bicarbonate, pH9.6, between 21 mM and 0.7M over a total volume of 20 mL. Samples were collected in 0.5 mL fractions at a flow rate of 1 mL/min. Fractions were vacuum-dried at 70 °C for 2 h, re-suspended in 0.5 mL water and then vacuum-dried again at 70 °C for 2 h. Finally, samples were re-suspended in 50 µL $Ap_4A$ assay buffer (25 mM HEPES-NaOH, pH7.8, 5 mM magnesium acetate) and assayed for $Ap_4A$ as described previously (pg. 46).

### 2.2.8 Synthesis of ADP-ribosylated $Ap_4A$ *in vitro*

Synthesis of ADP-ribosylated $Ap_4A$ *in vitro* was carried out based on the procedure published by Tanaka *et al.*, 1981. A total reaction volume of 50 µL was used containing 25 mM Tris-HCl, pH8.0, 1 mM DTT, 100 µM $Ap_4A$, 25 µM $NAD^+$, 5 µg histone H1 (Calbiochem), 10 µg PARP active DNA (R&D Systems) and 20 µg recombinant PARP-1-HSA (high specific activity) enzyme (Trevigen). PARP active DNA is a sample of dsDNA fragments containing single-strand nicks that specifically bind to PARP-1, thus activating its catalytic activity. Reactions were incubated at 25 °C for 18 h and then the enzyme was deactivated by incubating for 10 min at 95 °C and centrifuging for 10 min at 9,000 x *g*. The supernatant was removed and stored until further analysis.

### 2.2.9 Treatment of cell extracts with poly(ADP ribose) glycohydrolase

Nucleotide extracts were prepared from untreated EM9 cells and then incubated at 37 °C for 18 h in a total reaction volume of 100 µL containing 25 mM Tris-HCl, pH8.0, 10 mM β-

mercaptoethanol (Sigma-Aldrich) and 10 μg recombinant poly(ADP ribose) glycohydrolase (PARG) enzyme (Enzo Life Sciences). Following incubation, the enzyme was deactivated by incubating for 10 min at 95 °C and centrifuging for 10 min at 9,000 x *g*, after which the supernatant was removed and stored until further analysis.

### 2.2.10 Treatment of cells with PARP-1 inhibitor

The PARP-1 inhibitor NU1025 was obtained from Sigma-Aldrich. A concentrated stock solution (5 mg/mL) was prepared in DMSO and stored at -20 °C. Cells were treated with 100 μM of NU1025 by direct addition of the stock solution to the growth medium. An equal volume of DMSO was added to untreated cells as a control. Cell monolayers were extracted for analysis 18 h after addition.

### 2.2.11 Molecular cloning of *NUDT2* cDNA

**Amplification of plasmid DNA and miniprep:** Bacterial cells carrying pOTB7 plasmid DNA were amplified by inoculating 3 mL Luria-Bertani (LB) medium containing 100 μg/mL ampicillin and incubating for 18 h at 37 °C in a shaker set to 225 rpm. Plasmid DNA was subsequently extracted using a QIAGEN miniprep extraction kit.

**Polymerase chain reaction (PCR):** PCR amplification of human NUDT2 cDNA was performed using 50 μL Bioline 2X BioMix$^{TM}$ (*Taq* DNA polymerase, 2 mM dNTPs, 32 mM $(NH_4)_2SO_4$, 4 mM $MgCl_2$, 125 mM Tris-HCl (pH8.8), 0.02% (v/v) Tween-20), 0.5 μg of each primer (Sigma-Aldrich), 1 mg template DNA and deionised water up to a total reaction volume of 100 μL. Cycling conditions were as follows: 1 cycle at 94 °C for 1 min followed by 35 cycles at 94 °C for 1 min, 54 °C for 1 min, 72 °C for 30 s, and final extension 72 °C for 5 min. PCR products were purified using a QIAquick PCR purification kit (QIAGEN).

**Restriction digests:** Restriction digests were carried out using restriction enzymes supplied by Promega. A total reaction volume of 20 µL was used consisting of 2 µL enzyme buffer (6 mM Tris-HCl, pH7.5, 50 mM NaCl, 6 mM $MgCl_2$, 1 mM DTT), 5 units of each enzyme, 1 µg DNA and deionised water. The reaction was incubated at 37 °C for 4 h, after which the restriction enzymes were inactivated by heating to 65 °C for 15 min. The digested products were then purified using the QIAquick PCR purification kit (QIAGEN).

**Agarose gel electrophoresis:** Electrophoresis of DNA fragments was carried out using a 50 mL gel containing 1% (w/v) agarose dissolved in TAE (Tris-Acetic acid-EDTA) buffer (40 mM Tris-HCl, pH8.0, 1 mM EDTA and 0.1% (v/v) acetic acid), with ethidium bromide added to a final concentration of 0.5 µg/mL prior to pouring. DNA fragments for separation were mixed with loading gel (Sigma-Aldrich) and the gel was run in TAE buffer at 100V for 1 h, after which the DNA fragments were visualised in a UV transilluminator (Alpha Innotech).

**Ligation:** Ligation was carried out using T4 DNA ligase supplied by Promega. A total reaction volume of 10 µL was used consisting of 1 µL ligase buffer (300 mM Tris-HCl, pH7.8, 100 mM $MgCl_2$, 100 mM DTT, 10 mM ATP), 1 unit ligase, 100 ng vector DNA, 20 ng insert DNA and deionised water. The reaction was incubated at 15 °C for 16 h to allow ligation to occur.

**Transformation and blue-white screening:** For transformation, 5 µL of the ligation mix was added to 100 µL of competent *E. coli* cells, and the mixture left on ice for 30 min. Cells were heat-shocked at 42 °C for 90 s and placed on ice for a further 2 min. Nine hundred µL of super-optimal catabolite-repression medium was then added and the cells incubated at 37

°C while being shaken at 225 rpm for 1 h. Following incubation, 200 µL of the cell suspension was plated out on each of four Luria-Bertani (LB) agar plates containing 100 µg/mL ampicillin (Sigma-Aldrich), 40 µg/mL 5-bromo-4-chloro-3-indolyl β-D-galactopyranoside (X-Gal, Sigma-Aldrich) and 0.2 mM isopropyl β-D-1-thiogalactopyranoside (IPTG, Sigma-Aldrich). Plates were incubated for 18 h at 37 °C to allow colony formation. Colonies containing the correct ligation product were identified by their lack of blue colouring. Plasmid DNA was subsequently extracted using a miniprep extraction kit (QIAGEN).

**DNA Sequencing:** The NUDT2 cDNA sequence cloned into the pNEBR-X1Hygro vector was sequenced using the BigDye sequencing method and ABI 3100 genetic analyzer (Applied Biosystems), according to the protocol given by the manufacturer and using the sequencing primers supplied with the vector.

**DNA precipitation:** To precipitate DNA, 0.1 volumes of 3M sodium acetate and 2.5 volumes of ice-cold 100% (v/v) ethanol were added to the sample, which was then stored overnight at -18 °C. Following centrifugation at 12,000 x *g* for 15 min, the supernatant was discarded and the pellet washed with 70% (v/v) ethanol. The pellet was air-dried and re-suspended in the appropriate buffer or sterile deionised water and stored at -18 °C.

**DNA quantification:** DNA was quantified by measuring the absorbance of the solution using a nanodrop ND-1000 spectrophotometer (Nanodrop Technologies, USA), according to the instructions provided by the manufacturer.

### 2.2.12 Transfection

For transfection, a 75 $cm^2$ culture flask was seeded with ~2 x $10^6$ cells in their normal growth medium and incubated overnight. Prior to transfection, 1 μg of vector DNA and 50 μl of lipofectamine (Invitrogen) were each added to separate 1.5 mL aliquots of OptiMEM-1 medium (Invitrogen), mixed well and left at room temperature for 30 min. The two aliquots were then combined, mixed well and left for a further 15 min at room temperature to allow DNA/lipofectamine complex formation, after which a further 3 mL of fresh OptiMEM medium was added. The cells were drained of medium, washed in HBSS and the DNA/lipofectamine/OptiMEM mixture was added. The cells were then incubated for 5 h, after which the medium was removed, the cells washed in HBSS and fresh normal growth medium added. The cells were then incubated overnight under normal conditions. Following the transfection procedure, cells were harvested and a portion of them spread at 200, 500, 5,000 and 10,000 cells/dish in 500 μg/μl G418 or 500 μg/μl hygromycin for ten days. In order to determine transfection frequency, dishes were fixed and stained with methylene blue for 1 h, after which they were rinsed, air-dried and the surviving colonies counted. From other dishes, 25 colonies were picked in order to obtain cell populations derived from single colonies. Successfully transfected cells containing the plasmid were cultured in medium containing 500 μg/mL G418 or 500 μg/mL hygromycin in order to maintain selective pressure.

### 2.2.13 Luciferase reporter gene expression assay

For transient transfection with pNEBR-X1GLuc, cells of each clone were seeded in their normal growth medium into 2 wells each of a 24-well plate and incubated until reaching ~60% confluence. Prior to transfection, 9.6 μg of the pNEBR-X1GLuc plasmid and 36 μl of TransPass™ D2 transfection reagent (NEB) were added to 2.4 mL serum-free DMEM

(Lonza) and mixed gently. The mixture was left at room temperature for 30 min, after which 100 µL was added to each well, and the cells were returned to the incubator for 1 h. For each clone, 10 µL of RSL1 (500 µM in DMSO) was added to one well (final conc. 500 nM) to induce luciferase gene expression, while 10 µL DMSO was added to the other well as a negative control. Cells were incubated for a further 18 h, after which a 20 µL sample of medium was taken and assayed for luciferase activity using the reagents and protocol provided in the kit. Briefly, a working solution of GLuc substrate was produced by diluting 20 µL substrate to a total volume of 2 mL with GLuc assay buffer. For each 20 µL sample, 50 µL of GLuc working solution was added, mixed well and the level of luminescence was promptly measured in a luminometer (BioOrbit 1250) at 25 °C.

### 2.2.14 Immunoblotting

Cells were grown to near-confluence, harvested and washed twice with HBSS. Cells were then lysed with protein extraction buffer (50 mM Tris-HCl, pH6.8, 10% (w/v) sodium dodecyl sulphate (SDS), 10% (w/v) EDTA, 5% (v/v) glycerol, 5% (v/v) β-mercaptethanol) and the lysate boiled for 10 min. Following centrifugation for 10 min at 9,000 x *g*, the supernatant was subjected to SDS polyacrylamide gel electrophoresis with an acrylamide concentration of 7.5% (w/v). Following separation, proteins were transferred to a Hybond™ nitrocellulose membrane (GE Healthcare) using a submerged transfer apparatus (Wolf labs) filled with 20 mM Tris base, 150 mM glycine and 20% (v/v) methanol at a constant current of 350 mA for 4 h. After blocking for 1 h with 5% (w/v) non-fat dried milk in Tris-buffered saline (TBS, 50 mM Tris-HCl, pH8.8, 150 mM NaCl, 1% (v/v) Tween 20), the membrane was incubated with the primary antibody (1:1000 dilution in TBS) or anti-β-actin antibody (1:5000 dilution in TBS) for 18 h at 4 °C. After washing thoroughly with TBS, the membrane was incubated with anti-rabbit horseradish peroxidase-linked secondary antibody (GE

Healthcare) (1:1000 dilution in TBS and 5% (w/v) non-fat dried milk) for 2 h, and the membrane washed thoroughly again with TBS. Proteins were detected by enhanced chemiluminescence (GE Healthcare), using the protocol and reagents supplied with the kit. Briefly, equal volumes of luminol and enhancer solutions were added to the membrane, mixed well and the excess liquid drained away. The membrane was then exposed to X-ray film (GE Healthcare) for 2 h in a hyper cassette before development. Protein size was determined using Full Range Rainbow (GE Healthcare) molecular weight markers (10-250 kDa).

### 2.2.15 $Ap_4A$ hydrolase activity assay of cell lysates

Cells were grown to near-confluence, harvested and washed twice with phosphate-buffered saline (PBS). Cells were lysed with a non-denaturing protein extraction buffer (50 mM Tris-HCl, pH7.6, 150 mM NaCl, 1 % (v/v) Igepal CA-630) and smaller cellular proteins (<50 kDa) were partially purified by centrifugal filtration using Microcon filter columns (Millipore) to remove any possible contaminating high-molecular-weight nucleotide pyrophosphatase/phosphodiesterase I activity. Two 10 µL samples were assayed from each extract by adding to a 3 mL tube containing 50 µL assay buffer (70 mM Hepes-KOH, pH7.8, 10 mM $MgCl_2$), 20 µL ATP monitoring reagent (Lonza) and excess $Ap_4A$ substrate (final concentration 10 µM) in a final volume of 100 µL. The tube was immediately placed in a luminometer at 25 °C (BioOrbit 1250) attached to a chart recorder and the linear increase in luminescence over an initial time period of approximately 10 min was recorded as a measure of the rate of ATP production by hydrolysis of the substrate.

### 2.2.16 Clonal survival assays

Sub-confluent cell cultures (in exponential growth) were harvested by trypsinisation, counted by haemocytometry, diluted to known cell concentrations and plated into 90 mm tissue culture dishes. Five control dishes were prepared at 200 cells/dish, while those with the chemical to be added were prepared in triplicate with increasing cell numbers used at higher drug doses. For the EMS survival assays, dishes were incubated for 4 h to allow attachment of the cells, after which the medium was removed and attached cells were washed once with HBSS. Cells were then treated with EMS for 1 h in serum-free medium, which was then removed and replaced with normal medium. Dishes were incubated for 10 days under normal growth conditions to allow colony formation. For survival assays to G418 and hygromycin, dishes were incubated for 2 h after cell plating, after which the chemical was added. Cells were then incubated for 10 days under normal growth conditions to allow colony formation, with G418 or hygromycin present for the entire period. In both cases following colony formation dishes were then fixed and stained with methylene blue for 1 h, after which they were rinsed, air dried and the colonies counted.

# CHAPTER 3

# Intracellular $Ap_4A$ is increased in CHO cells under conditions that cause an accumulation of DNA strand breaks and specifically by the absence of XRCC1

## 3.1 Introduction

As discussed previously (pg. 31-38), there are various pieces of evidence that, taken together, suggest that $Ap_4A$ is in some way involved in the DNA damage response and/or DNA repair. The aim of this project is to determine whether or not this is the case, and if so, to probe the exact molecular details of this involvement. There are a great many strategies and techniques that could potentially be used to achieve this aim and one particularly useful tool is likely to be the extensive collection of well characterised Chinese hamster ovary (CHO) DNA repair mutant cell lines that are available in the laboratory. Examining cells deficient in various specific components of DNA repair pathways, and investigating what effect this may have on cellular $Ap_4A$, could provide some important information about the possible biological function of the molecule. Therefore, it was decided to carry out some initial experiments to examine the level of $Ap_4A$ in CHO cell lines and how this may change under certain conditions.

## 3.2 Results

### 3.2.1 CHO cells have a comparable level of intracellular $Ap_4A$ to human cells

The normal intracellular level of $Ap_4A$ has previously been reported for a variety of different cell lines and types, but the level present in the CHO cells that are being used in this study is unknown. Initial experiments were carried out to determine the normal background level of $Ap_4A$ in the wild-type CHO cell line AA8, in order to compare this with existing data on $Ap_4A$ levels in human cells and to provide a reference point for future work.

To determine the normal basal level of $Ap_4A$, nucleotides were extracted from AA8 cells grown under normal culture conditions and the level of $Ap_4A$ was measured using a specific luminometric assay (see pg. 45-46). The data obtained indicates a level of 0.63 ± 0.07 pmol/$10^6$ cells [mean ± S.E.M, $n$=6], which is comparable to the levels previously reported for various human cell lines (Murphy *et al.*, 2000). Based on an approximate cell diameter of 12 μm for AA8 (Dr. N.J. Jones, personal communication), this equates to an intracellular $Ap_4A$ concentration of around 0.69 μM, which is also consistent with previous reports that the intracellular $Ap_4A$ concentration is usually between 0.05 and 1 μM during normal cellular growth (Garrison & Barnes, 1992). The fact that the level of intracellular $Ap_4A$ detected in AA8 cells was within the range already reported for a number of different human cell lines further validates the use of CHO cells as a model system and confirms the efficiency of the assay technique.

### 3.2.2 $Ap_4A$ is increased in CHO cells following DNA alkylation damage and under conditions that cause an accumulation of DNA strand breaks

Previous evidence from human fibroblastic cells indicates that a 2-8-fold increase in the level of intracellular $Ap_4A$ occurs following DNA damage and an accumulation of DNA strand breaks (Baker & Ames, 1988). To determine if this was also the case in CHO cells, the wild-type cell line AA8 was treated for 4 h with increasing doses of the DNA alkylating agent ethyl methanesulphonate (EMS; Fig. 3.1A). EMS induces DNA alkylation damage, primarily producing N7-ethylguanine, which is removed by the BER pathway. Following EMS treatment, the level of $Ap_4A$ was found to be increased by up to 2.1-fold at the maximum concentration (Fig. 3.2) and analysis of the data using a paired t-test indicated that this observed increase in $Ap_4A$ was statistically significant ($P=0.041$).

Previous reports suggest that the increase in intracellular $Ap_4A$ observed following DNA damage is caused specifically by an accumulation of DNA strand breaks with the highest levels of $Ap_4A$ correlating with the greatest incidence of DNA strand breaks (Baker & Ames, 1988). DNA strand breaks are caused indirectly by alkylating agents such as EMS and occur during the incision stage of the BER process, in which the DNA strand is nicked by APE1 to allow excision of the damaged nucleotide. Since this is part of a co-ordinated process, it is likely that the steady-state level of strand-breaks remains limited regardless of the level of DNA base damage, since an equilibrium may be reached in which DNA strand breaks are continually sealed at a rate equal to which new incisions are made. If this were the case, it would be expected that specific inhibition of gap-filling and re-sealing during BER would produce a much higher level of $Ap_4A$ since breaks would then be allowed to accumulate.

To test this hypothesis in AA8, cells were treated with EMS following a pre-incubation with cytosine arabinoside (araC; Fig. 3.1B). This nucleotide analogue prevents re-synthesis and gap-filling during the BER process, but since the incision stage is not affected, DNA strand breaks will accumulate in cells throughout the EMS treatment. As expected, under these conditions, the level of $Ap_4A$ increased considerably, reaching a maximum of ~14-fold higher than the basal level (Fig. 3.2) and analysis of the data using a paired t-test indicated that this increase in $Ap_4A$ was statistically significant (P=0.021). Therefore, this data supports existing evidence that $Ap_4A$ is increased under conditions that cause an accumulation of DNA strand breaks.

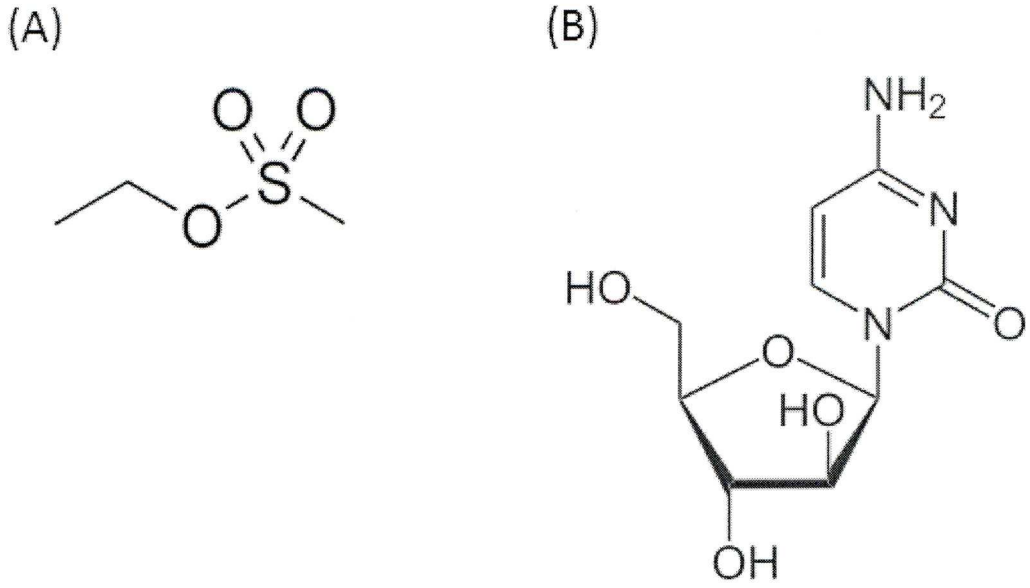


**Figure 3.1** (A) Chemical structure of ethyl methanesulphonate (EMS). (B) Chemical structure of cytosine arabinoside (araC).

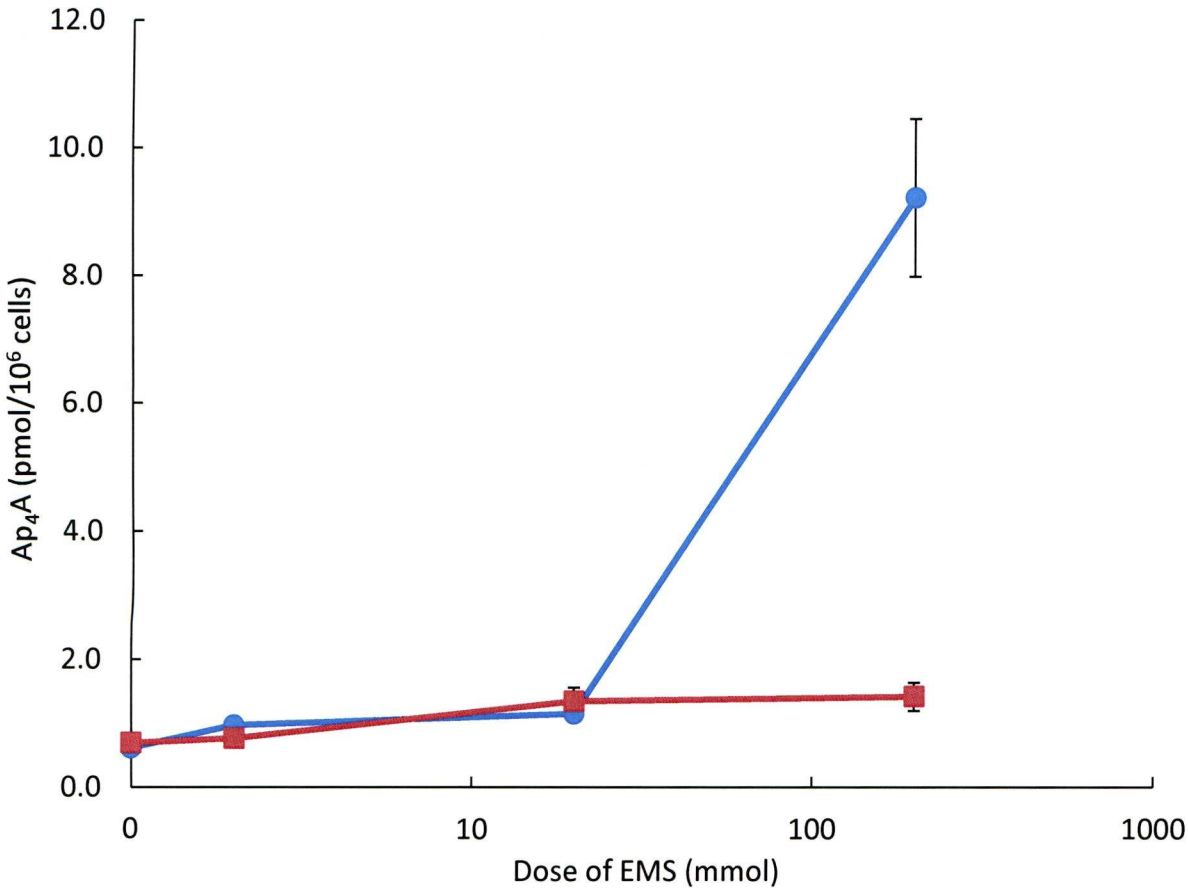


**Figure 3.2** Increase in intracellular $Ap_4A$ in the wild-type CHO cell line AA8 in response to treatment with increasing doses of ethyl methanesulphonate (EMS). Cells were treated with EMS in serum free medium for 4 h, both in the presence (blue circles) and absence (red squares) of 200 μM cytosine arabinoside (araC) and then intracellular $Ap_4A$ was immediately extracted and assayed. Each data point represents the mean of three independent determinations and the error bars represent the S.E.M. Some error bars are smaller than the marker size and are therefore not visible in the figure.

### 3.2.3 The XRCC1-deficient CHO cell line EM9 has a very high level of $Ap_4A$

Although there is evidence that the level of $Ap_4A$ is increased by treatment of cells with various agents that induce different types of DNA damage (Baker & Ames, 1988; Gilson *et al.*, 1988), it appears that the largest increases in $Ap_4A$ occur in response to the types of damage that are specifically repaired by the SSBR and BER pathways. Based on this observation, it was decided to examine the level of $Ap_4A$ in cells that are deficient in these processes to determine what effect this may have.

The CHO cell line EM9 is an AA8-derived *XRCC1* mutant, which was originally isolated by its hypersensitivity to EMS (Thompson *et al.*, 1980b). It has since been determined that EM9 carries the premature termination mutation Q221X in the *XRCC1* gene and as a result, fails to express functional XRCC1 (Thompson *et al.*, 1990; Shen *et al.*, 1998). As discussed previously (pg. 11-13), XRCC1 is a scaffold protein that co-ordinates the processes of SSBR and BER through multiple interactions with a number of different repair enzymes. Cells deficient in XRCC1 are defective in these processes and consequently have a reduced ability to repair DNA damage and are hypersensitive to DNA alkylating agents such as EMS. Examination of the intracellular level of $Ap_4A$ in EM9 cells revealed a very striking increase when compared to the parental wild-type strain AA8, with a 16-fold higher level of $Ap_4A$ detected (Table 3.2). Interestingly, in response to EMS treatment, a decrease in $Ap_4A$ occurred after a dose of 20 mM, which contrasts with the increase in $Ap_4A$ observed in wild-type AA8 cells following the same treatment (Table 3.1, Fig. 3.3). This may possibly be due to a higher rate of cell death for EM9 cells under the treatment conditions, since they are 21-fold more sensitive to EMS than AA8 (Thompson *et al.*, 1982). However, at a much higher dose of 200 mM, an increase in $Ap_4A$ was recorded.

**Table 3.1** Change in $Ap_4A$ levels in the *xrcc1*$^-$ cell line EM9 in response to treatment with increasing doses of ethyl methanesulphonate (EMS). Cells were treated with EMS for 4 h in serum free medium and then intracellular $Ap_4A$ was immediately extracted and assayed. Each value is the mean ± S.E.M. of independent triplicate determinations. P values were calculated using a paired t-test and represent the statistical significance of the observed difference between the level of $Ap_4A$ in cells following the treatment indicated and that in untreated cells.

| Dose of EMS (mM) | $Ap_4A$ (pmol/$10^6$ cells) | Fold difference to untreated cells | P value |
|---|---|---|---|
| 0 | 12.4 ± 1.32 | - | - |
| 2 | 9.86 ± 2.42 | 0.79 | 0.23 |
| 20 | 6.64 ± 1.77 | 0.54 | 0.029 |
| 200 | 17.4 ± 1.35 | 1.40 | 0.035 |

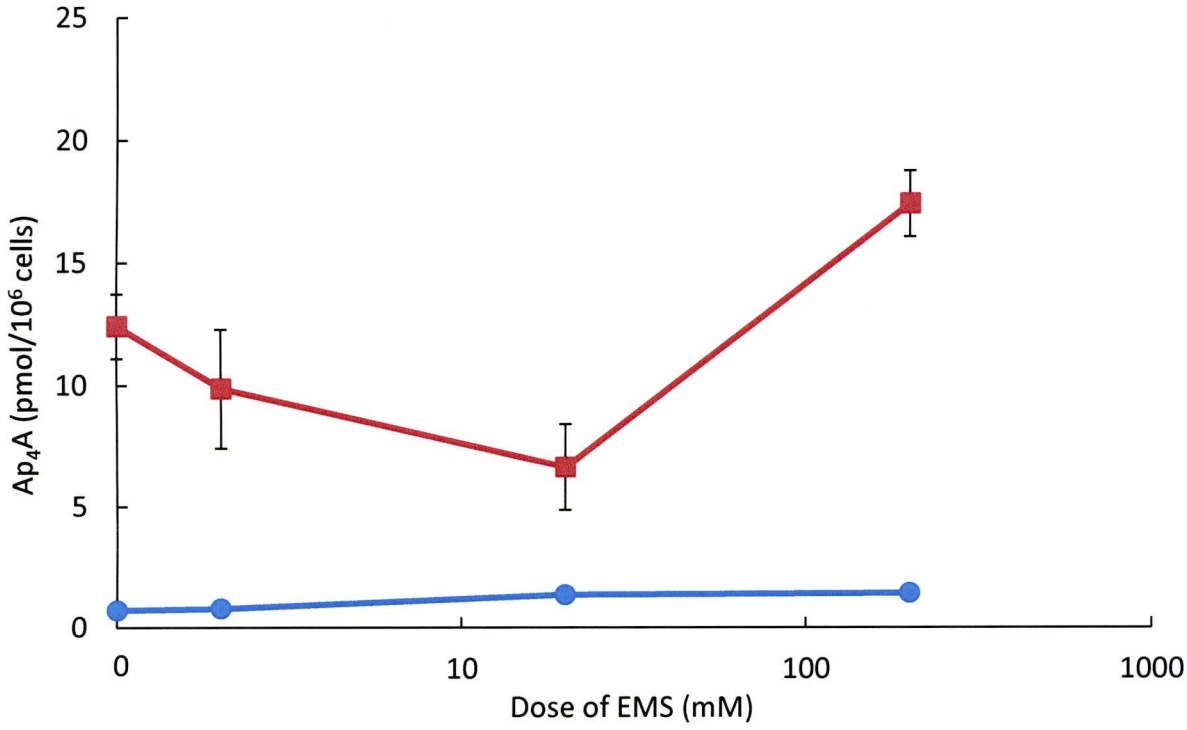


**Figure 3.3** Change in $Ap_4A$ levels in the *xrcc1*$^-$ cell line EM9 (red squares) in response to treatment with increasing doses of ethyl methanesulphonate (EMS). Cells were treated with EMS for 4 h in serum free medium and then intracellular $Ap_4A$ was immediately extracted and assayed. Data for the wild-type cell line AA8 is also shown for comparison (blue circles). Each data point represents the mean of three independent determinations and the error bars represent the S.E.M. Some error bars are smaller than the marker size and are therefore not visible in the figure.

### 3.2.4 Increased $Ap_4A$ appears to be specifically associated with a lack of XRCC1 in CHO cells

Following on from the observations made above which indicate a 16-fold higher level of $Ap_4A$ in the XRCC1-deficient cell line EM9, it was decided to next examine the level of $Ap_4A$ in a second XRCC1-deficient cell line. This is important to provide confirmation that the elevated level of $Ap_4A$ in EM9 is specifically associated with the lack of XRCC1, and not simply a result of some other unknown change in the cells which may have been induced by the mutagenesis process or occurred randomly during prolonged growth of the cell line in culture.

EM7 is an independent AA8-derived *XRCC1* mutant, which was also isolated by its hypersensitivity to EMS (Thompson *et al.*, 1980). The specific mutation is different than that in EM9 cells, in this case being a point mutation in the first intron of the *XRCC1* gene, which prevents normal splicing from occurring. However the result of this is that like EM9, cells fail to express functional XRCC1 (Thompson *et al.*, 1990; Shen *et al.*, 1998). Examination of the level of $Ap_4A$ in EM7 revealed that it was also elevated significantly compared to the parental strain AA8, and was comparable to the very high levels detected previously in EM9 cells (Table 3.2). This suggests that this effect is specifically associated with the lack of XRCC1 in both cases.

To provide further confirmation of this, the level of $Ap_4A$ was also measured in H9T3-7-1 cells, which are derived from EM9 by transfection with full-length human *XRCC1* cDNA, thus restoring XRCC1 expression. These cells are proficient in DNA repair and show correction of their mutant phenotype with respect to sensitivity to DNA damaging agents

(Thompson *et al.*, 1990). In these cells, intracellular $Ap_4A$ was found to have been restored to levels comparable to the wild-type strain AA8 (Table 3.2).

Immediately following these measurements of $Ap_4A$ levels, an XRCC1 immunoblot was carried out on the four cell lines, which confirmed that XRCC1 expression was as expected in each case (Fig. 3.4). Taken together, the data reported here indicate a normal low level of $Ap_4A$ in the parental wild-type strain and a high level in the two independent AA8-derived mutant strains EM7 and EM9, both of which fail to express XRCC1. Where XRCC1 expression is restored in EM9 by transfection with human *XRCC1* cDNA, the level of $Ap_4A$ is restored to levels comparable to the wild-type strain AA8 (Fig. 3.4, Table 3.2). These findings appear to indicate that the substantial increase in the level of $Ap_4A$ in CHO cells is specifically associated with the lack of XRCC1 protein.

**Table 3.2** Increased intracellular $Ap_4A$ in XRCC1-deficient Chinese hamster ovary (CHO) cells. AA8 is a wild-type CHO cell line while EM7 and EM9 are independent AA8-derived *XRCC1* mutant strains which lack functional XRCC1. H9T3-7-1 is derived from EM9 and has been complemented with *XRCC1* cDNA, thus restoring XRCC1 expression. Cell monolayers were extracted and analysed for intracellular $Ap_4A$ using a specific luminometric assay. Each value is the mean ± S.E.M. with the number of independent determinations ($n$) in brackets. P values were calculated using an unpaired t-test and represent the statistical significance of the observed difference between the level of $Ap_4A$ in each cell line compared to that in AA8.

| Cell line | $Ap_4A$ (pmol/$10^6$ cells) | Fold difference to AA8 | P value |
|---|---|---|---|
| AA8 | 0.63 ± 0.07 ($n$=6) | - | - |
| EM7 | 8.77 ± 0.84 ($n$=3) | 13.9 | 0.0002 |
| EM9 | 9.96 ± 1.65 ($n$=6) | 15.8 | <0.0001 |
| H9T3-7-1 | 0.78 ± 0.06 ($n$=4) | 1.24 | 0.17 |

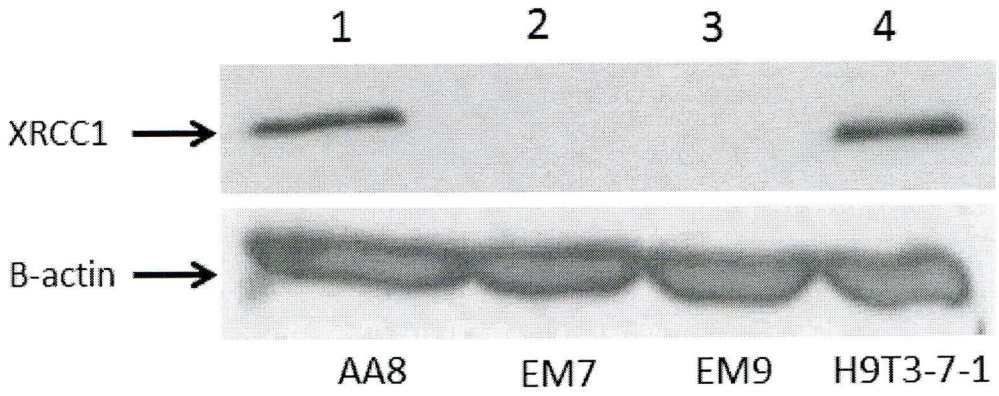


**Figure 3.4** Detection of XRCC1 expression in CHO cells by immunoblotting. Whole cell extracts were prepared from the cell lines indicated and cellular proteins were immunoblotted with an anti-XRCC1 antibody. The wild-type cell line AA8 (lane 1) shows normal expression of XRCC1 while the *xrcc1*$^{-}$ mutant cell lines EM7 (lane 2) and EM9 (lane 3) show no expression. Expression of XRCC1 is restored in EM9 cells transfected with human *XRCC1* cDNA (lane 4). β-actin was detected in all cell lines as a loading control.

### 3.2.5 Mouse XRCC1 knockout cells also have an elevated level of $Ap_4A$

Based on the data above from CHO cells, it appears that the normal background level of intracellular $Ap_4A$ is significantly increased by the specific lack of XRCC1 protein. However, since no measurements had been made in other cell types lacking XRCC1, it was not known if this is also the case in other species or is simply an effect limited to CHO cells.

The availability of an *Xrcc1*$^{-/-}$ mouse embryonic fibroblast (MEF) cell line in which XRCC1 has been stably knocked out (Tebbs *et al.*, 1999) provided an excellent opportunity to also investigate the effect of a lack of XRCC1 on the level of $Ap_4A$ in mouse cells. The wild-type cell line *Xrcc1*$^{+/+}$ expresses XRCC1 normally and provided an appropriate control strain. Examination of the normal background level of $Ap_4A$ in each of these cell lines determined that the XRCC1 knockout cells have a 5.3-fold increased level of $Ap_4A$ in comparison with cells which express XRCC1 normally (Table 3.3). This appears to indicate that the lack of XRCC1 also produces an increase in the level of intracellular $Ap_4A$ in mouse cells as well as CHO cells.

**Table 3.3** Increased intracellular $Ap_4A$ in mouse embryonic fibroblast (MEF) cells in the absence of XRCC1. *Xrcc1*$^{-/-}$ is a stable XRCC1-knockout cell line, while *Xrcc1*$^{+/+}$ is the control strain that expresses XRCC1 normally. Cell monolayers were extracted and analysed for intracellular $Ap_4A$ using a specific luminometric assay. Each value is the mean ± S.E.M. of four independent determinations. The P value was calculated using an unpaired t-test and represents the statistical significance of the observed difference between the level of $Ap_4A$ in the two cell lines.

| Cell line | $Ap_4A$ (pmol/$10^6$ cells) | Fold difference | P value |
|---|---|---|---|
| *Xrcc1*$^{+/+}$ | 0.04 ± 0.01 | - | - |
| *Xrcc1*$^{-/-}$ | 0.21 ± 0.07 | 5.3 | 0.047 |

### 3.2.6 siRNA knockdown of XRCC1 in the human cell line HeLa appears not to alter the background level of $Ap_4A$

Having established that the normal basal level of intracellular $Ap_4A$ appears to be substantially increased by the lack of XRCC1 in both CHO and MEF cells, it was next decided to examine if this might also be the case in human cells. Unfortunately, no stable XRCC1-deficient human cell lines were available, so it was instead decided to suppress XRCC1 levels using siRNA technology in order to determine the effect that this has on the level of $Ap_4A$. Efficient siRNA knockdown of XRCC1 in the human cell line HeLa has already been reported (Fan *et al.*, 2007), and this produced a cellular phenotype similar to EM9 in terms of a reduced level of DNA ligase IIIα and an increased sensitivity to DNA alkylating agents. Therefore, it seemed possible that XRCC1 knockdown may also result in an increased level of $Ap_4A$, consistent with what was observed in EM9 cells.

The procedure used was based on that previously used by Fan *et al.*, 2007, and utilised the same XRCC1-targetting siRNA sequence that was successfully used in that study (Materials and Methods, Table 2.1). Four days following siRNA transfection, an XRCC1 immunoblot was carried out on both transfected and untransfected HeLa cells, which confirmed that expression of XRCC1 had been successfully reduced, with no detectable protein present in the knockdown cells (Fig. 3.5). However, surprisingly, this knockdown of XRCC1 appeared have no effect the level of $Ap_4A$, (Table 3.4), which contrasts with what might be expected given the observations made previously in XRCC1-deficient rodent cells (Table 3.2, Table 3.3). To confirm that this was not an effect specific to HeLa cells, the same experiment was repeated using a different human cell line HEK-293 and again, no detectable decrease in the level of $Ap_4A$ was recorded.

**Table 3.4** Effect of siRNA knockdown of XRCC1 on the level of intracellular $Ap_4A$ in human cell lines. The cell lines indicated were transfected with XRCC1-targetting siRNA and after 4 days, cell monolayers were extracted and analysed for intracellular $Ap_4A$ using a specific luminometric assay. Each value is the mean of independent duplicate determinations.

| Cell line and treatment | $Ap_4A$ (pmol/$10^6$ cells) |
|---|---|
| HeLa | 0.30 |
| HeLa + siRNA | 0.30 |
| HEK-293 | 0.20 |
| HEK-293 + siRNA | 0.21 |

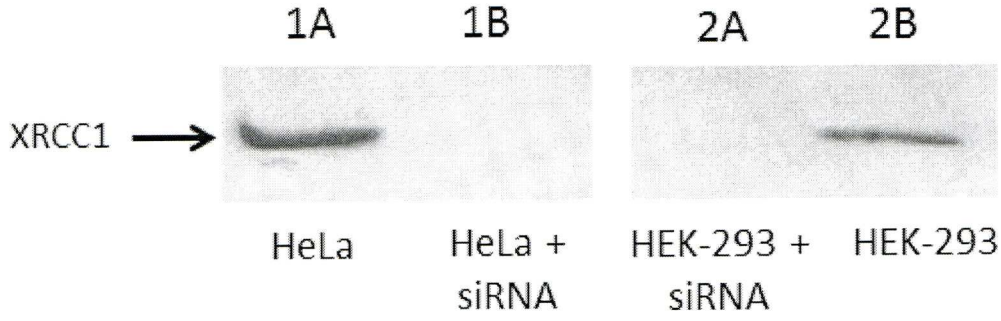


**Figure 3.5** Detection of XRCC1 expression in human cells following protein down-regulation by siRNA. Cells were transfected with XRCC1-targetting siRNA and after 4 days, whole cell extracts were prepared from the cell lines indicated and cellular proteins were immunoblotted with an anti-XRCC1 antibody. Untransfected HeLa (lane 1A) and HEK-293 (lane 2B) show normal expression of XRCC1 while expression is not detectable in siRNA transfected HeLa (lane 1B) or HEK-293 (lane 2A).

### 3.2.7 Lack of XRCC1 appears to have no effect on the level of $Ap_3A$ in CHO cells

As discussed previously (pg. 25), other dinucleotides in addition to $Ap_4A$ also exist in cells at varying concentrations. One such dinucleotide is $Ap_3A$, of which the level has been reported to vary from almost undetectable levels to around 2.4 pmol/$10^6$ cells depending on *FHIT* status (see below). Since the level of $Ap_4A$ appears to be substantially elevated in XRCC1-deficient cells, it was decided to examine if this effect was specific to $Ap_4A$, or if the level of $Ap_3A$ was also altered by the presence or absence of XRCC1.

Examination of the level of $Ap_3A$ in the wild-type cell line AA8 and the AA8-derived *xrcc1*$^-$ mutant EM9 revealed no significant difference in $Ap_3A$ between the two cell lines (Table 3.5), suggesting that the presence or absence of XRCC1 has no effect on intracellular $Ap_3A$. However, it is noteworthy that the level of $Ap_3A$ detected in both cases is relatively high compared with the values reported for other cells (McLennan & Murphy, 1999; Murphy *et al.*, 2000).

Previous findings have indicated that the level of $Ap_3A$ is regulated by Fragile histidine triad protein (Fhit), an $Ap_3A$ hydrolase encoded by the *FHIT* tumour suppressor gene. In cells that have high Fhit expression, the level of $Ap_3A$ is very low and often undetectable, whereas in Fhit negative cells including many tumour tissues and other cell lines, the level of $Ap_3A$ is much higher. The high level of $Ap_3A$ detected in both AA8 and EM9 cells strongly suggests that at some point they have lost Fhit expression, which is not surprising given the length of time they have been grown in culture and the apparent instability of the fragile site containing the *FHIT* gene (Huebner & Croce, 2003).

**Table 3.5** Effect of the lack of XRCC1 on the level of intracellular $Ap_3A$ in CHO cell lines. AA8 is a wild-type CHO cell line while EM9 is an AA8-derived *XRCC1* mutant strain that lacks functional XRCC1. Cell monolayers were extracted and analysed for intracellular $Ap_3A$ using a specific luminometric assay. Each value is the mean ± S.E.M. of independent triplicate determinations. The P value was calculated using an unpaired t-test and represents the statistical significance of the observed difference between the level of $Ap_4A$ in the two cell lines.

| Cell line | $Ap_3A$ (pmol/$10^6$ cells) | Fold difference | P value |
|---|---|---|---|
| AA8 | 3.05 ± 0.27 | - | - |
| EM9 | 2.98 ± 0.32 | 0.98 | 0.76 |

### 3.2.8 Lack of XRCC4 appears to causes an increase in the level of $Ap_4A$ in CHO cells

The substantial increase in $Ap_4A$ detected in XRCC1-deficient CHO cells raises the question of whether or not cells deficient in other DNA repair proteins may also have an elevated level of $Ap_4A$. One obvious candidate for investigation is XRCC4, a 38 kDa DNA repair protein which is involved in DNA double-strand break (DSB) repair by non-homologous end-joining (NHEJ). Interestingly, in a manner analogous to XRCC1/Lig3α, XRCC4 forms a tight complex with DNA ligase IV (Lig4) that stimulates Lig4 and is important for maintaining its stability *in vivo* (Bryans *et al.*, 1999).

The CHO cell line XR-1 lacks functional XRCC4 protein due to the complete deletion of the *XRCC4* gene and is therefore deficient in DSB repair by NHEJ (Li *et al.*, 1995). The intracellular level of $Ap_4A$ in XR-1 was found to be elevated in comparison with the parental strain CHO-K1 (Table 3.6), although to a much smaller extent than that found in the absence of XRCC1.

**Table 3.6** Increased intracellular $Ap_4A$ in CHO cells in the absence of XRCC4. CHO-K1 is a wild-type CHO cell line while XR-1 is a CHO-K1-derived mutant strain deficient in XRCC4 due to the deletion of the *XRCC4* gene. Cell monolayers were extracted and analysed for intracellular $Ap_4A$ using a specific luminometric assay. Each value is the mean ± S.E.M. of independent triplicate determinations. The P value was calculated using an unpaired t-test and represents the statistical significance of the observed difference between the level of $Ap_4A$ in the two cell lines.

| Cell line | $Ap_4A$ (pmol/$10^6$ cells) | Fold difference | P value |
|---|---|---|---|
| CHO-K1 | 0.62 ± 0.08 | - | - |
| XR-1 | 1.73 ± 0.20 | 2.8 | 0.007 |

## 3.3 Discussion

The 2.1-fold increase in $Ap_4A$ detected in the wild-type CHO cell line AA8 following treatment with the DNA alkylating agent EMS is consistent with previous reports of 2-8-fold increases in $Ap_4A$ following treatment of cells with various agents which induce DNA damage (Baker & Ames, 1988). EMS is a monofunctional alkylating agent that induces ethylation of DNA bases, primarily producing N7-ethylguanine (~70%) and to a lesser extent N3-ethyladenine (~10%). These adducts are recognised by DNA glycosylase enzymes such as alkyladenine DNA glycosylase (AAG) which initiates the process of BER by cleaving the damaged base to produce an AP site. This is then recognised by AP endonuclease 1 (APE1) which makes an incision adjacent to the site, allowing excision of the damaged nucleotide and creating a gap which is subsequently filled in by DNA polymerase β and sealed by DNA ligase IIIα.

Existing evidence has suggested that the increase in $Ap_4A$ following DNA damage is caused specifically by an accumulation of DNA strand breaks. In the case of EMS treatment, DNA strand breaks are produced indirectly by incision repair and since these breaks are subsequently removed by re-synthesis and ligation, it is likely that the steady-state level of strand breaks remains limited. Where wild-type cells were treated with EMS in combination with araC, the $Ap_4A$ increase was much greater, reaching levels 13-fold higher than untreated cells (Fig. 3.2). AraC prevents re-synthesis and gap-filling during BER, but since the incision stage is not affected, the level of DNA strand breaks will accumulate throughout the treatment (Hiss & Preston, 1977; Dunn & Regan, 1979). Therefore the findings here support the existing hypothesis that $Ap_4A$ is increased under conditions that cause an accumulation of DNA single strand breaks (Baker & Ames, 1988).

Possibly the most intriguing observation made here is that the basal level of $Ap_4A$ is increased by up to 16-fold in the AA8-derived *XRCC1* mutant cell lines EM7 and EM9 compared to the parental strain AA8 (Table 3.2). This also appeared to be the case in mouse *Xrcc1* knockout cells, albeit to a lesser extent (~5-fold), suggesting that this is not an effect specific to CHO cells (Table 3.3). This increase in $Ap_4A$ could simply be produced indirectly as result of a high background level of DNA strand breaks in XRCC1-deficient cells, although such a high level did not occur in wild-type cells, even after treatment with very high doses of EMS/araC to produce an extremely high level of DNA strand breaks. Therefore, XRCC1 may have a more direct involvement in DNA-damage related $Ap_4A$ synthesis and regulation, and may provide a good opportunity to further investigate this.

A number of possible explanations for the increase in $Ap_4A$ in the absence of XRCC1 can be hypothesised and will be addressed later (Chapter 4), but one such explanation is that uncomplexed Lig3α produces $Ap_4A$ as a result of its inability to bind to XRCC1. In the absence of DNA, Lig3α produces $Ap_4A$ *in vitro* (McLennan, 2005) and since Lig3α usually exists in complex with XRCC1, which is responsible for localising it to sites of ligation activity on DNA strands (Caldecott *et al.*, 1994; Caldecott *et al.*, 1995), $Ap_4A$ synthesis may also occur *in vivo* in the absence of XRCC1 and the resulting lack of Lig3α contact with DNA.

The fact that no increase in the level of intracellular $Ap_4A$ was detected in human cells following siRNA knockdown of XRCC1 is somewhat surprising, and initially appears inconsistent with the data from CHO and MEF cells. While there is certainly the possibility that increased $Ap_4A$ in the absence of XRCC1 is a rodent specific phenomenon, the unavoidable differences in the experimental strategies mean that this is not necessarily the

case. In both the CHO and MEF cell lines, expression of functional XRCC1 has been completely eliminated, whereas in human cells expression has been supressed to some degree by siRNA, but not eliminated completely. The extent of this XRCC1 suppression was not quantified here, but was estimated to be in the region of 80% by Fan *et al.*, 2007, using the same experimental procedure and cells. These authors also reported that the loss of XRCC1 was accompanied by a substantial reduction in the level of DNA ligase IIIα, as might be expected given the known requirement of XRCC1 for the stability of the enzyme (Caldecott *et al.*, 1995). XRCC1 is thought to exist normally at approximately $8x10^4$ molecules per cell, in excess of DNA ligase IIIα, which is thought to exist at approximately $3x10^4$ molecules per cell (Leppard *et al.*, 2003; Dong & Tomkinson, unpublished results). Therefore, it is likely that the remaining XRCC1 following siRNA down-regulation is sufficient to stabilise a significant portion (>50%) of DNA ligase IIIα, whereas in completely XRCC1-deficient cells this would not be the case. Given the overall reduction in DNA ligase IIIα levels that also occurs, it could actually be the case that no uncomplexed enzyme is present to synthesise $Ap_4A$. It is also possible that uncomplexed human Lig3α is simply too unstable to survive *in vivo*. In EM9 cells the level of Lig3α is reduced 5-fold due to its increased rate of degradation by the proteasome (Moore *et al.*, 2000), but the remaining Lig3α must certainly be uncomplexed and may rapidly produce $Ap_4A$ as a result of its inability to localise to DNA and carry out its normal ligation activity. The findings made here do not necessarily mean that $Ap_4A$ would not also be increased in human cells if a full XRCC1 knockout was made.

Another interesting finding made here is that the XRCC4-deficient cell line XR-1 also has an elevated level of $Ap_4A$ in comparison with its parental strain CHO-K1. Similar to the XRCC1/Lig3α complex, XRCC4 forms a tight complex with Lig4, which stabilises the enzyme and is essential for its normal function *in vivo* (Li *et al.*, 1995). Although Lig4 has

not specifically been shown to synthesise $Ap_4A$, it is certainly possible that this may occur in the absence of DNA or XRCC4, similar to the model proposed above for Lig3α. One notable difference is that where XRCC1-deficient cells retain around 20% Lig3α activity, Lig4 is reduced to only around 5% in XRCC4-deficient cells (Bryans *et al.*, 1999). This could possibly provide some explanation as to why the increase in $Ap_4A$ is much smaller in XR-1 compared to EM7 and EM9.

In summary, a number of interesting findings have been made so far which appear to support a role for $Ap_4A$ in the DNA damage response and provide some interesting clues as to the possible mechanism of this involvement. This provides some excellent opportunities to further investigate the exact details of this involvement in the subsequent stages of this project.

# CHAPTER 4

# Possible source and covalent modification of $Ap_4A$ by ADP-ribose

## 4.1 Introduction

The observations made in the previous chapter demonstrate that the level of intracellular $Ap_4A$ is increased in CHO cells in response to treatment with EMS, an agent which induces alkylated base damage, a type of damage normally repaired by the BER pathway. Furthermore, the key observation was made that in cells lacking XRCC1, a protein which plays a pivotal role in BER, the normal background level of intracellular $Ap_4A$ is substantially elevated by almost 16-fold compared to wild-type cells. This finding both strengthens the existing evidence supporting a role for $Ap_4A$ in the DNA damage response, and provides a good opportunity to further investigate the details of this involvement. Following on from the observations made in the previous chapter, the primary focus of the investigation was to determine both the mechanism of this DNA damage-related $Ap_4A$ synthesis, and the possible function that this $Ap_4A$ may have in the DNA damage response.

As discussed previously (pg. 11-13), XRCC1 is a scaffold protein which co-ordinates the processes of SSBR and BER through interactions with a number of different repair enzymes. It forms a tight complex with DNA ligase IIIα (Lig3α) (Caldecott *et al.*, 1994; Caldecott *et al.*, 1995), which binds to sites of DNA damage and recruits other repair proteins including the DNA end-processing enzymes aprataxin (APTX) and polynucleotide kinase (PNK), as well as DNA polymerase β, which is responsible for DNA gap-filling during repair. Based on the information available about XRCC1 and its interaction partners, a number of possible sources for the increased $Ap_4A$ can be hypothesised.

## 4.2 Results

### 4.2.1 XRCC1 has no detectable $Ap_4A$ hydrolase activity *in vitro*

The simplest explanation for the increased level of $Ap_4A$ detected in the absence of XRCC1 is that XRCC1 itself has a previously unreported $Ap_4A$ hydrolase activity, the loss of which leads to an increase in intracellular $Ap_4A$. This seemed a very unlikely scenario given the apparent lack of any enzymatic activity in XRCC1, and the lack of any sequence or putative domain features which may suggest the protein has a nucleotide hydrolase activity. However, it was important that this possibility be ruled out before further investigation into other potential sources of the increased $Ap_4A$ observed in the absence of XRCC1.

To determine if XRCC1 did have $Ap_4A$ hydrolase activity, purified recombinant XRCC1 was directly assayed *in vitro*, using a specific luminometric enzyme activity assay, as described on pg. 49. Although human NUDT2 is known to hydrolyse $Ap_4A$ asymmetrically (producing AMP and ATP products), the possibility also existed that hydrolysis by XRCC1 may be symmetrical, producing only ADP as a product, as is the case for a number of other enzymes, such as the *E. coli* $Ap_4A$ hydrolase ApaH (Guranowski, 2000). Therefore, both types of hydrolysis were investigated and it was found that XRCC1 appeared to have no detectable $Ap_4A$ hydrolase activity *in vitro* (Table 4.1).

### 4.2.2 XRCC1 has no detectable effect on NUDT2 $Ap_4A$ hydrolase activity *in vitro*

An alternative hypothesis for the increased level of $Ap_4A$ in the absence of XRCC1 is that XRCC1 stimulates the activity of another $Ap_4A$ hydrolase, and that the loss of this stimulation reduces the activity of that enzyme and results in elevated levels of $Ap_4A$. Since

the primary $Ap_4A$ hydrolase in mammalian cells is NUDT2 (Guranowski, 2000), this seemed an obvious potential candidate for investigation.

The normal rate of $Ap_4A$ hydrolysis by NUDT2 was first determined by direct assay of the recombinant human protein *in vitro*. NUDT2 was found to have a very high level of hydrolytic activity on $Ap_4A$ (Table 4.1), and the presence of recombinant XRCC1 at an equimolar ratio to NUDT2 appeared to have no effect on the rate of activity, with only a very slight decrease recorded. This indicates that the presence of XRCC1 alone does not appear to have a stimulative effect on the $Ap_4A$ hydrolytic activity of NUDT2 which might have contributed to the substantially elevated levels of $Ap_4A$ in the absence of XRCC1.

**Table 4.1** $Ap_4A$ hydrolase activity of XRCC1 *in vitro* and the effect of XRCC1 on the $Ap_4A$ hydrolase activity of NUDT2 *in vitro*. Purified, recombinant proteins (100 ng XRCC1 or 45 ng NUDT2) were incubated at 25 °C in a total reaction volume of 100 µL containing 70 mM HEPES-NaOH, pH7.8, 10 mM $MgCl_2$ and 10 µM $Ap_4A$ substrate. To measure possible asymmetrical hydrolysis of $Ap_4A$ by XRCC1, phosphoenolpyruvate (PEP) was added to a final concentration of 5 mM along with pyruvate kinase to a final concentration of 50 ng/mL. For the NUDT2 + XRCC1 reaction, XRCC1 was added at equimolar ratio to NUDT2. The rate of $Ap_4A$ hydrolysis was determined by measuring the rate of ATP product formation using a specific luminometric assay, as described on pg. 49. Each value is the mean of at least two determinations.

| Reaction components | Specific activity (fmol $Ap_4A$ hydrolysed/min/pmol protein) |
|---|---|
| XRCC1 | No detectable hydrolysis |
| XRCC1 + PK + PEP | No detectable hydrolysis |
| NUDT2 | 126 |
| NUDT2 + XRCC1 | 118 |

### 4.2.3 The level of intracellular $Ap_4A$ is increased when DNA ligase IIIα is inhibited from binding its DNA substrate

A more plausible explanation for the increase in $Ap_4A$ in the absence of XRCC1 is that un-complexed Lig3α produces $Ap_4A$ as either a direct or indirect result of its inability to bind to XRCC1. Lig3α has already been shown to produce $Ap_4A$ *in vitro*, and importantly, this reaction is inhibited by both ligatable and non-ligatable DNA (McLennan, 2000). Since Lig3α usually exists in complex with XRCC1, which is responsible for localising it to sites of ligation activity on DNA strands (Caldecott *et al.*, 1994; Caldecott *et al.*, 1995; Cappelli *et al.*, 1997), it seems entirely possible that $Ap_4A$ synthesis by Lig3α may be initiated or increased in the absence of XRCC1, and the resulting lack of Lig3α contact with DNA. Although XRCC1 is required to maintain the stability of Lig3α *in vivo*, and in EM9 cells the level of Lig3α is actually reduced 5-fold due to its increased rate of degradation by the proteasome (Moore *et al.*, 2000), it could still be the case that the remaining unstable Lig3α, unable to localise to sites of ligation activity, rapidly produces $Ap_4A$ until its degradation occurs.

To further investigate the hypothesis that Lig3α may produce $Ap_4A$ as a result of its inability to contact its normal DNA substrate, experiments were carried out using inhibitors which interfere with the normal function of the enzyme. The DNA ligase inhibitor L67 (ChemDiv) was originally identified using a computer-aided drug design technique to screen a large database of commercially available low molecular weight compounds that were predicted to bind the DNA-binding pocket of DNA ligase I (Chen *et al.*, 2008). These authors found L67 to be a simple competitive inhibitor, which interacts with the DNA binding domain of both DNA ligase I and III and prevents binding to the correct DNA substrate by both enzymes. The chemical structure of this molecule is shown in Fig. 4.1A.

The normal process of DNA ligation proceeds by a three step reaction mechanism (Fig. 4.2). L67 has no detectable effect on the first stage of ligation, which involves the formation of a covalent DNA ligase-AMP intermediate, and which occurs completely independently of the DNA substrate. The second stage of ligation involves the transfer of the AMP moiety from the enzyme to the 5′ phosphate terminus of the nick, and L67 causes a substantial reduction in the level at which this occurs due to its interference with the ability of the enzyme to bind the substrate. The final stage of ligation involves the catalysis of a phosphodiester bond by the nonadenylated enzyme, which releases AMP. L67 was most potent at inhibiting this stage of ligation, again by preventing the DNA substrate from correctly binding to the DNA binding pocket of the enzyme (Chen *et al.*, 2008).

Since the effect of L67 is limited to preventing Lig3α from binding to DNA, it does not prevent the formation of a DNA ligase-AMP intermediate, or presumably the transfer of the AMP moiety to an ATP acceptor, thereby producing $Ap_4A$. Indeed, it seemed quite possible this activity may be increased by the inability of the enzyme to properly contact the DNA substrate, as appears to be the case *in vitro*. To test this hypothesis, wild-type AA8 cells were treated with L67 and the level of intracellular $Ap_4A$ was measured and compared to untreated cells. Following treatment, a 4.8-fold increase in intracellular $Ap_4A$ was detected (Table 4.2). Since L67 is active on both DNA ligase I and DNA ligase III, a similar molecule L82 (ChemDiv) was also used as a control. L82 affects the same stage of ligation as L67, but is active on DNA ligase I only, with no detectable effect reported on Lig3. The chemical structure of this molecule is shown in Fig. 4.1B. Unlike with L67, treatment of AA8 cells with L82 did not cause a substantial increase in the level of intracellular $Ap_4A$, suggesting that the increase in $Ap_4A$ observed following L67 treatment is most likely to be caused by DNA ligase III, rather than DNA ligase I

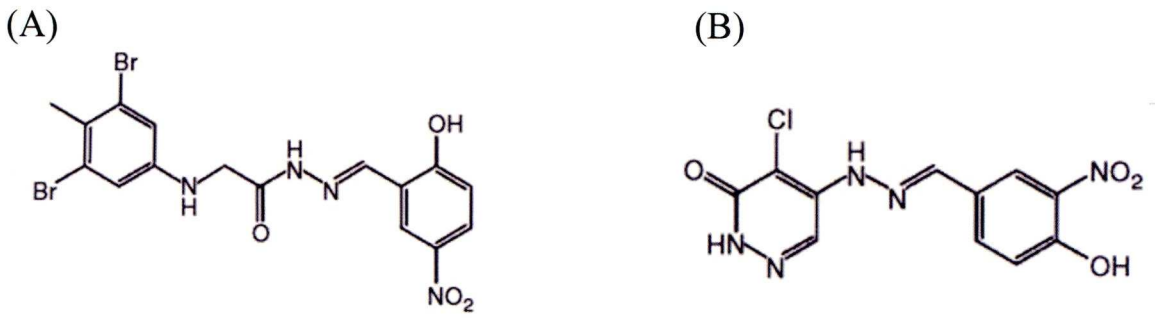


**Figure 4.1** Chemical structures of the DNA ligase inhibitors L67 (A) and L82 (B).

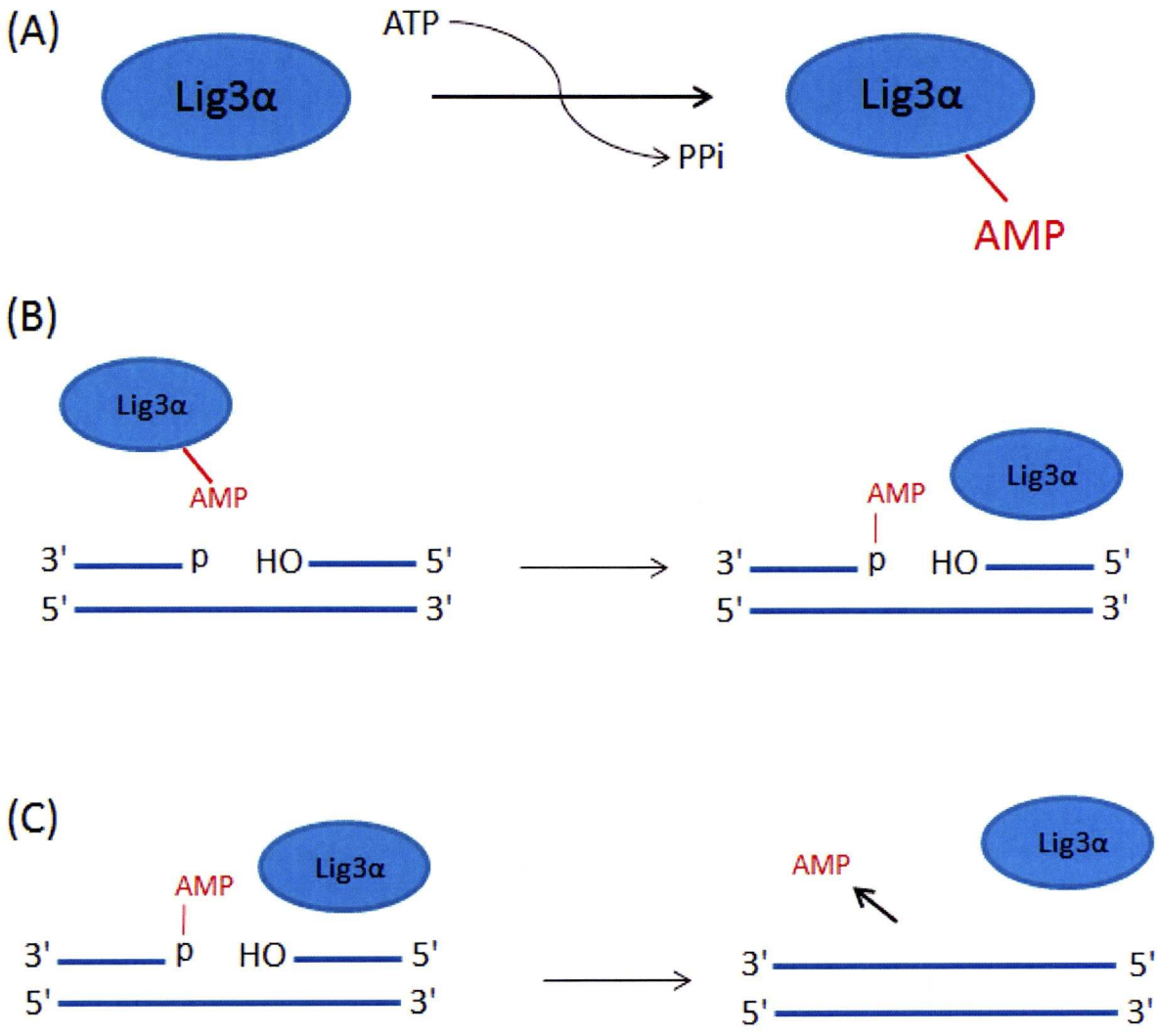


**Figure 4.2** Stages of DNA ligation. (A) DNA ligase reacts with ATP and forms a covalent ligase-AMP intermediate. (B) the AMP residue is transferred to the 5′ phosphate terminus of the DNA nick. (C) The ligase enzyme catalyses the formation of a phosphodiester bond to re-seal the gap, with the release of AMP.

**Table 4.2** Increase in intracellular $Ap_4A$ in wild-type CHO cells following treatment with the DNA ligase inhibitor L67. Cells were treated with 50 μM L67 or 50 μM L82 (ChemDiv) by addition of concentrated stock solutions (5 mM in DMSO) to the growth medium. An equal volume of DMSO was added to untreated AA8 cells as a control. Cell monolayers were extracted for analysis 18 h after addition and assayed for $Ap_4A$ using a specific luminometric assay. Each value is the mean of independent duplicate determinations.

| Cell line and treatment | $Ap_4A$ (pmol/$10^6$ cells) | Fold difference to untreated AA8 |
|---|---|---|
| AA8 | 0.57 | - |
| AA8 + L67 | 2.72 | 4.8 |
| AA8 + L82 | 0.75 | 1.3 |

### 4.2.4 Lack of Aprataxin causes an increase in the level of intracellular $Ap_4A$

Another possible explanation for the increased $Ap_4A$ in XRCC1-deficient cells is that a reduction in the previously reported $Ap_4A$ hydrolytic activity of APTX (Kijas *et al.*, 2006) may occur when it is not complexed with XRCC1. APTX normally directly interacts with CK2-phosphorylated XRCC1 protein and this is required for its recruitment to sites of DNA damage (Hirano *et al.*, 2007). In addition to its reported roles in DNA end processing during damage repair (Ahel *et al.*, 2006; Takehashi *et al.*, 2007), the central catalytic HIT domain of aprataxin is also able to bind $Ap_4A$ and to utilise it as a substrate, resulting in its hydrolysis (Kijas *et al.*, 2006). This activity is low when measured *in vitro* using uncomplexed aprataxin, although the possibility exists that it may be increased by complex formation with XRCC1. Indeed, there is already evidence that XRCC1 stimulates the activity of various other enzymes, including APE1 (Vidal *et al.*, 2001) and PNK (Whitehouse *et al.*, 2001), the latter of which binds to the same region of CK2-phosphorylated XRCC1 as APTX, by means of a similar FHA domain (Clements *et al.*, 2004; Date *et al.*, 2004). Despite a report that the presence of triply phosphorylated XRCC1 peptide, which binds to the FHA domain of APTX, does not appear increase its $Ap_4A$ hydrolase activity *in vitro* (Kijas *et al.*, 2006), it could be the case that the presence of other components of the XRCC1 complex, and the participation of APTX in its multiprotein complex does increase the activity *in vivo*.

FD105 M20 is a human skin fibroblastic cell line derived from a patient with ataxia with oculomotor apraxia type 1 (AOA1), the autosomal recessive neurological syndrome resulting from the lack of functional APTX. These cells carry the premature termination mutation W279X in the *APTX* gene and as a result, fail to express APTX protein (Clements *et al.*, 2004). FD105 M21 is derived from FD105 and has been complemented with full length human *APTX* cDNA under the control of a constitutive expression promoter, and therefore

stable expression of APTX has been restored (El-Khamisy *et al.*, 2009). Together, these two cell lines provided an opportunity to investigate the effect that the lack of APTX has on the level of intracellular $Ap_4A$, and to examine the possible role that APTX may have in the regulation of $Ap_4A$ levels *in vivo*.

The level of intracellular $Ap_4A$ was determined in both FD105 M20 and FD105 M21 cell lines using the standard assay technique (Table 4.3). These data indicate that the specific lack of APTX causes a substantial (5.7-fold) increase in the level of intracellular $Ap_4A$. This suggests that despite only a very low level of $Ap_4A$ hydrolase activity reported *in vitro*, APTX may have a role in the regulation of its levels *in vivo*. However, this increased $Ap_4A$ could alternatively be simply an indirect effect caused by accumulation of endogenously generated SSBs in these cells due to defective SSBR in the absence of APTX.

**Table 4.3** Increase in intracellular $Ap_4A$ caused by the lack of APTX. FD105 M20 is an immortalized human skin fibroblast cell line derived from an AOA patient and deficient in APTX due to a premature termination mutation in *APTX*. FD105 M21 has been corrected by transfection of full length *APTX* cDNA under the control of a constitutive expression vector, thus restoring cellular APTX. Cell monolayers were extracted and analysed for intracellular $Ap_4A$ using a specific luminometric assay. Each value is the mean ± S.E.M. of independent triplicate determinations. The P value was calculated using an unpaired t-test and represents the statistical significance of the observed difference between the level of $Ap_4A$ in the two cell lines.

| Cell line | $Ap_4A$ (pmol/$10^6$ cells) | Fold difference | P value |
|---|---|---|---|
| FD105 M21 | 0.22 ± 0.03 | - | - |
| FD105 M20 (APTX $^{-/-}$) | 1.26 ± 0.29 | 5.7 | 0.031 |

### 4.2.5 Aprataxin has a low level of $Ap_4A$ hydrolase activity *in vitro*, and this appears to be reduced in the presence of DNA

Although only a low level of $Ap_4A$ hydrolase activity has been reported *in vitro* for APTX (Kijas *et al.*, 2006) it was decided to re-examine this using the more sensitive luminometric assay described previously (pg. 44-45). Purified, recombinant and catalytically active APTX was assayed for $Ap_4A$ hydrolase activity *in vitro* and, consistent with the previous findings, a low level of activity was detected (Table 4.4). To further probe the possible effect that XRCC1 complex formation may have on this activity, full length CK2-phosphorylated XRCC1 was added to the sample of APTX, and this appeared to produce no significant change in the subsequent rate of $Ap_4A$ hydrolysis. The presence of phosphate in the reaction produced no detectable change in the level of $Ap_4A$ hydrolysis either, ruling out the possibility that APTX was in fact an $Ap_4A$ phosphorylase ($Ap_4A + Pi \rightarrow ATP + ADP$), rather than a hydrolase. Although unlikely for a true HIT protein like APTX, this activity was recently been reported for one such protein isolated from *Mycobacterium tuberculosis* (Mori *et al.*, 2010), raising the interesting possibility that the same may have been true for APTX. Addition of DNA however, did cause a decrease in relative $Ap_4A$ hydrolase activity, both in the absence and presence of XRCC1.

**Table 4.4** $Ap_4A$ hydrolase activity of APTX measured *in vitro*. A 150 ng sample of purified, recombinant APTX was incubated at 25 °C in a total reaction volume of 100 µL containing 50 mM HEPES-NaOH, pH7.6, 1 mM $MgCl_2$ and 100 µM $Ap_4A$ substrate. The rate of $Ap_4A$ hydrolysis was determined by measuring the rate of ATP product formation using a specific luminometric assay, as described on pg. 49. Purified recombinant XRCC1 was added at equimolar ratio to APTX, DNA was added to a final concentration of 0.05 µM and phosphate was added to a final concentration of 5 mM. Each value is the mean of at least two determinations.

| Reaction components | Specific activity (pmol $Ap_4A$ hydrolysed/min/pmol APTX) |
|---|---|
| APTX | $5.01 \times 10^{-3}$ |
| APTX + XRCC1 | $4.70 \times 10^{-3}$ |
| APTX + DNA | $2.48 \times 10^{-3}$ |
| APTX + XRCC1 + DNA | $2.04 \times 10^{-3}$ |
| APTX + phosphate | $5.02 \times 10^{-3}$ |

### 4.2.6 Lack of APLF appears not to cause an increase in the level of intracellular $Ap_4A$

APLF (aprataxin and polynucleotide kinase-like factor; also known as PALF and Xip1) is a DNA repair protein which has been recently identified through the similarity of its FHA domain to those present in both APTX and PNK (Iles *et al.*, 2007). As with these two proteins, the FHA domain mediates an interaction with phosphorylated XRCC1, and accumulation of APLF also occurs at sites of DNA strand breaks. Recruitment of APLF to these sites of DNA damage is mediated by two tandem poly-(ADP ribose) binding zinc finger (PBZ) domains which bind to poly-(ADP ribose) (PAR), present at DNA strand breaks due to the activity of PARP-1 (Rulten *et al.*, 2008). Depletion of cellular APLF results in a delay to the repair of DNA single strand breaks following ionising radiation and produces a phenotype resembling that of PARP-1 deficient cells. Given the known interaction between XRCC1 and APLF, the effect of APLF depletion on the level of intracellular $Ap_4A$ was also examined.

A549-pSC5 is a strain of the human lung epithelial cell line A549, which has been stably transfected with the constitutive expression vector pS, encoding a human APLF siRNA knockdown sequence which results in constitutive depletion of cellular APLF (Iles *et al.*, 2007). A549-pS1 is a control A549 cell line which harbours the empty pS vector. To investigate the possible involvement of APLF in regulating $Ap_4A$ levels *in vivo*, the level of $Ap_4A$ was measured in both cell lines (Table 4.5). The lack of any significant difference in $Ap_4A$ between normal cells and those depleted in APLF suggests that this protein does not immediately appear have a involvement in the regulation of intracellular $Ap_4A$.

**Table 4.5** Effect of APLF depletion on the level of intracellular $Ap_4A$. A549 pSC5 cells constitutively express an siRNA knockdown sequence which results in depleted APLF, while A549 pS1 cells carry only the empty expression vector as a control. Cell monolayers were extracted and analysed for intracellular $Ap_4A$ using a specific luminometric assay. Each value is the mean ± S.E.M. of independent triplicate determinations. The P value was calculated using an unpaired t-test and represents the statistical significance of the observed difference between the level of $Ap_4A$ in the two cell lines.

| Cell line | $Ap_4A$ (pmol/$10^6$ cells) | Fold difference | P value |
|---|---|---|---|
| A549 pS1 | 0.14 ± 0.01 | - | - |
| A549 pSC5 | 0.12 ± 0.02 | 0.86 | 0.35 |

### 4.2.7 The majority of adenyl dinucleotides in untreated wild-type cells co-elute with an $Ap_4A$ standard following fractionation by HPLC

The luminometric $Ap_4A$ assay using NUDT2 detects nucleotides in the form $Ap_nA$, where $n$ is >4, not only $Ap_4A$. To confirm the exact nature of the dinucleotides being detected in these experiments, high performance liquid chromatography (HPLC) was used to fractionate the cell extracts, and the amount of $Ap_nA$ in each fraction was subsequently assayed. Fractionation of a sample of mixed adenine dinucleotide standards, containing an equal 1 μM concentration of $Ap_4A$, $Ap_5A$ and $Ap_6A$, showed clear separation of the different nucleotides according to the size of their negative charge (Fig. 4.3), confirming the effectiveness of the separation technique and conditions used.

Following fractionation of untreated AA8 cell extracts, almost all of the material detected by the $Ap_4A$ assay co-eluted with the $Ap_4A$ standard (Fig. 4.4), indicating that that the majority of $Ap_nA$ that was previously detected in untreated cells was indeed $Ap_4A$. A very low level of material co-eluted with each of the $Ap_5A$ and $Ap_6A$ standards, suggesting that as expected, these dinucleotides only exist at very low levels in untreated cells.

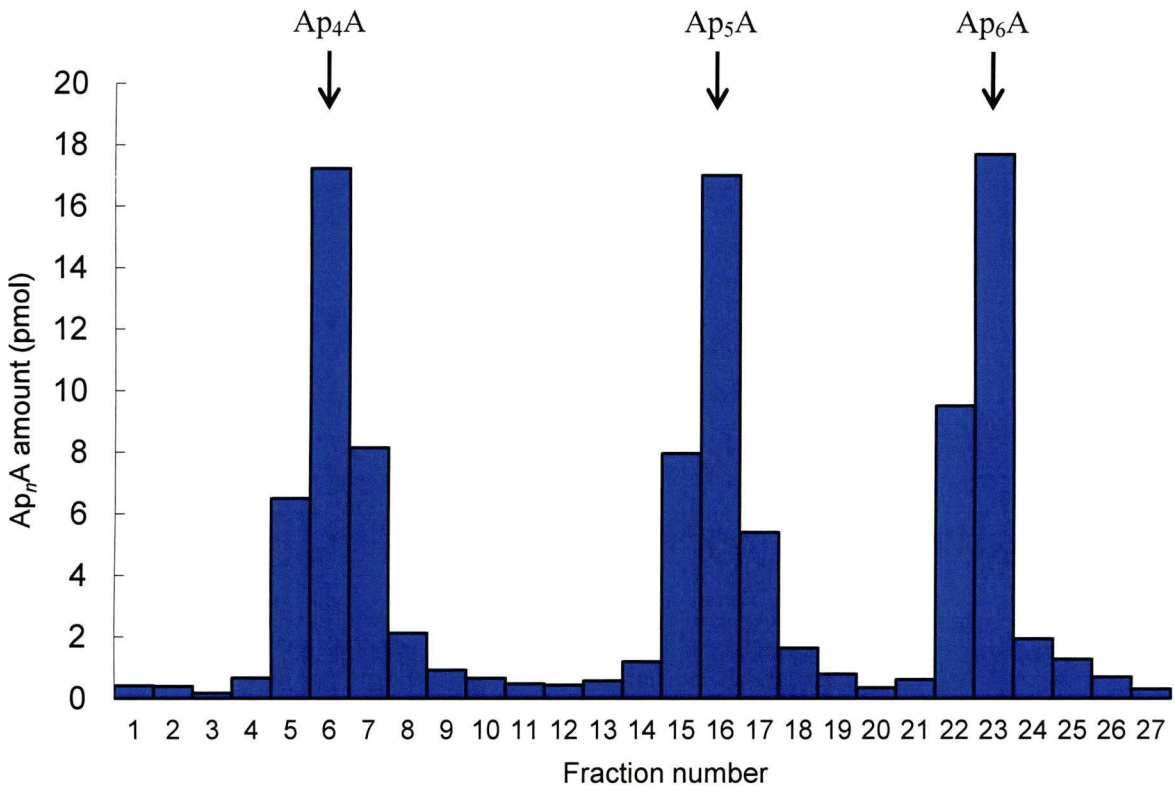


**Figure 4.3** Fractionation of adenine dinucleotide standards by HPLC. A 50 µL sample of mixed adenine dinucleotide standards, containing an equal 1 µM concentration of $Ap_4A$, $Ap_5A$ and $Ap_6A$, was bound to a MonoQ ion exchange column and eluted at 1 mL/min with a linear gradient of ammonium bicarbonate, pH9.6, between 21 mM and 0.7 M over a total volume of 20 mL. Fractions (0.5 mL) were collected and the amount of adenine dinucleotide in each was determined using a specific luminometric assay, as described on pg. 47.

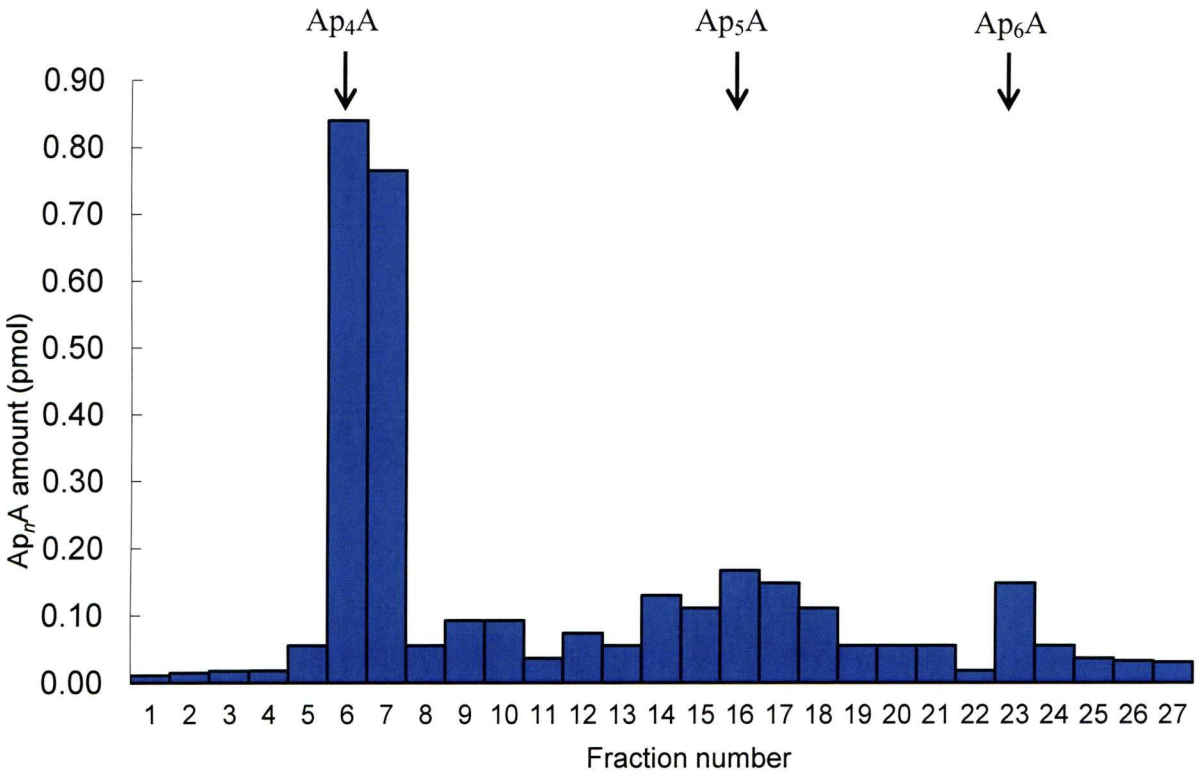


**Figure 4.4** Fractionation of cell extracts by HPLC. A nucleotide was extract prepared from approximately 4 x $10^7$ wild-type AA8 cells, bound to a MonoQ ion exchange column and eluted at 1 mL/min with a gradient of ammonium bicarbonate, pH9.6, between 21 mM and 0.7 M. Fractions (0.5 mL) were collected and the amount of adenine dinucleotide in each was determined using a specific luminometric assay, as described on pg. 46. The arrows indicate the elution fraction of the dinucleotide standards.

### 4.2.8 The increase in adenyl dinucleotides following DNA damage appears not to consist of $Ap_4A$ alone

To further characterise the nature of the increased level of adenyl dinucleotides which accumulates in cells following DNA damage, an extract from EMS and araC-treated AA8 cells was also fractionated by HPLC and each fraction subsequently assayed for $Ap_nA$. The treatment conditions were identical to those which were previously found to increase the overall level of $Ap_nA$ (Fig. 3.2, pg. 62), although the additional use of HPLC enabled this $Ap_nA$ to be examined in more detail and its exact composition determined. In comparison to untreated AA8 cells (Fig. 4.4), the EMS and araC-treated AA8 cells showed a striking difference (Fig. 4.5A). In addition to the peak of material co-eluting with the $Ap_4A$ standard, a second, much larger peak of material was also detected eluting after the $Ap_4A$. Similarly, this was also observed in untreated EM9 cells, which were earlier found to have a constitutively high level of $Ap_4A$ (Fig. 4.5B). This important finding appears to indicate that the previously reported increase in $Ap_4A$ following EMS-treatment is actually not $Ap_4A$ alone, and in fact a substantial portion of it is another, as yet unidentified compound which is also detected by the assay technique. Although eluting in a similar position, this material appeared not to co-elute with the $Ap_5A$ standard, yet it must be sensitive to hydrolysis by NUDT2 in order to be detected by the assay. Based on this, the most likely explanation is that it is in fact a form of $Ap_4A$ which has been modified in some way which causes it to be separated from unmodified $Ap_4A$ during HPLC.

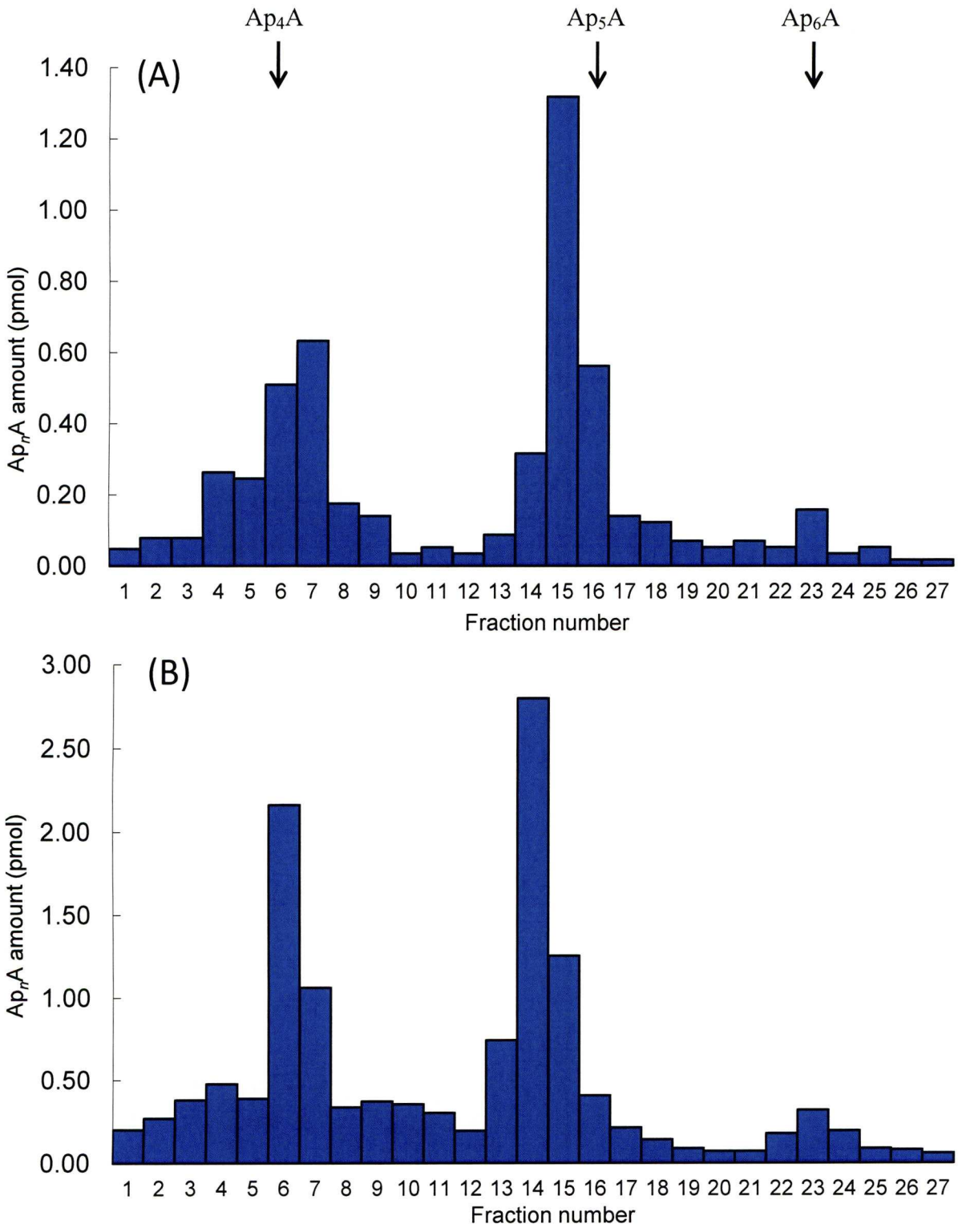


**Figure 4.5** Fractionation of cell extracts by HPLC. (A) AA8 cells were treated for 4 h with 200 mM ethyl methanesulphonate (EMS) in combination with 200 mM cytosine arabinoside (araC) and immediately extracted for analysis. (B) Untreated EM9 cells (XRCC1 deficient). In each case, nucleotide extracts from approximately 4 x $10^7$ cells were bound to a MonoQ ion exchange column and eluted at 1 mL/min with a gradient of ammonium bicarbonate, pH9.6, between 21 mM and 0.7 M. Fractions (0.5 mL) were collected and the amount of adenine dinucleotide in each was determined using a specific luminometric assay, as described on pg. 46. The arrows indicate the elution fraction of the dinucleotide standards.

### 4.2.9 The increased $Ap_4A$ detected following DNA damage appears to be modified by ADP-ribosylation

An intriguing possibility for the identity of the unknown molecule is ADP-ribosylated $Ap_4A$ (Fig. 1.4), which has been reported to be produced under certain conditions *in vitro* (Yoshihara & Tanaka, 1981), however until now has never been detected *in vivo*. Given that ADP-ribosylation is primarily carried out by PARP enzymes, which have an important role in DNA single strand break repair, this seemed a very interesting hypothesis to investigate.

To examine if this might be the case, a sample of ADP-ribosylated $Ap_4A$ was initially synthesised *in vitro* using purified, recombinant PARP-1 enzyme to produce ADP-ribose from $NAD^+$ substrate and attach it onto $Ap_4A$ as an acceptor. This has previously been shown to occur efficiently under certain conditions, and in the presence of histone H1 (Tanaka *et al.*, 1981). As shown in Fig. 4.6A, following the synthesis reaction and subsequent fractionation of the products, a second peak of material elutes after the unmodified $Ap_4A$, which presumably corresponds to mono-ADP-ribosylated $Ap_4A$, since it was not detected in a control reaction in the absence of PARP-1 (Fig. 4.6B). This co-eluted with the peak of unknown material detected in both EM9 cells and EMS-treated AA8 cells, supporting the theory that it is in fact ADP-ribosylated $Ap_4A$. An additional, smaller peak also elutes later (fraction 20) which probably corresponds to di-ADP-ribosylated $Ap_4A$, modified by the addition of two ADP ribose units.

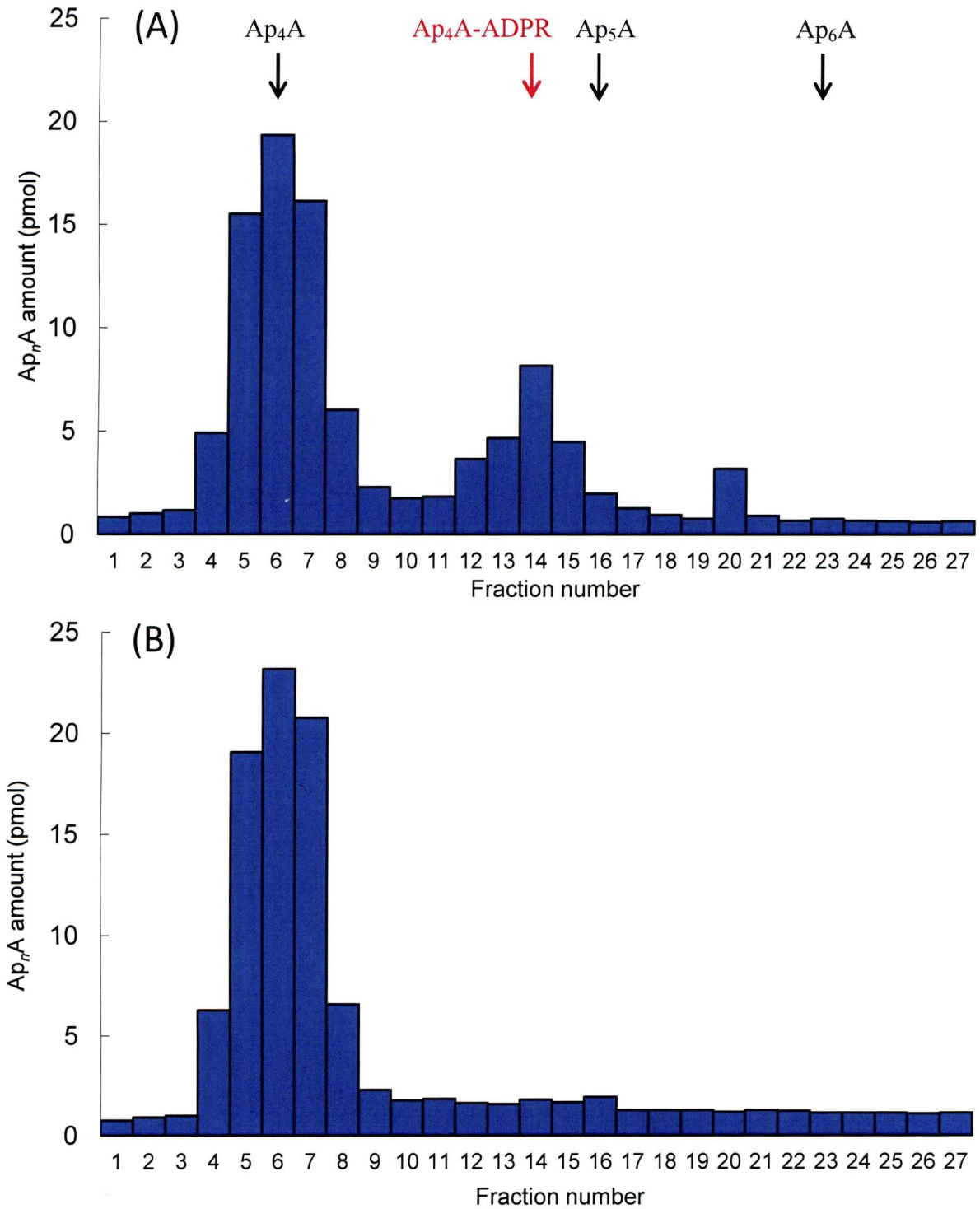


**Figure 4.6** (A) Synthesis of ADP-ribosylated $Ap_4A$ *in vitro* by PARP-1. A total reaction volume of 50 µL was used, containing 25 mM Tris-HCl, pH8.0, 1 mM DTT, 100 µM $Ap_4A$, 25 µM $NAD^+$, 5 µg histone H1, 10 µg PARP active DNA and 20 µg PARP-1 enzyme. (B) Negative control reaction, as above except without PARP-1. Reactions were incubated at 25 °C for 18 h and then the enzyme was deactivated by incubating for 10 minutes at 95 °C and centrifuging for 10 mins at 9,000 x *g*. The supernatant was bound to a MonoQ ion exchange column and eluted at 1 mL/min with a gradient of ammonium bicarbonate, pH9.6, between 21 mM and 0.7 M. Fractions (0.5 mL) were collected and the amount of adenine dinucleotide in each was determined using a specific luminometric assay, as described on pg. 46. The arrows indicate the elution fraction of the dinucleotide standards.

To provide further evidence that ADP-ribosylated $Ap_4A$ had been detected *in vivo*, EM9 cell extracts were treated with purified recombinant poly(ADP-ribose) glycohydrolase (PARG), the enzyme which functions to reverse the poly(ADP-ribosylation) reaction by removing ADP-ribose and restoring the acceptor molecule to its original, unmodified state. Following treatment of EM9 cell extracts with PARG and subsequent fractionation, there was a distinct change in the elution pattern of the nucleotides (Fig. 4.7B). The second peak thought to correspond to ADP-ribosylated $Ap_4A$ was no longer present and all of the material now co-eluted with the $Ap_4A$ standard. Since the unidentified material detected in untreated EM9 extracts (Fig. 4.7A) is clearly sensitive to PARG, and is apparently restored to unmodified $Ap_4A$ following treatment with PARG, this provides fairly strong evidence that it is in fact ADP-ribosylated $Ap_4A$.

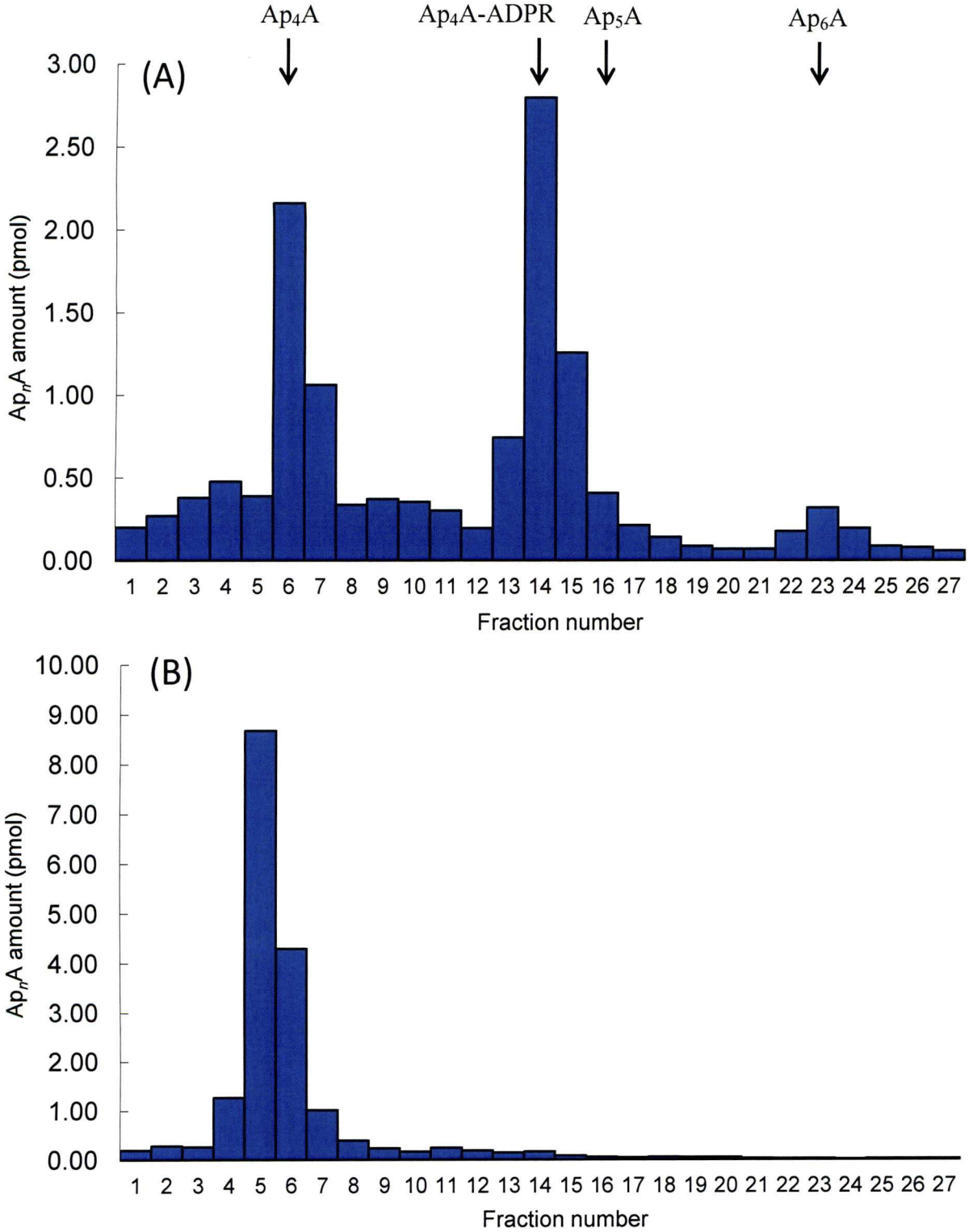


**Figure 4.7** Treatment of EM9 cell extracts with poly-(ADP ribose) glycohydrolase (PARG). (A) Untreated nucleotide extract prepared from approximately 4 x $10^7$ EM9 cells (B) Nucleotide extract prepared as above and then incubated at 37 °C for 18 h in a total reaction volume of 100 µL containing 25 mM Tris-HCl, pH8.0, 10 mM β-mercaptoethanol and 10 µg recombinant PARG. Following incubation, the enzyme was deactivated by incubating for 10 minutes at 95°C and centrifuging for 10 mins at 9,000 x *g*. The supernatant was bound to a MonoQ ion exchange column and eluted at 1 mL/min with a gradient of ammonium bicarbonate, pH9.6, between 21 mM and 0.7 M. Fractions (0.5 mL) were collected and the amount of adenine dinucleotide in each was determined using a specific luminometric assay, as described on pg. 46. The arrows indicate the elution fraction of the dinucleotide standards.

### 4.2.10 ADP-ribosylated $Ap_4A$ might not be synthesised by PARP-1 *in vivo*

Poly(ADP-ribosylation) of various proteins during SSBR is primarily carried out by PARP-1, which was also shown above to carry out ADP-ribosylation of $Ap_4A$ *in vitro*. To investigate whether PARP-1 might also be responsible for ADP-ribosylation of $Ap_4A$ *in vivo*, it was decided to examine nucleotide extracts from EM9 cells grown in the presence of a PARP-1 inhibitor. NU1025 (Fig. 4.8B) is a structural analogue of $NAD^+$ (Fig. 4.8A) and is a potent PARP-1 inhibitor since it has a greater ability to interact with the enzyme compared to $NAD^+$ (Griffin *et al.*, 1995). The results obtained (Fig. 4.9) initially appear to indicate that PARP-1 inhibition had no effect on the $Ap_nA$ detected, suggesting that PARP-1 might not be responsible for ADP-ribosylation of $Ap_4A$ *in vivo*. However, the lack of a control mechanism to confirm the success of PARP-1 inhibition prevents any valid conclusions from being made. Furthermore, the data is very puzzling since the elution fractions appear to have shifted, with the nucleotides eluting from the column earlier than expected. This inconsistency with previous experiments could be indicative of a problem with the HPLC process on this particular run.

Given the ambiguous data and the concerns about its validity, it is certainly not possible to draw any definitive conclusions from this experiment. However, the data has been included here because it worth considering the interesting possibility that ADP-ribosylation of $Ap_4A$ may actually be carried out by another enzyme besides PARP-1. There are 17 human genes encoding PARP family enzymes, although only two of these appear to have a role in DNA repair. The second such member besides PARP-1 is PARP-2, which is also activated in both the SSBR and BER pathways (Ame *et al.*, 1999). It has a different DNA binding domain to PARP-1 and seems to be involved in later stages of repair (Mortusewicz *et al.*, 2007), although it does also interact with XRCC1, pol-β and Lig3α (Schreiber *et al.*, 2002). The high

potency of the NU1025 inhibitor appears to be specific to PARP-1 with its structure giving it an improved ability to interact with that enzyme in comparison with the usual $NAD^+$ substrate (Griffin *et al.*, 1995; Ruf *et al.*, 1998). Since NU1025 is a structural analogue of $NAD^+$, it is likely to inhibit all PARP enzymes to a certain degree, although at the low concentration used here, this effect is unlikely to be significant for other PARP enzymes besides PARP-1. Therefore, it could be the case that PARP-2 actually carries out ADP-ribosylation of $Ap_4A$ which would provide an explanation of why this appeared not to be affected by NU1025 treatment. It is also a possibility that ADP-ribosylation of $Ap_4A$ is carried out by a different enzyme such as a mono-ADP-ribosylase unrelated to PARP. Due to time and equipment constraints, it was not possible to repeat this experiment within the present study or to investigate further by using a specific PARP-2 inhibitor such as UPF1035 (Moroni *et al.*, 2005) or a general inhibitor of both PARP-1 and PARP-2. However this is certainly something that should be carried out as part of further investigation in this area.

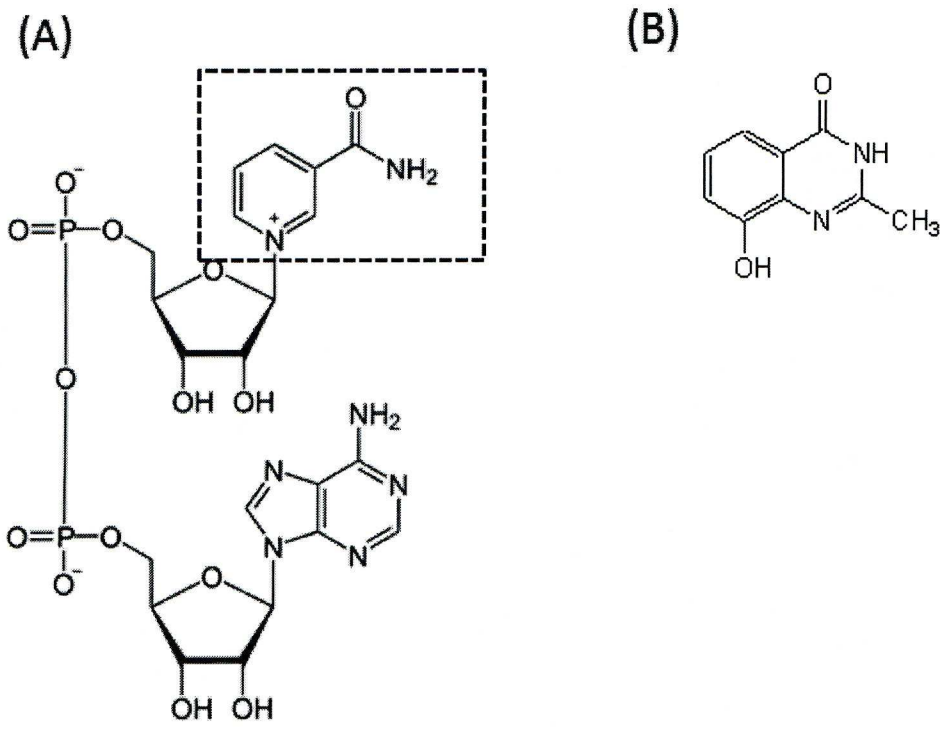


**Figure 4.8** (A) Chemical structure of $NAD^+$ with the nicotinamide moiety (recognised by PARP-1) highlighted within the box. (B) Chemical structure of the PARP-1 inhibitor NU1025.

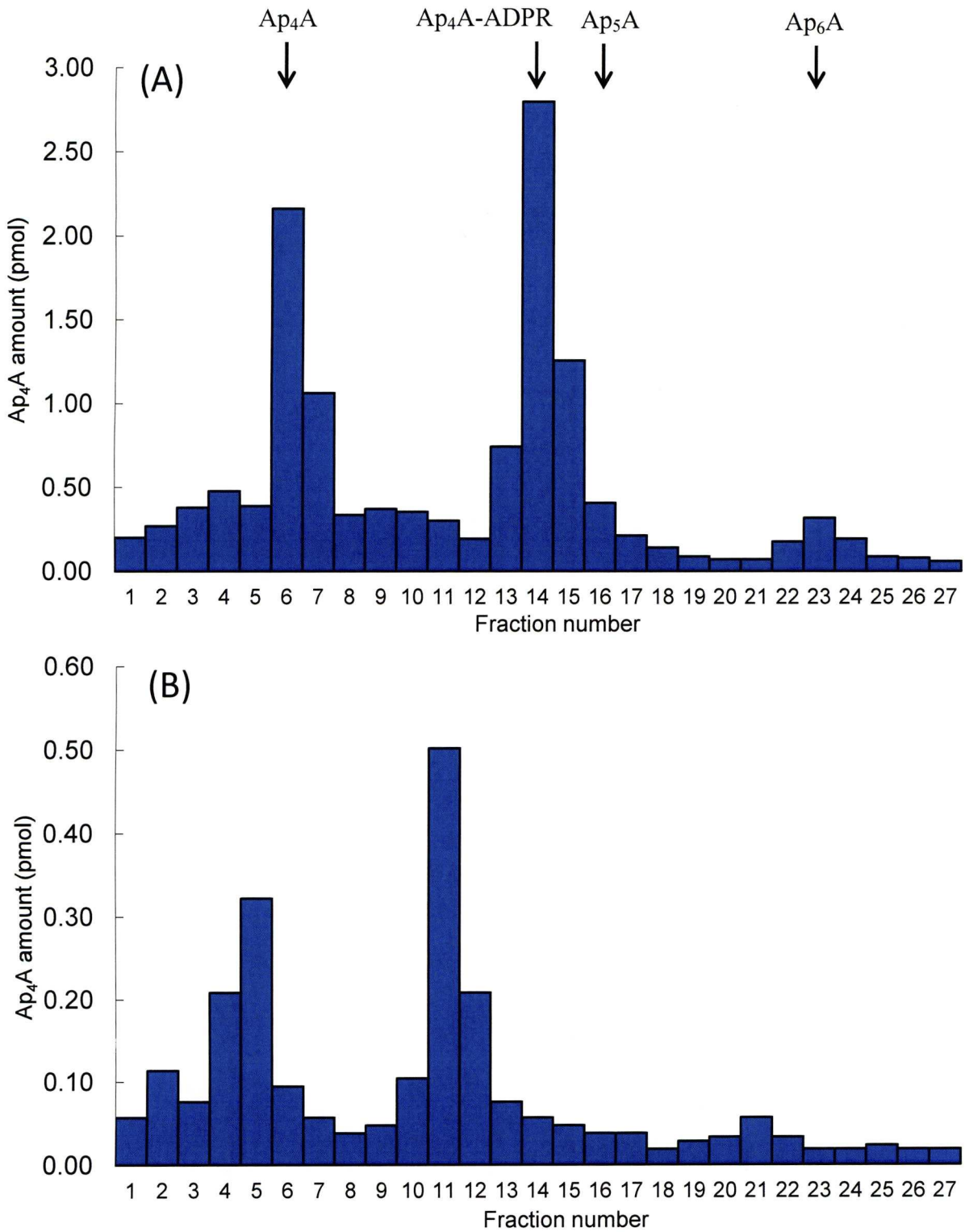


**Figure 4.9** Fractionation of cell extracts by HPLC. (A) Untreated EM9 cells extracts. (B) EM9 cells were treated with NU1025 for 18 h and then extracted for analysis. In each case, nucleotide extracts from approximately 4 x $10^7$ cells were bound to a MonoQ ion exchange column and eluted at 1 mL/min with a gradient of ammonium bicarbonate, pH9.6, between 21 mM and 0.7 M. Fractions (0.5 mL) were collected and the amount of adenine dinucleotide in each was determined using a specific luminometric assay, as described on pg. 46. The arrows indicate the elution fraction of the dinucleotide standards.

## 4.3 Discussion

While further work is clearly required to conclusively prove the origin of DNA-damage related $Ap_4A$ accumulation, the evidence gathered here provides a strong suggestion of its source and the mechanism of its synthesis.

Synthesis of $Ap_4A$ is already known to be carried out by ligase family enzymes and Lig3α has specifically been shown to be one such enzyme (McLennan, 2000). This $Ap_4A$ synthesis is inhibited *in vitro* by the presence of either ligatable or non-ligatable DNA, suggesting it specifically occurs only when Lig3α is not bound to DNA. The finding here that the level of intracellular $Ap_4A$ is increased in cells treated with L67, appears to indicate that Lig3α also produces $Ap_4A$ *in vivo* as a result of its inability to bind to DNA due to the effect of the inhibitor. This is supported by the increased level of $Ap_4A$ also detected in EM9 cells, in which XRCC1-Lig3α complex formation does not occur due to the lack of XRCC1. In these cells, Lig3α is not targeted to DNA since this is mediated by its interaction with XRCC1 (Caldecott *et al.*, 1995; Cappelli *et al.*, 1997). Taken together, these observations support a model in which Lig3α produces $Ap_4A$ *in vivo* as a consequence of its inability to bind to DNA, or its inability to participate in a multiprotein complex required for this to occur, as is the case in EM9. This is also consistent with the increased $Ap_4A$ in wild-type cells following DNA damage, since Lig3α may be prevented from binding to DNA immediately following DNA damage due to the prior transient binding of PARP-1. To further examine the possible role of Lig3α in producing $Ap_4A$ *in vivo*, it would be extremely useful to examine DNA damage-related $Ap_4A$ accumulation in Lig3α-deficient cells. If this did not occur normally, it would provide a very strong indication that this function was indeed carried out by Lig3α. Unfortunately, such cells were unavailable while the work reported here was being carried out, although a Lig3α knockout mouse cell line has recently been produced (K.W. Caldecott,

personal communication), which is likely to prove a valuable tool for uncovering further information on the role of Lig3α.

Despite the apparent role of Lig3α in the synthesis of $Ap_4A$, it appears that the level of $Ap_4A$ is substantially higher in EM9 cells which lack XRCC1 entirely than in L67 treated cells (data summarised in Table 4.6). This suggests that there may be another factor responsible for the increased $Ap_4A$ in EM9 cells in addition to Lig3α. The important finding that APTX deficient cells clearly do have a significantly increased level of $Ap_4A$ (Table 4.3) gives a strong suggestion that this protein also has some involvement in the regulation of $Ap_4A$ levels, and the DNA damage related increases in $Ap_4A$ which occur. The catalytic HIT domain of APTX has previously been reported to have a low level of $Ap_4A$ hydrolase activity *in vitro* (Kijas *et al.*, 2006), and this was confirmed here with a similar, low level of activity being detected (Table 4.4). This relatively weak $Ap_4A$ hydrolase activity is arguably too low to make a significant change to the $Ap_4A$ level *in vivo*, and its activity did not appear to be increased by binding to recombinant phosphorylated XRCC1, as is the case for PNK which shares a similar XRCC1-binding FHA domain with APTX (Whitehouse *et al.*, 2001; Clements *et al.*, 2004). However, since XRCC1-APTX is actually part of a much larger multiprotein complex *in vivo*, it could be the case that APTX activity is increased by the presence and interaction of other components of the complex, besides XRCC1. Since APTX interacts with these other proteins indirectly through XRCC1 (Hirano *et al.*, 2007), this would not occur in EM9 cells, resulting in reduced hydrolytic activity and increased $Ap_4A$. Also, it is possible that the stability of APTX is reduced without XRCC1 binding, which may lead to reduced APTX, also contributing to reduced $Ap_4A$ hydrolysis and higher $Ap_4A$.

**Table 4.6** Summary table showing the level of $Ap_4A$ present in various cell lines and conditions.

| Cell line and treatment | $Ap_4A$ (pmol/$10^6$ cells) | Fold difference to untreated AA8 |
|---|---|---|
| AA8 | 0.63 ± 0.07 ($n$=6) | - |
| AA8 + L67 (ligase inhibitor) | 2.72 ($n$=2) | 4.3 |
| EM9 | 9.96 ± 1.65 ($n$=6) | 15.8 |
| H9T3-7-1 (EM9 + XRCC1) | 0.78 ± 0.06 ($n$=4) | 1.24 |

Taken together, the data reported here are consistent with a model in which the very high level of $Ap_4A$ in EM9 is caused by a combination of both increased synthesis (by Lig3α), and decreased degradation (by APTX). Where either only Lig3α or only APTX is affected, an increase in $Ap_4A$ does occur, but it is lower than that occurring in the absence of XRCC1, which is likely to affect both proteins.

The apparent synthesis of ADP-ribosylated $Ap_4A$ in response to DNA damage provides a very interesting clue as to the potential role of increased $Ap_4A$ in the DNA damage response. ADP-ribosylation of proteins is an important feature of SSBR and is primarily carried out by PARP-1 (de Murcia *et al.*, 1994). Despite the earlier identification of ADP-ribosylated $Ap_4A$ *in vitro* (Yoshihara & Tanaka, 1981), its occurrence has never been reported before *in vivo*. Its synthesis in cells in response to DNA damage is particularly intriguing since it has been previously found to be an effective inhibitor of SV40 DNA replication *in vitro*. Therefore, it could form a novel part of the cellular mechanism to inhibit and stall DNA replication in response to DNA damage while repair occurs.

# CHAPTER 5

## $Ap_4A$ increases the ability of cells to survive after exposure to EMS

### 5.1 Introduction

The experiments carried out in the previous chapters have added to the existing evidence which suggests that $Ap_4A$ has a role in the DNA damage response, and have provided some important information about a possible source of the DNA damage related increase in $Ap_4A$. However, until now, there has been no clear evidence that the excess $Ap_4A$ synthesised in response to DNA damage actually has any function and what the nature, importance or relevance of this function may be.

To investigate the possible functional significance of $Ap_4A$ in the DNA damage response, it would be extremely useful to have cell lines available in which the level of intracellular $Ap_4A$ could be increased or decreased independently of DNA damage, in order to examine what effect this has on the cells' ability to respond normally to DNA damage. By using various techniques to measure DNA damage and repair, such cells could provide valuable information about the possible role of $Ap_4A$ in these important cellular processes.

## 5.2 Results

### 5.2.1 Production of $Ap_4A$-deficient AA8 cells

To gather some information about the possible functional significance of $Ap_4A$ in the DNA damage response, it was decided to first examine the effects that the absence of $Ap_4A$ has on this response. In order to do this, a stably transfected cell line was established in which the human NUDT2 enzyme can be over-expressed in order to continually hydrolyse intracellular $Ap_4A$, thus eliminating it from the cell.

To achieve this, the 'Rheoswitch' mammalian expression system (New England Biolabs) was used. This system uses two individual plasmids, both a regulatory plasmid (pNEBR-R1) and a separate vector plasmid (pNEBR-X1Hygro) in which the expression sequence is cloned. The pNEBR-R1 plasmid (Fig. 5.1) constitutively expresses two regulatory molecules (termed RheoReceptor-1 and RheoActivator) that interact to form a heterodimer which binds tightly to a region of the pNEBR-X1Hygro vector plasmid (Fig. 5.2A), just upstream of the cloned gene. The heterodimer is normally in a transcriptionally inactive form and this binding to pNEBR-X1Hygro tightly represses expression of the cloned gene. However, addition of the RSL1 inducer ligand (Fig. 5.3), which binds to the RheoReceptor-1 protein, induces a conformational change in the RheoActivator that stabilises and activates the heterodimer. This results in recruitment of the basal transcription machinery and a high level of expression of the cloned gene. The benefits of this system are a very low background level of expression, and the fact that gene expression can be induced and tightly controlled by varying the concentration of RSL1 in the cells' growth medium.

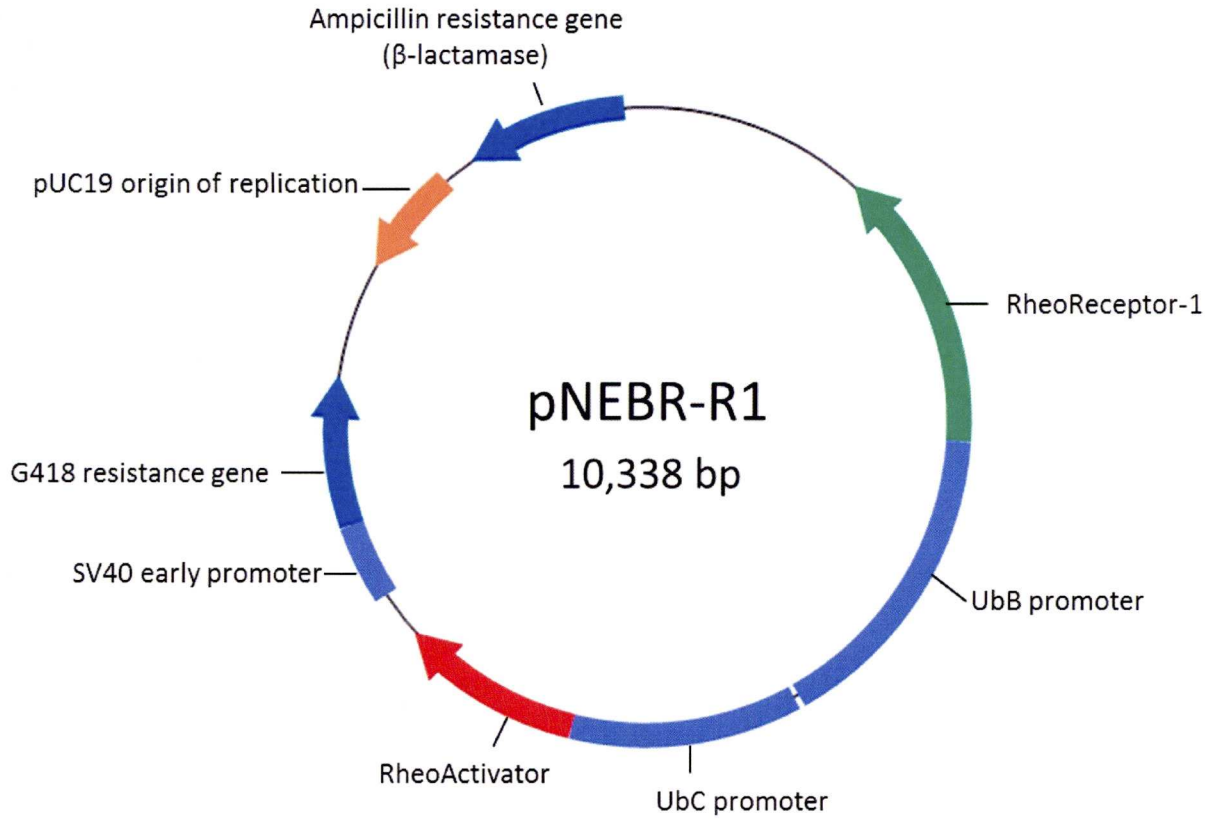


**Figure 5.1** Plasmid map of the 'Rheoswitch' regulatory plasmid pNEBR-R1. This plasmid expresses two regulatory proteins termed RheoReceptor-1 and RheoActivator from the constitutive UbC and UbB promoters respectively. Together, these molecules form a heterodimer which regulates the transcription of genes cloned into the pNEBR-X1Hygro vector. The plasmid also contains the G418 resistance gene under the control of the SV40 early promoter to allow selection of cells carrying the plasmid and the generation of stably transfected cell lines. The diagram is based on the sequence information provided by the manufacturer.

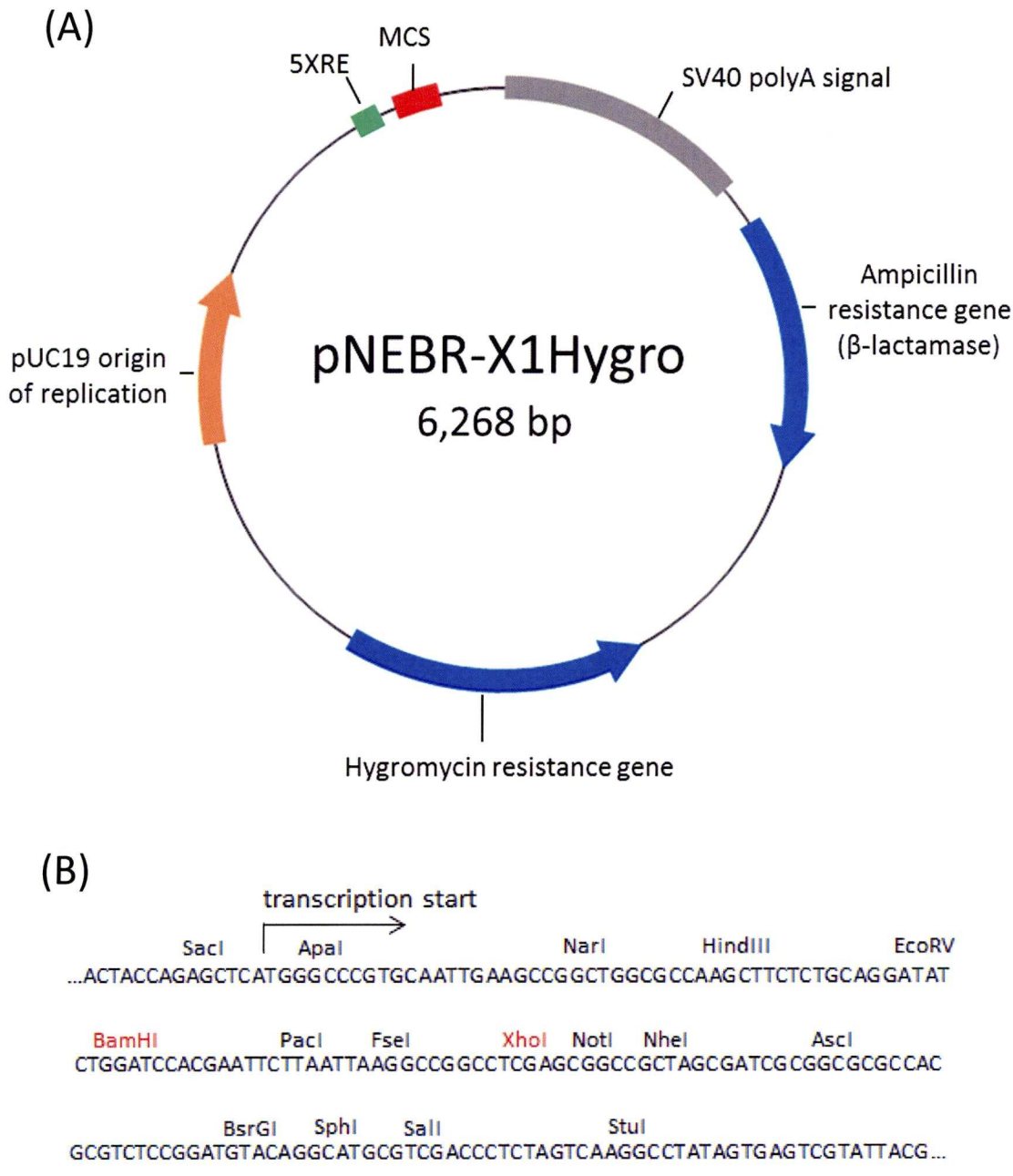


**Figure 5.2** (A) Plasmid map of the 'Rheoswitch' expression vector plasmid pNEBR-X1Hygro. The gene for expression is cloned into the multiple cloning site (MCS), ahead of a TATA box and short leader sequence, and followed by an SV40 polyA signal. There are five copies of the GAL4 response element (5XRE) also upstream of the MCS which function as a binding site for the RheoReceptor-1/RheoActivator heterodimer that regulates transcription of the cloned gene. The plasmid also contains the hygromycin resistance gene to allow selection of cells carrying the plasmid and the generation of stably transfected cell lines. (B) Multiple cloning site (MCS) of the pNEBR-X1Hygro vector plasmid. The *Bam*HI and *Xho*I restriction enzyme sites were used to clone the NUDT2 cDNA into the vector. The diagrams are based on the sequence information provided by the manufacturer.

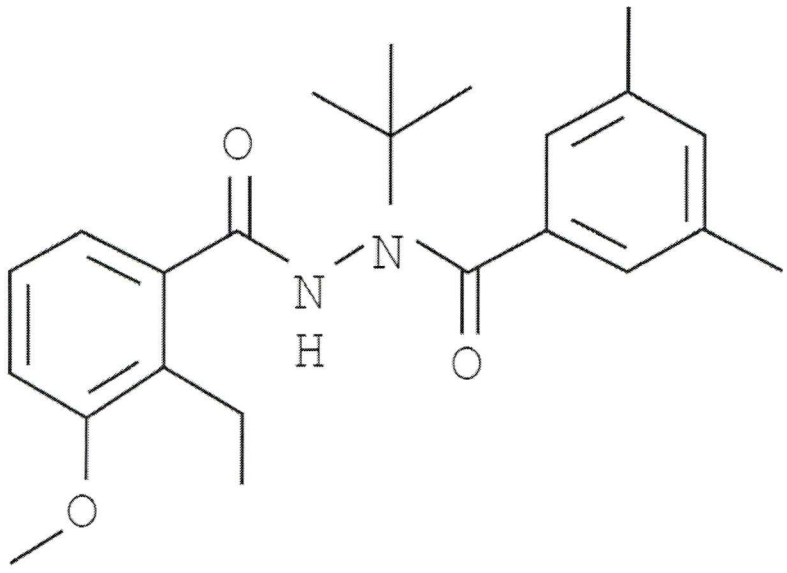


**Figure 5.3** Chemical structure of the 'Rheoswitch' inducer ligand RSL1.

Initially, the wild-type CHO cell line AA8 was stably transfected with the regulatory plasmid pNEBR-R1, and successfully transfected cells were selected by resistance to G418, which is conferred by the plasmid. The appropriate concentration of G418 to use for selection was determined experimentally by first constructing a G418 survival curve (Fig. 5.4). Based on the findings, a concentration of 500 μg/mL was chosen for selection, since this was sufficient to result in 100% lethality of untransfected cells. The transfection efficiency was calculated to be 22.0% from the proportion of cells able to form colonies in the presence of G418, compared to that in the absence of G418. Following selection, a G418 survival curve was also constructed for the transfected cells to measure the increase in G418 resistance relative to untransfected cells (Fig 5.4). Comparison of the two $D_{37}$ values (Table 5.1) indicates a four-fold increase in resistance, confirming the presence of the pNEBR-R1 plasmid and the success of transfection.

**Table 5.1** Resistance to G418 of wild-type AA8 cells and AA8 transfected with the pNEBR-R1 plasmid. Resistance is presented as $D_{37}$ values (concentration of G418 required to produce 37% survival) and fold resistance is in relation to the wild type cell line AA8.

| Cell line | $D_{37}$ value (μg/mL G418) | Fold resistance |
|---|---|---|
| AA8 WT | 232 | - |
| AA8 pNEBR-R1 | 946 | 4.0 |

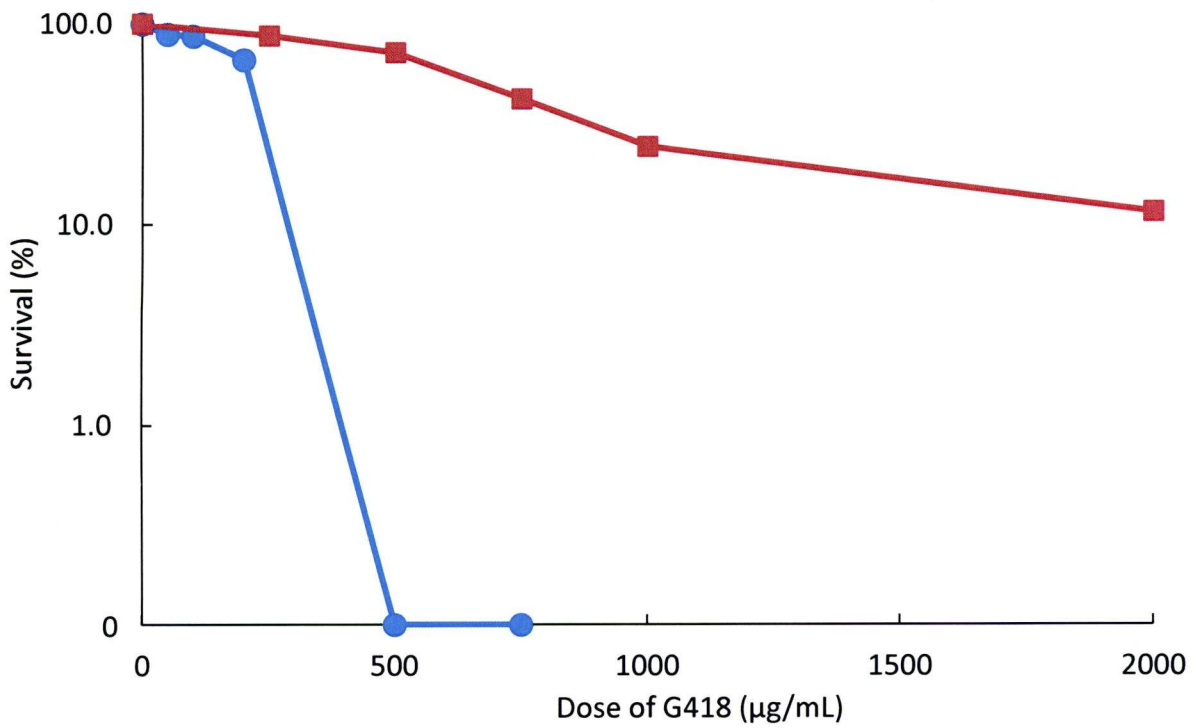


**Figure 5.4** Survival response of cells to increasing doses of G418. Wild-type AA8 cells (blue circles) are sensitive to G418, with 100% lethality occurring at 500 μg/mL. Cells transfected with the pNEBR-R1 plasmid (red squares) are resistant to G418 due to the presence of the resistance gene on the plasmid. In both cases at least 200 cells were plated out into dishes, G418 was added to the medium and dishes were incubated for 10 days, after which the surviving colonies were counted. At least three replicates were used for each dose and each data point represents the mean of 2 independent experiments.

Following transfection and selection, cells were plated out to form a series of individual single cell derived clones, which were each examined for the level of gene expression, both before and after RSL1 induction, using a luciferase based reporter assay. Twelve clones were each transiently transfected with the pNEBR-X1GLuc reporter plasmid (Fig. 5.5), which is derived from the pNEBR-X1Hygro vector plasmid, and encodes an excreted luciferase enzyme isolated from the marine copepod *Gaussia princeps*. The enzyme catalyses the hydrolysis of the substrate coelenterazine which produces light. Following transfection of cells with pNEBR-X1GLuc, maximum luciferase expression was induced in each clone by addition of RSL1. A sample of culture medium was taken both immediately before, and 18 h after RSL1 addition and the level of luciferase activity was assayed as a measure of the level of induced gene expression by RSL1 (Table 5.2). Based on this data, clone 8 was chosen for transfection with the *NUDT2* expression vector, based on the low level of background gene expression, and more importantly, the extremely high level of expression when induced by RSL1.

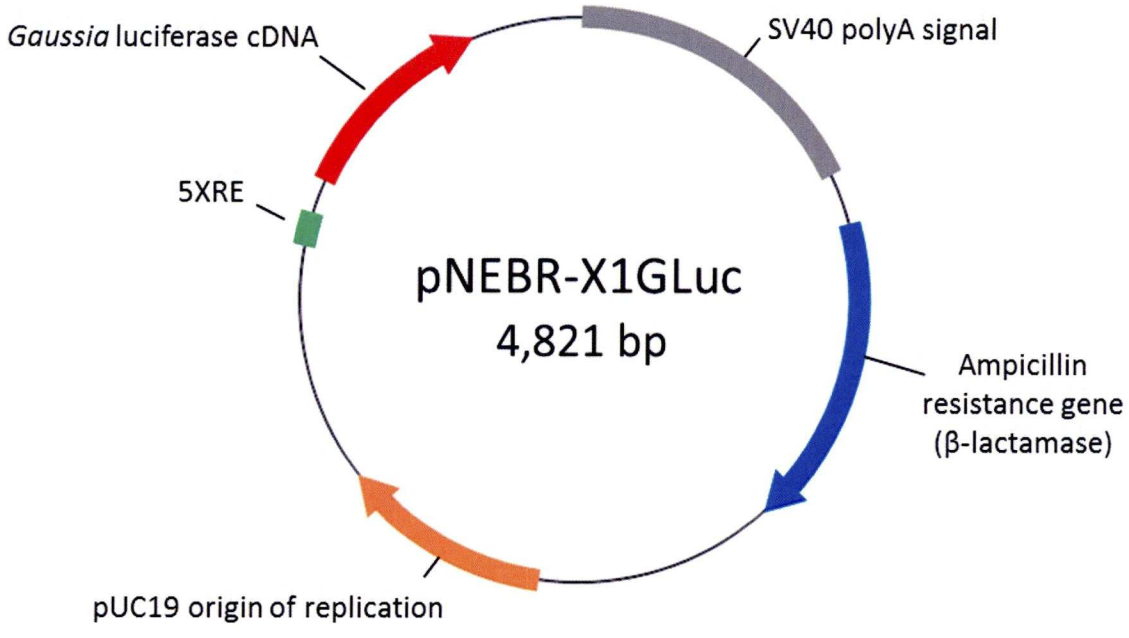


**Figure 5.5** Plasmid map of the 'Rheoswitch' control plasmid pNEBR-X1GLuc. This plasmid is derived from pNEBR-X1Hygro and contains the *Gaussia princeps* luciferase reporter cDNA sequence under the control of the RheoReceptor-1/RheoActivator heterodimer which binds to the five copies of the GAL4 response element (5XRE) just upstream of the sequence. Upon induction by the RSL1 ligand, luciferase is expressed and secreted, allowing an accurate measure of gene expression by the assay of luciferase activity in the cells growth medium. The diagram is based on the sequence information provided by the manufacturer.

**Table 5.2** Comparison of luciferase reporter gene expression in clones of AA8 cells transfected with the 'Rheoswitch' pNEBR-R1 regulatory plasmid. Each clone was transiently transfected with the pNEBR-X1GLuc plasmid, which encodes a secreted luciferase under the control of the pNEBR-R1 plasmid. The relative level of luciferase activity in the cells growth medium was measured in the medium by luminometric assay both before and after induction of gene expression by the addition of 500 nM RSL1. Clone 8 (bold) shows the highest level of gene induction following RSL1 addition and the highest induction ratio.

| Clone number | Relative gene expression before RSL1 addition | Relative gene expression after RSL1 addition | Induction ratio |
|---|---|---|---|
| 1 | 24 | 2009 | 83.7 |
| 2 | 17 | 780 | 45.9 |
| 3 | 28 | 3778 | 134.9 |
| 4 | 5 | 1110 | 222.0 |
| 5 | 13 | 4270 | 305.0 |
| 6 | 25 | 1456 | 58.24 |
| 7 | 27 | 892 | 33.0 |
| **8** | **6** | **4834** | **805.7** |
| 9 | 12 | 2137 | 178.1 |
| 10 | 57 | 3344 | 58.7 |
| 11 | 24 | 357 | 14.8 |
| 12 | 30 | 4552 | 151.7 |

The human *NUDT2* cDNA sequence was supplied as a bacterial clone carrying a recombinant pOTB7 plasmid with the *NUDT2* cDNA sequence cloned into the plasmid between the *Eco*RI and *Xho*I restriction enzyme sites (Fig. 5.6). Following miniprep extraction, a restriction digest and subsequent agarose gel electrophoresis were carried out on the plasmid DNA to confirm that the correct clone had been received (Fig. 5.7). The *NUDT2* cDNA sequence was then amplified from the recombinant plasmid by PCR. The primers used (Table 5.3) were designed to incorporate appropriate restriction enzyme sites on to the ends of the PCR product to facilitate its cloning into the multiple cloning site (MCS) of the pNEBR-X1Hygro expression vector (Fig. 5.2B). Following PCR, amplification of the correct 464 bp product was confirmed by agarose gel electrophoresis (Fig. 5.8).

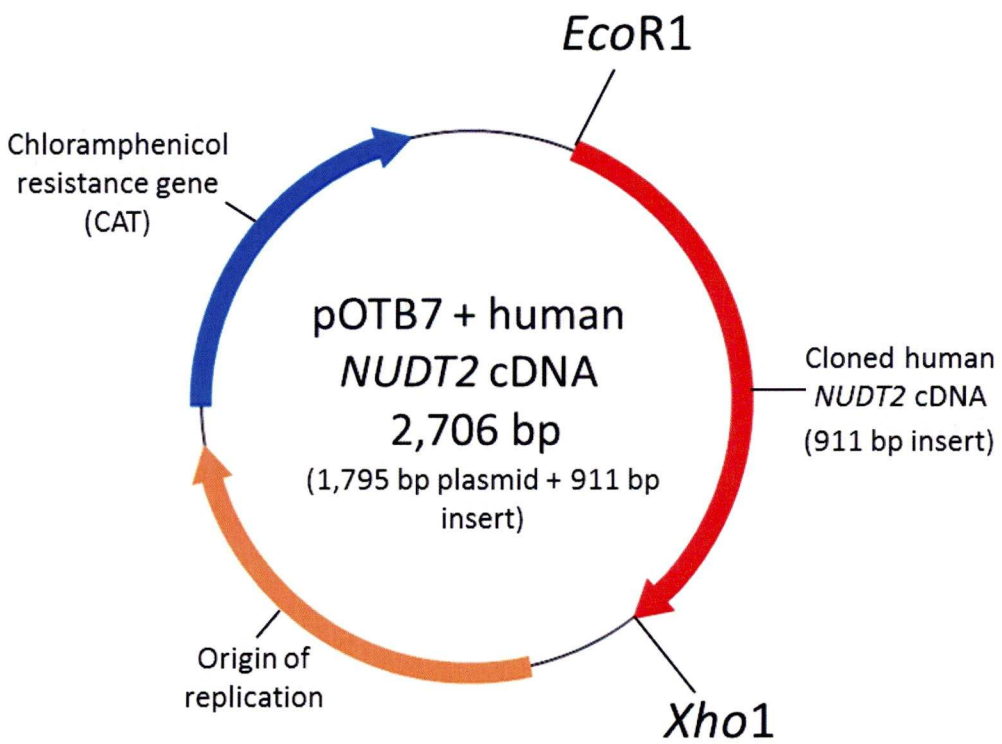


**Figure 5.6** Plasmid map of the pOTB7 vector as received from the I.M.A.G.E. consortium (ID: 3623134), with the human *NUDT2* cDNA sequence cloned between the *Eco*R1 and *Xho*1 restriction enzyme recognition sites. The diagram was constructed using the information provided by the supplier.

**Table 5.3** PCR primers used for the amplification of *NUDT2* cDNA sequence from recombinant plasmid DNA. Primers were designed to incorporate appropriate restriction sites (lowercase) into the PCR product in order to facilitate cloning into the pNEBR-X1Hygro expression vector.

| Primer | Sequence | Melting temperature ($T_m$) |
|---|---|---|
| | *Bam*HI | |
| F primer | 5′-TggatccGACCATGGCCTTGAGAGC-3′ | 59 °C |
| | *Xho*I | |
| R primer | 5′-TctcgagGCTCAGGCCTCTATGGAG-3′ | 59 °C |

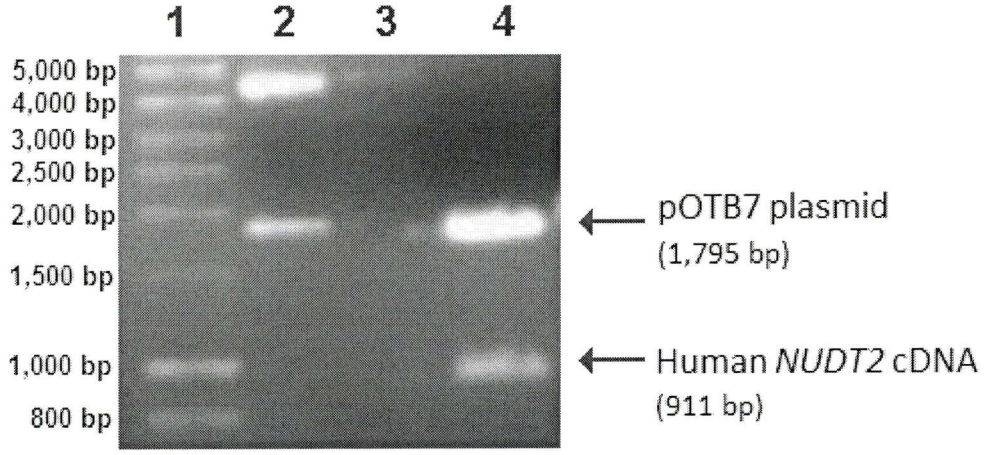


**Figure 5.7** Restriction digest of recombinant pOTB7 plasmid containing human *NUDT2* cDNA following agarose gel electrophoresis. Lane 1 contains the DNA size markers. Lanes 2 and 3 contain undigested plasmid, while lane 4 contains plasmid following digestion by *Eco*R1 and *Xho*I. The 1,795 bp fragment corresponds to the pOTB7 plasmid itself, while the 911 bp fragment corresponds to the inserted cDNA sequence.

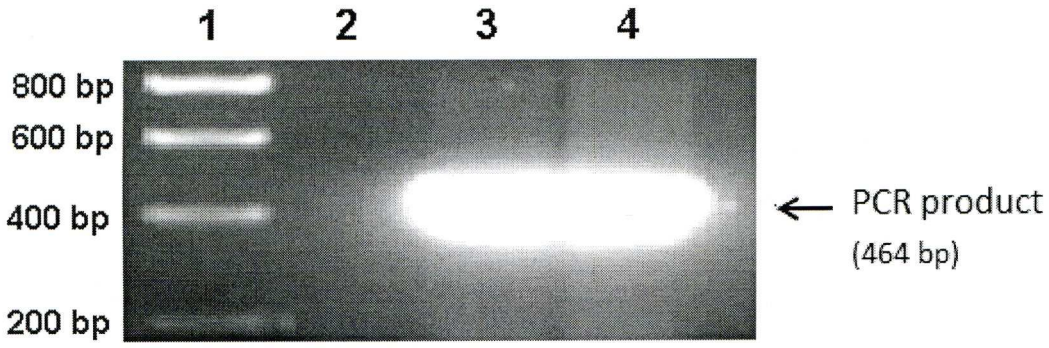


**Figure 5.8** Amplification of human *NUDT2* cDNA sequence by PCR and visualisation of products following agarose gel electrophoresis. Lane 1 is the DNA size markers, while lane 2 is a negative control (no DNA template). The presence of a band in lanes 3 and 4 at approximately 464 bp indicates product amplification.

The PCR product was purified and both the PCR product and pNEBR-X1Hygro expression vector plasmid were digested by *Bam*HI and *Xho*I restriction enzymes to produce complementary cohesive ends. The insert was then ligated into the vector and the reaction product mixture was used to transform competent *E. coli* cells. Those cells transformed with the correct product (vector+insert) were identified by blue-white screening of colonies, before further amplification and subsequent miniprep extraction of the vector. The insert was then fully sequenced using appropriate primers to ensure that no mutations had been introduced and that the sequence was in the correct reading frame (data not shown).

Finally, the previously selected AA8 pNEBR-R1 clone (Table 5.2) was stably transfected with the pNEBR-X1Hygro expression vector containing the cloned human *NUDT2* cDNA sequence. This plasmid contains a hygromycin resistance gene, which allows the selection of successfully transfected cells. As described earlier for G418, the appropriate concentration of hygromycin to use for selection was determined experimentally to be 500 μg/mL by first constructing a hygromycin survival curve (Fig. 5.9). The transfection efficiency in this case was calculated to be 30.2%. Following selection, a hygromycin survival curve was also constructed for transfected cells and comparison of the two $D_{37}$ values indicates a 4.5-fold increase in hygromycin resistance (Table 5.4). This cell line was plated out to form a series of single cell derived clones and all further experiments were carried out on the same single clone.

**Table 5.4** Resistance to hygromycin of wild-type AA8 cells and AA8 transfected with the pNEBR-X1Hygro plasmid. Resistance is presented as $D_{37}$ values (concentration of hygromycin required to produce 37% survival) and fold resistance is in relation to the wild type cell line AA8.

| Cell line | $D_{37}$ value (μg/mL hygromycin) | Fold resistance |
|---|---|---|
| AA8 WT | 218 | - |
| AA8 pNEBR-X1Hygro | 982 | 4.5 |

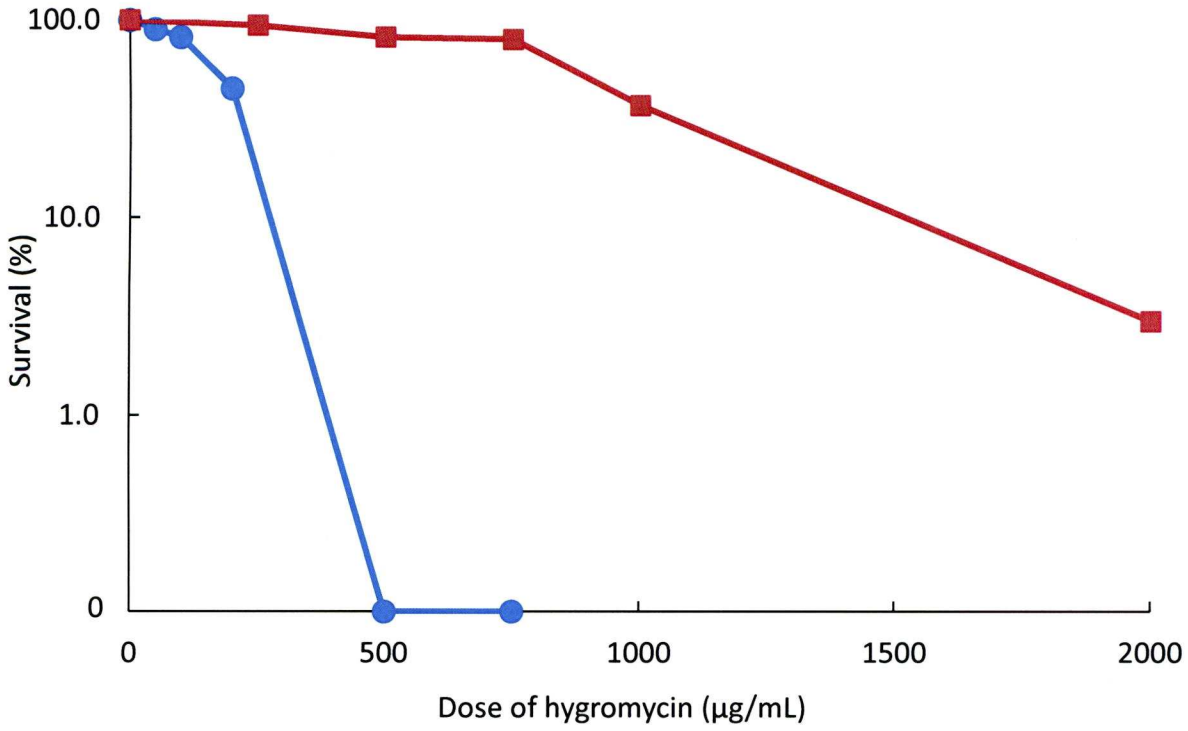


**Figure 5.9** Survival response of cells to increasing doses of hygromycin. Wild-type AA8 cells (blue circles) are sensitive to hygromycin, with 100% lethality occurring at 500 μg/mL. Cells transfected with the pNEBR-X1Hygro plasmid (red squares) are resistant to hygromycin due to the presence of the resistance gene on the plasmid. In both cases, at least 200 cells were plated out in dishes, hygromycin was added to the medium and dishes were incubated for 10 days, after which the surviving colonies were counted. At least two replicates were used for each dose.

### 5.2.2 Characterisation of $Ap_4A$-deficient cells

In order to confirm that the transfected *NUDT2* cDNA was expressed and under the control of RSL1, an immunoblot using an anti-NUDT2 antibody was carried out on extracts from the transfected cell line grown in increasing concentrations of RSL1 (Fig. 5.10). The visual intensity of the target protein band increased considerably with increasing concentration of RSL1, indicating an increase in the level of NUDT2 expression. To further confirm that the increased NUDT2 was catalytically active, and to provide a quantitative measurement of this activity, an $Ap_4A$ hydrolase enzyme activity assay was also carried out on the cell lysates. At the maximum level of expression (500 nM RSL1), a 42-fold increase in $Ap_4A$ hydrolytic activity was detected in the transfected cell lysates over wildtype cells (Fig. 5.11).

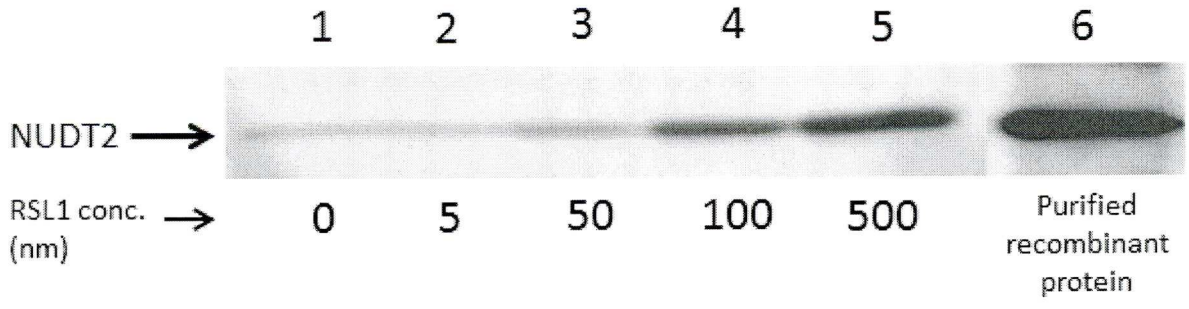


**Figure 5.10** Expression of human NUDT2 as detected by immunoblotting. Whole cell extracts were prepared from AA8 cells transfected with pNEBR-R1/pNEBR-X1Hygro+*NUDT2* and cellular proteins were immunoblotted with an anti-NUDT2 antibody. Un-induced cells express a relatively low level of NUDT2 (lane 1) which increases as cells are grown in increasing concentrations of the inducer ligand RSL1 (lanes 2-5). Purified recombinant NUDT2 was also detected as a positive control (lane 6). β-actin was detected in all cell extracts as a loading control (data not shown).

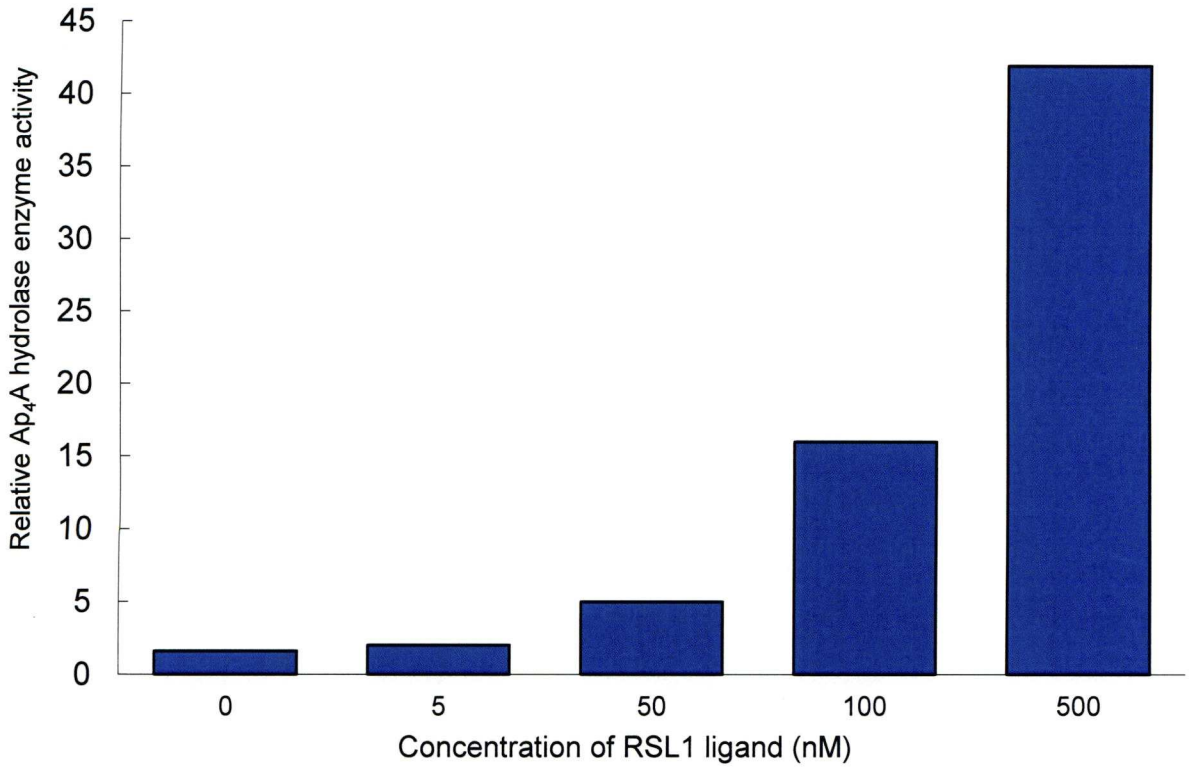


**Figure 5.11** Measurement of relative $Ap_4A$ hydrolase enzyme activity in extracts from pNEBR-R1/pNEBR-X1Hygro+*NUDT2* transfected cells grown in increasing concentrations of the inducer ligand RSL1. Whole cell extracts were prepared using a non-denaturing protein extraction buffer and enzyme activity was determined by addition of a portion of the extract to an excess of $Ap_4A$ substrate. The activity was measured by the rate of formation of ATP (a product of the reaction) as detected by a luminometric assay (pg. 56). All values show the activity relative to that detected in wild-type AA8 cell extracts.

To determine the extent to which this level of NUDT2 over-expression is capable of reducing or eliminating intracellular $Ap_4A$, the basal level of $Ap_4A$ was measured in both the wild-type cell line and the fully induced transfected cell line. Even at the maximum level of NUDT2 expression, a low background level of $Ap_4A$ was found to persist in transfected cells (Table 5.5), although this is possibly due to a compartmentalised pool of $Ap_4A$, inaccessible to the enzyme and unlikely to be related to the possible role of $Ap_4A$ in the nucleus. Indeed, synthesis of $Ap_4A$ by mitochondrial enzymes has previously been reported (Krauspe *et al.*, 1988), and given its widespread presence, it is likely that a pool of $Ap_4A$ exists within these organelles.

In order for the transfected cell line to be useful in establishing a role for $Ap_4A$ in DNA repair, it must be able to resist the increase in $Ap_4A$ that usually occurs in response to DNA damage. Therefore, it was important to examine the ability of the transfected cell line to maintain a low level of $Ap_4A$ under conditions which normally cause it to increase. As found previously (Table 3.2, pg. 66), in wild-type AA8 cells, the level of $Ap_4A$ is increased 2.1-fold following a 4 hour treatment with ethyl methanesulphonate (EMS). Upon examination of the level of $Ap_4A$ in the transfected cell line following the same EMS treatment, there was no increase (Table 5.5), indicating that the over-expression of $Ap_4A$ hydrolase was sufficient to prevent this from occurring. To assess the ability of the transfected cell line to resist a much larger increase in the level of $Ap_4A$, both cell lines were treated with a combination of EMS and araC, which was previously found to significantly increase the level of $Ap_4A$ in wild-type cells up to 13-fold higher than the basal level. In the transfected cell line, a small increase in $Ap_4A$ was observed, although the maximum level remained low and was comparable to the basal level of wild-type cells (Table 5.5, Fig. 5.12).

**Table 5.5** $Ap_4A$ levels in wild-type AA8 cells and in transfected AA8 cells over-expressing human *NUDT2*. Both cell lines were treated for 4 hours with 200 mM ethyl methanesulphonate (EMS) in the presence and absence of 200 μM cytosine arabinoside (araC), and then intracellular $Ap_4A$ was immediately extracted and assayed. Each value is the mean ± S.E.M. of independent triplicate determinations. P values were calculated using a paired t-test and represent the statistical significance of the observed difference between the level of $Ap_4A$ in cells after the treatment indicated and that in untreated cells.

| Cell line | Treatment | $Ap_4A$ (pmol/$10^6$ cells) | Fold difference to untreated cells | P value |
|---|---|---|---|---|
| AA8 | None | 0.69 ± 0.07 | - | - |
| | EMS | 1.42 ± 0.22 | 2.1 | 0.036 |
| | EMS + araC | 9.23 ± 1.24 | 13.4 | 0.0023 |
| AA8 (transfected) | None | 0.22 ± 0.04 | - | - |
| | EMS | 0.21 ± 0.07 | 0.95 | 0.97 |
| | EMS + araC | 0.84 ± 0.19 | 3.8 | 0.03 |

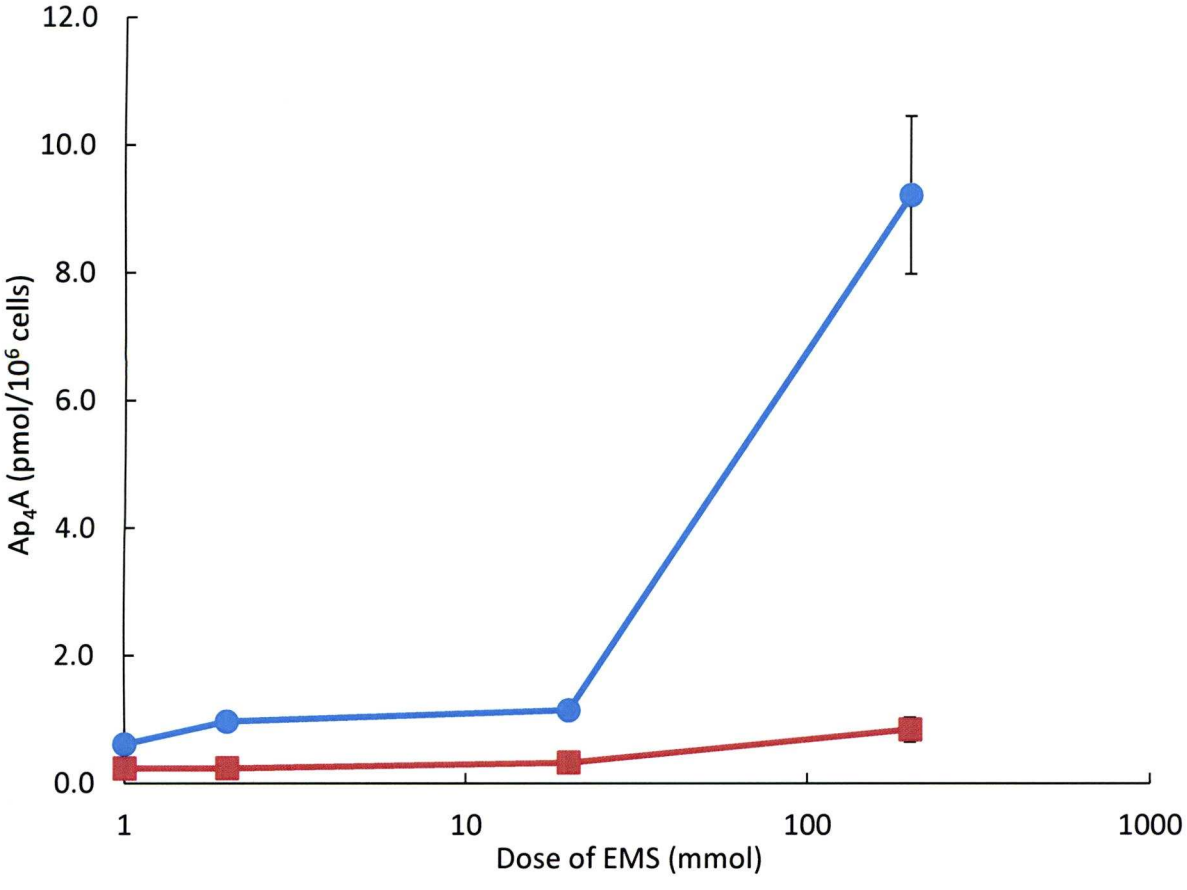


**Figure 5.12** Increase in $Ap_4A$ levels of wild-type AA8 cells (blue circles) and transfected AA8 cells over-expressing human *NUDT2* cDNA (red squares) in response to treatment with increasing doses of EMS in combination with 200 μM araC. Cells were treated for 4 h and then intracellular $Ap_4A$ was immediately extracted and assayed. The data represents the mean of three independent determinations and the error bars represent the standard error of the mean (S.E.M.). Some error bars are smaller than the marker size and are therefore not visible in the figure.

Based on the information gathered about the newly engineered cell line, it appears that the intracellular level of NUDT2 activity can be increased by up to 40 times the normal level and this results in both a low background level of $Ap_4A$, and a substantial reduction in the usual DNA damage-induced increase. Therefore, this cell line has the potential to be an extremely useful tool to examine what effects the lack of $Ap_4A$ has on various aspects of the DNA damage response, and therefore to provide an insight into a possible role for $Ap_4A$ in this.

### 5.2.3 $Ap_4A$-deficient cells are more sensitive to EMS than wild-type cells

Following the successful establishment of a cell line deficient in $Ap_4A$ through the over-expression of *NUDT2*, it was decided to use these cells for some preliminary investigations as to what effects this may have on the DNA damage response. Previous evidence suggests a possible role for $Ap_4A$ in the SSBR and BER pathways, and the level of $Ap_4A$ normally increases following treatment with agents which induce the type of damage repaired by these pathways, such as EMS and MMS. In addition, the level of $Ap_4A$ is substantially elevated in XRCC1-deficient cells, which are defective in the SSBR and BER processes. To determine if this DNA damage-related increase in $Ap_4A$ may have a function in the cell, it was decided to firstly examine the ability of $Ap_4A$-deficient cells to survive following treatment with EMS.

Both wild-type AA8 cells and the transfected cells deficient in $Ap_4A$ through *NUDT2* over-expression were treated with increasing concentrations of EMS and the proportion of surviving cells was measured by their ability to form colonies. The data showed a clear difference between the two cell lines (Fig. 5.13), with the $Ap_4A$ deficient cell line showing a much higher sensitivity to EMS than the wild-type cell line. Comparison of the two $D_{37}$ values (Table 5.6) indicates that the cells lacking $Ap_4A$ have a 3.4-fold higher sensitivity to EMS than those with a normal level of $Ap_4A$. This very interesting finding provides the strongest suggestion yet that $Ap_4A$ may be functionally involved in the DNA damage response and/or DNA repair processes. Clearly, further work is required to confirm these findings and to substantiate them by examining the response of $Ap_4A$-deficient cells to various other DNA damaging agents and by probing the exact mechanism by which the lack of $Ap_4A$ contributes to the increased sensitivity of the cells to EMS.

**Table 5.6** Sensitivity to EMS of wild-type AA8 cells and transfected AA8 cells deficient in $Ap_4A$ due to the over-expression of human *NUDT2* cDNA. Sensitivity is presented as $D_{37}$ values (concentration of EMS required to produce 37% survival) and fold sensitivity is in relation to the wild type cell line AA8.

| Cell line | $D_{37}$ value (mM EMS) | Fold sensitivity |
|---|---|---|
| AA8 | 18.0 | - |
| AA8 transfected | 5.27 | 3.4 |

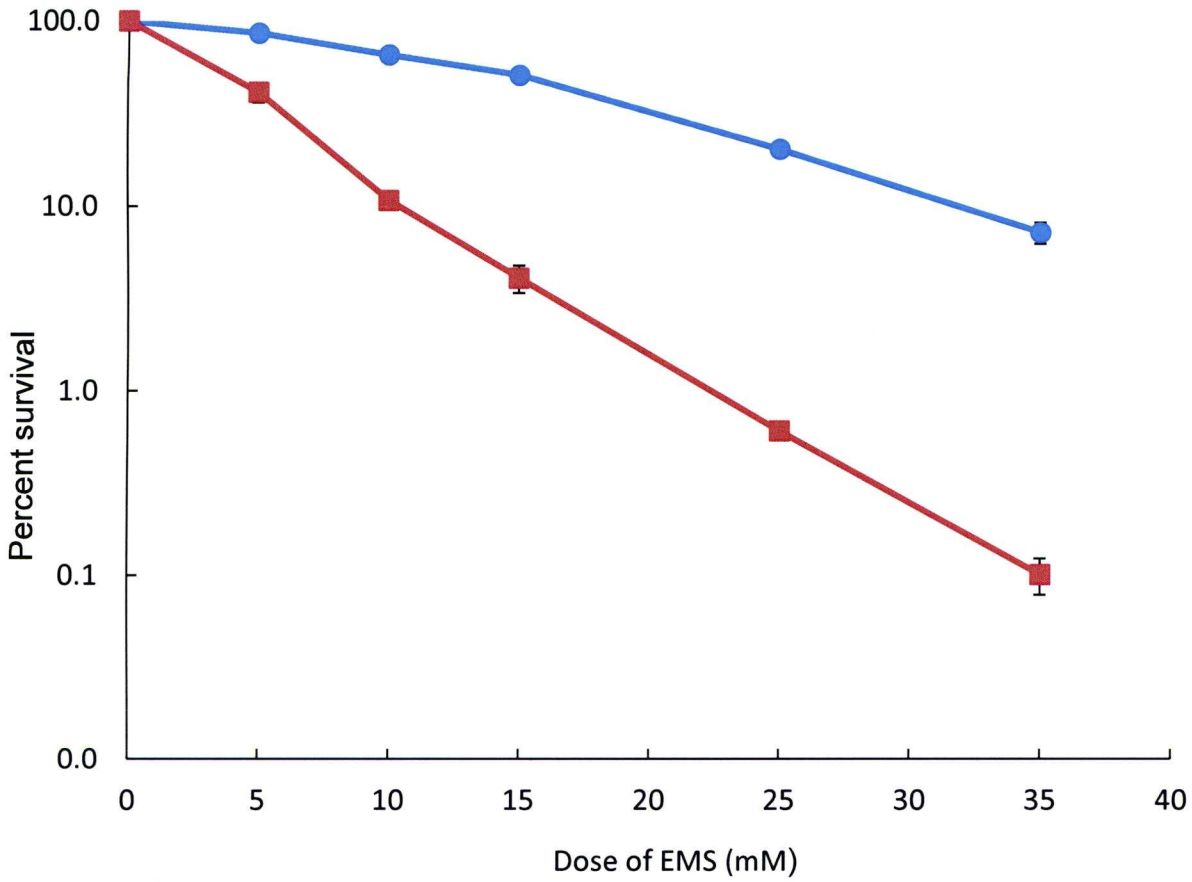


**Figure 5.13** Survival responses of wild-type AA8 cells (blue circles) and transfected cells deficient in $Ap_4A$ due to the over-expression human *NUDT2* cDNA (red squares) after treatment with increasing doses of EMS. At least 200 cells were plated out in each dish and allowed to attach for 4 h, after which the medium was removed and attached cells were washed once with HBSS. Cells were then treated with EMS for 1 h in 10 mL serum free medium, which was then removed and replaced with normal medium. Dishes were incubated for 10 days, after which the colonies were counted and used to calculate the proportion of surviving cells compared to untreated controls. At least three replicates were used for each dose and each data point represents the means of 3 independent experiments. The error bars represent the standard error of the mean (S.E.M.). Some error bars are smaller than the marker size and are therefore not visible in the figure.

### 5.2.4 Production of $Ap_4A$-deficient *XRCC1* mutant EM9 cells

It was previously found that cells lacking the DNA repair protein XRCC1 have a substantially increased level of intracellular $Ap_4A$ in comparison to wild-type cells. These cells have a number of distinctive phenotypic characteristics, including a hypersensitivity to DNA alkylating agents, a reduced ability to repair DNA strand breaks and a high background level of sister chromatid exchanges (Thompson *et al.*, 1982). An interesting possibility is that some of the cellular phenotypes of XRCC1-deficient cells might actually be partially caused by the increased level of $Ap_4A$, rather than directly caused by the lack of XRCC1. To investigate this, it was decided to also produce a strain of the XRCC1-deficient cell line EM9 in which over-expression of *NUDT2* can be induced and controlled, in order to eliminate intracellular $Ap_4A$, or to reduce it back to the level occurring in wild-type cells.

As described above for AA8, EM9 cells were transfected with the pNEBR-R1 regulatory plasmid and successfully transfected cells were selected by resistance to G418. The transfection efficiency was 27.3%, and following transfection, cells were subsequently plated out to form a series of single cell-derived clones. These were then examined for the level of luciferase reporter gene expression both before and after the addition of RSL1. Based on this data, one clone was chosen for transfection with the pNEBR-X1Hygro expression vector plasmid containing the *NUDT2* cDNA sequence. Following transfection, cells were selected by their resistance to hygromycin and plated out to form single cell derived clones. Unfortunately, examination of the basal level of $Ap_4A$ in these cells found that it remained high in each case, even at the maximum induction of *NUDT2* expression by RSL1. Since the maximum level of *NUDT2* over-expression is insufficient to reduce $Ap_4A$ to levels to levels comparable with wild-type cells, it appears that these cells are not useful for the further experimental work that was planned.

### 5.2.5 Increasing intracellular $Ap_4A$ by expression of firefly luciferase *in vivo*

In addition to investigating the possible effects that a lack of $Ap_4A$ might have on the DNA damage response, it would also be useful to investigate the reverse situation and examine the possible effects caused by an increase in the level of intracellular $Ap_4A$. To achieve this, it was decided to use a system based on the expression of firefly luciferase, which has previously been reported to synthesise $Ap_4A$ *in vitro* in the presence of its D-luciferin substrate (Guranowski *et al.*, 1990). The mechanism involves D-luciferin acting as an adenylate acceptor from ATP, forming luciferyl-AMP which is then converted to dehydroluciferyl-AMP. The AMP moiety is subsequently transferred to another molecule of ATP, thus producing $Ap_4A$ (Fontes *et al.*, 1998). More recently, it has been reported that firefly luciferase also produces $Ap_4A$ *in vivo*, subject to the presence of the substrate D-luciferin in the cells' growth medium. Over-expression of luciferase produces a very high level of intracellular $Ap_4A$ in COS-7 cells, and this can be controlled by altering the level of D-luciferin in the cells growth medium (Murphy & McLennan, 2004). Over-expression of luciferase is generally considered non-toxic, and it is widely used as a reporter gene, partly due to the lack of significant biochemical and physical side effects on transfected cells. It was therefore decided to exploit this system by over-expressing firefly luciferase in AA8 cells, in order to increase $Ap_4A$ and provide a direct comparison between the other AA8-derived cell lines available.

The wild-type CHO cell line AA8 was transiently transfected with the pGL3luc plasmid (Fig. 5.14), which encodes the firefly luciferase enzyme under the control of an SV40 promoter and enhancer sequences which results in a constitutively high level of luciferase expression. D-luciferin was added to the cells' growth medium 24 h after transfection and cells were extracted and analysed for $Ap_4A$ after a further 24 h. The level of $Ap_4A$ was found to be

increased substantially in cells transfected with pGL3luc and grown in the presence of D-luciferin compared to untransfected cells (Table 5.7). Although it is not possible to produce a cell line stably transfected with pGL3luc due to the lack of a eukaryotic selectable marker, this is still likely to be a useful tool to examine the possible effects of excess $Ap_4A$ on the DNA damage response response since it can be transiently applied to any cell line. If ADP-ribosylated $Ap_4A$ is found to be the functional form of $Ap_4A$ *in vivo*, another possible application for this technique could be as a negative control in order to increase unmodified $Ap_4A$ to confirm that it did not carry out the same function. Unfortunately pGL3luc transfection was not used further in the present study although the procedure established here has many potential applications in future work.

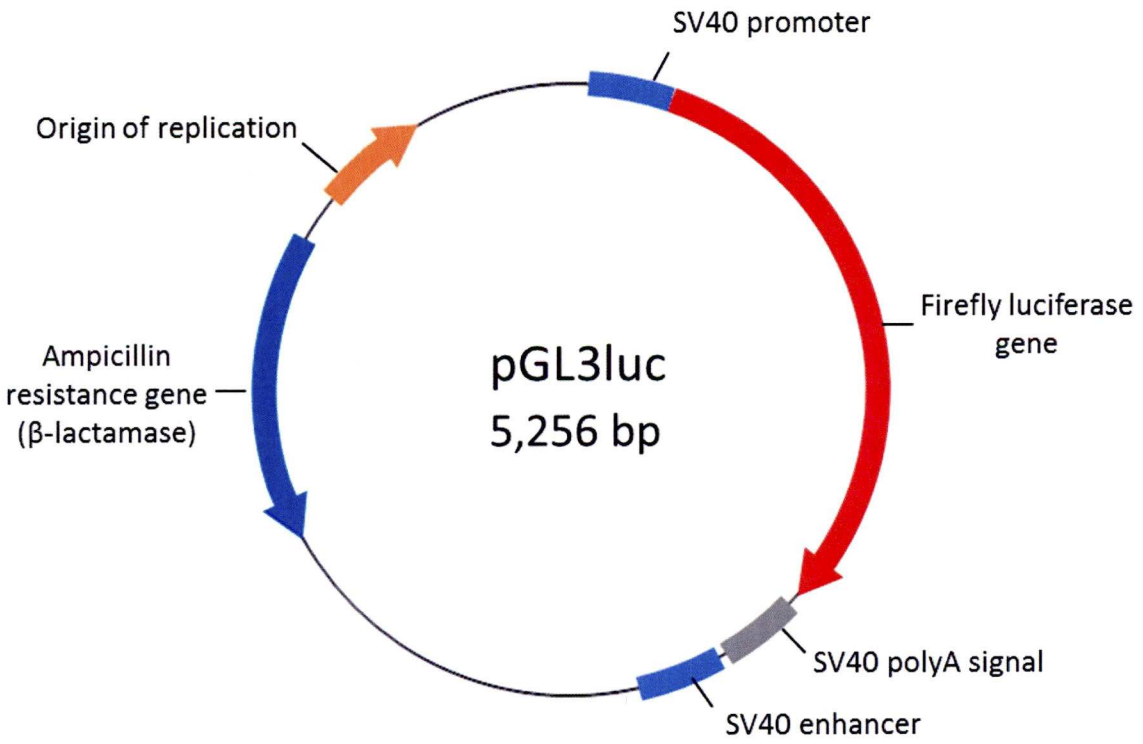


**Figure 5.14** pGL3luc plasmid map. This plasmid expresses the firefly luciferase gene under the control of the constitutive SV40 promotor and enhancer sequences. The diagram is based on the plasmid map and sequence information provided by the manufacturer.

**Table 5.7** $Ap_4A$ levels in wild-type AA8 cells and in AA8 cells transfected with the pGL3luc plasmid which constitutively expresses firefly luciferase. Cells were transfected with pGL3luc and after 24 h, D-luciferin was added to the medium to a final concentration of 0.5 mM. Cell monolayers were extracted for analysis after a further 24 h and the level of $Ap_4A$ was determined using a specific luminometric assay. Each value is the mean ± S.E.M. with the number of independent determinations (*n*) in barckets.

| Cell line | $Ap_4A$ (pmol/$10^6$ cells) | Fold difference |
|---|---|---|
| AA8 | 0.71 ± 0.14 (*n*=3) | - |
| AA8 pGL3luc | 22.1 ± 12.3 (*n*=4) | 31.1 |

## 5.3 Discussion

The work carried out here has produced and characterised a number of cell lines and expression systems that are likely to be valuable tools for further investigation into the role of $Ap_4A$ in the DNA damage response. The establishment of a stably transfected cell line which can be induced to significantly over-express the *NUDT2* $Ap_4A$ hydrolase enzyme has produced the first cells in which the level of $Ap_4A$ can be reduced *in vivo*, and which resist the normal increases in $Ap_4A$ following DNA damage. This provides a new opportunity to directly examine the phenotype of $Ap_4A$-deficient cells, in particular how this affects their ability to respond normally to DNA damage. The fact that the $Ap_4A$ deficient cell line has been derived from the wild-type CHO strain AA8 allows a direct comparison not only with wild-type cells, but also other AA8-derived mutants including the *XRCC1*-deficient strain EM9, which is also proving to be very important in investigating the possible role of $Ap_4A$. The establishment of an *in vivo* over-expression system for firefly luciferase in the same cell line further enhances the tools available for further work and allows investigation into the effects of increased $Ap_4A$ produced through a generally non-toxic and otherwise non-interfering system. Unfortunately, due to time constraints, the information gathered so far with these cell lines has been limited, however some interesting observations have been made.

The finding that cells deficient in $Ap_4A$ due to the over-expression of *NUDT2* have an increased sensitivity to the alkylating agent EMS is possibly the most important piece of information reported so far regarding the possible role of $Ap_4A$ in the DNA damage response. Although the possibility exists that the increased EMS sensitivity is caused by some other unintended effect of *NUDT2* over-expression, this seems unlikely given the specificity of the enzyme for dinucleotides such as $Ap_4A$. The level of EMS sensitivity found here for wild-

type AA8 cells is comparable to the level of sensitivity previously reported for the same cell line (Thompson *et al.*, 1982). The 3.4-fold increased EMS sensitivity of $Ap_4A$-deficient cells indicates that a lack of $Ap_4A$ has a significant negative impact on the ability of the cells to survive the induced DNA damage and therefore provides a strong suggestion of a functional involvement in the DNA damage response. However, it is important to note that the increased EMS sensitivity of $Ap_4A$-deficient cells is much lower than that of XRCC1-deficient cells such as EM9 (21-fold increased sensitivity), as would be expected given the core importance of XRCC1 to the BER and SSBR processes.

Following on from the findings reported here, the cellular tools produced provide an excellent opportunity to further probe the exact details of $Ap_4A$ involvement in the DNA damage response. The additional evidence supporting a role for $Ap_4A$ in this response makes it more important that the exact nature and mechanism of this be determined.

# CHAPTER 6

## Discussion

The aim of this project was to investigate the possible role of $Ap_4A$ in the DNA damage response. Although various pieces of existing evidence had suggested that $Ap_4A$ might have an involvement in signalling the inhibition of DNA replication in response to damage, this had never been investigated in detail until now. This project was intended to examine what function $Ap_4A$ might have in the DNA damage response and to probe the exact molecular details of that function.

The increase in $Ap_4A$ detected in response to EMS treatment is comparable to those increases previously reported in various other cell lines following treatment with similar agents, and supports the existing theory that $Ap_4A$ is increased specifically in response to DNA strand breaks (Baker & Ames, 1988). This is further supported by the much larger accumulation of $Ap_4A$ when araC was also present, which is known to result in an accumulation of DNA strand breaks (Hiss & Preston, 1977; Dunn & Regan, 1979). The data here are also consistent with the observations made by Gilson *et al.*, 1988, who showed that $Ap_4A$ accumulation was more pronounced when cells were incubated with the PARP-1 inhibitor 3-AB and that $Ap_4A$ persisted throughout the incubation period. Since the inhibition of PARP-1 would prevent the repair of SSBs, it would be expected that breaks would accumulate, therefore accounting for the $Ap_4A$ levels observed.

The increased $Ap_4A$ detected where Lig3α was prevented from binding to its normal DNA substrate *in vivo* by the ligase inhibitor L67 is also consistent with previous findings that

Lig3α synthesises $Ap_4A$ *in vitro* and that this is specifically inhibited by the presence of DNA (McLennan, 2000). Therefore, this supports the original hypothesis that Lig3α produces $Ap_4A$ *in vivo* as a result of its inability to bind its normal DNA substrate. This is likely to occur in the early stages of SSB repair since Lig3α would be prevented from binding the break immediately due to the transient binding of PARP-1 (Caldecott *et al.*, 1996). Although the primary function of Lig3α in ligating DNA single strand breaks is already well characterised, it is certainly not an unrealistic scenario that it may also synthesise $Ap_4A$ as a secondary function under certain conditions. Indeed, this has already been reported to be the case for LysRS, which primarily functions as an aminoacyl-tRNA synthetase, but also appears to also have a secondary function to produce $Ap_4A$ in immune system mast cells in response to FcεRI-mediated aggregation of these cells (Yannay-Cohen *et al.*, 2009). To confirm that DNA damage-induced $Ap_4A$ synthesis is primarily carried out by Lig3α, it would be important to examine DNA damage-related $Ap_4A$ accumulation in Lig3α deficient cells. If this did not occur normally, it would provide a very strong indication that this function was indeed carried out by Lig3α. Unfortunately such cells were unavailable during the present study, but have very recently been produced (K. W. Caldecott, personal communication).

Another key observation made in the present study is the apparent detection of ADP-ribosylated $Ap_4A$ accumulating in cells following DNA damage. ADP-ribosylation of proteins is already known to be an important feature of SSBR and is primarily carried out by PARP-1 (de Murcia *et al.*, 1994). Although the synthesis of ADP-ribosylated $Ap_4A$ has previously been reported *in vitro* (Yoshihara & Tanaka, 1981), until now there has been no evidence that it also occurs *in vivo*. The modified $Ap_4A$ detected here by HPLC of cell extracts was found to co-elute with ADP-ribosylated $Ap_4A$ synthesised *in vitro*, and treatment

of extracts with PARG appeared to convert this back to unmodified $Ap_4A$. Taken together, these observations provide a fairly strong indication that a substantial proportion of the increased $Ap_4A$ produced in response to DNA damage is modified by ADP-ribosylation. Since ADP-ribosylated $Ap_4A$ is an effective inhibitor of SV40 DNA replication *in vitro* (Baker *et al.*, 1987), this is consistent with its proposed function to stall DNA replication *in vivo*. It is also relevant that PARP-1 appears to be required for replication fork slowing in wild-type DT40 chicken cells in response to DNA damage (Sugimura *et al.*, 2008). Assuming that ADP-ribosylated $Ap_4A$ contributes to replication fork slowing, this is what would be expected since the lack of PARP-1 would likely prevent $Ap_4A$ from becoming ADP-ribosylated and therefore from carrying out its function. In order to confirm the identity of the modified $Ap_4A$, mass spectrometry should be carried out on at least partially purified cell extracts enriched for this material, which will provide definitive information that it is indeed ADP-ribosylated. In addition, it would also be very useful to examine whether or not this material accumulates in PARP-1 knockout cell lines or after the siRNA knockdown of various PARP family enzymes and/or mono-ADP ribosylases. These studies could provide further evidence supporting its identity as ADP-ribosylated $Ap_4A$ and the mechanism of its synthesis.

Taking into account the findings made in the present study, an updated model for the possible role of $Ap_4A$ in the DNA damage response is presented in Fig. 6.1. Overall, the original hypothesis remains valid, although there may be other factors involved that were not previously considered. For example, despite the low level of $Ap_4A$ hydrolase activity that APTX appears to have *in vitro*, the fact that a substantially elevated level of $Ap_4A$ was detected in APTX-deficient cells suggests it may also play some part in the regulation of

$Ap_4A$ levels. On the other hand, this could simply be an indirect effect caused by accumulation of SSBs in these cells due to defective SSBR in the absence of APTX.

A further key finding from the present study is that the basal level of $Ap_4A$ is increased by up to 16-fold in XRCC1-deficient cells. This is consistent with the theory that Lig3α produces $Ap_4A$ where it is unable to bind to DNA, since XRCC1 is required to target Lig3α to its sites of activity on DNA (Cappelli *et al.*, 1997). In addition, the model discussed above for the possible role of $Ap_4A$ is also supported by other observations made previously in XRCC1-deficient cells which would be consistent with the elevated level of $Ap_4A$/ADP-ribosylated $Ap_4A$ and its proposed function. Characterisation of the XRCC1-deficient CHO strain EM9 has previously shown that they show a delayed progression through S-phase, with a cell cycle that is 33% longer than in the parental strain AA8 (Kubota & Horiuchi, 2003). Furthermore, they show a reduced rate of initiation of DNA replication, even in the absence of DNA damaging agents (Thompson *et al.*, 1990). Given the substantially elevated $Ap_4A$ levels detected in EM9 cells and the apparent detection of ADP-ribosylated $Ap_4A$, these observations are consistent with a hypothesis that $Ap_4A$ and/or its ADP-ribosylated derivatives do have a role in slowing S-phase progression. This also presents a particularly interesting possibility that some of the other characteristic phenotypes of EM9 and other XRCC1-deficient cells may not be directly caused by the lack of XRCC1 *per se*, but rather the accompanying increase in the level of intracellular $Ap_4A$. These phenotypes include a 10-fold increase in the level of sister chromatid exchanges, defects in repairing SSBs and a hypersensitivity to the monofunctional alkylating agents EMS and MMS (Thompson *et al.*, 1982).

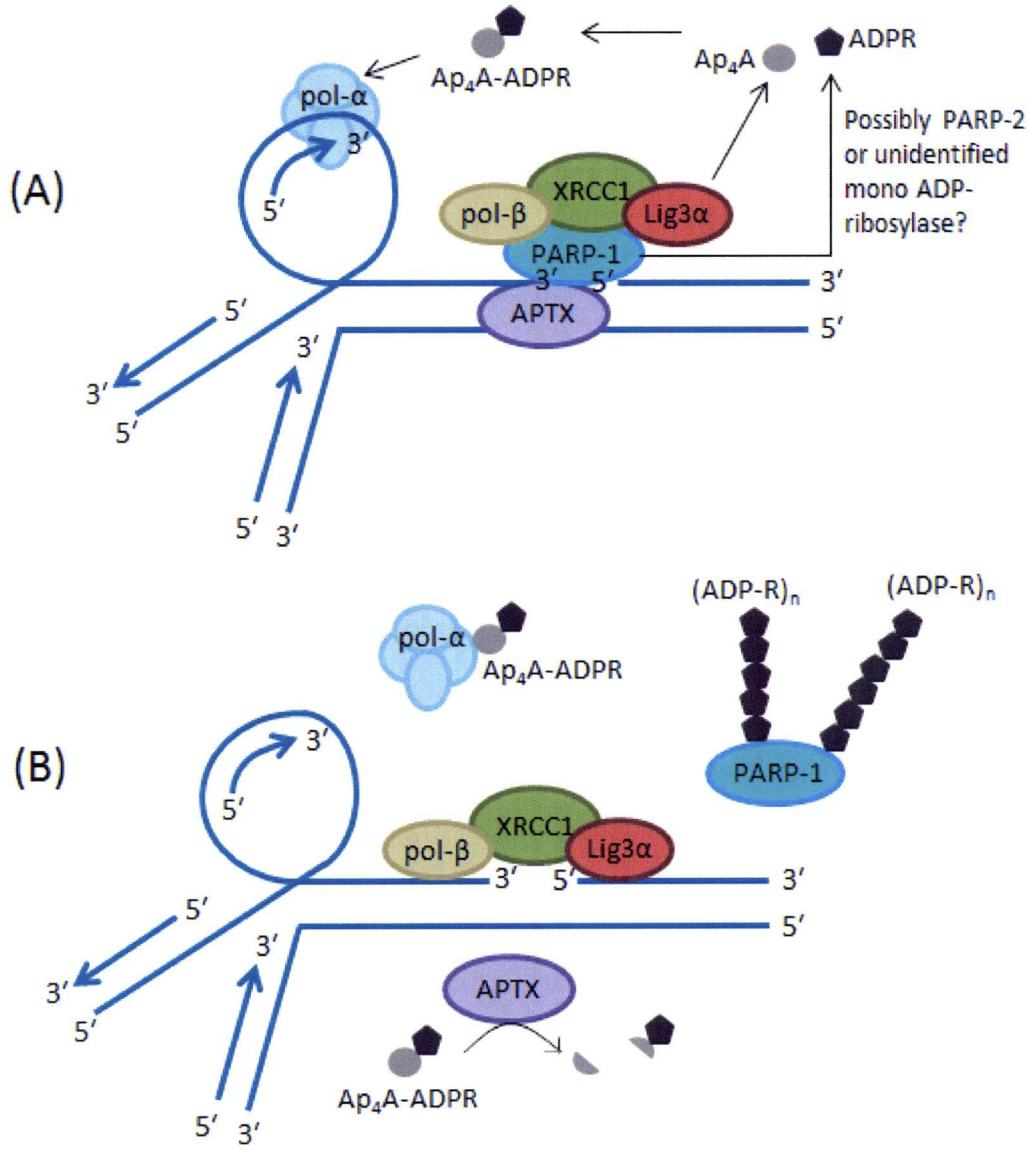


**Figure 6.1** Updated model for $Ap_4A$ involvement in intra-S phase checkpoint control. (A) Poly(ADP ribose) polymerase 1 (PARP-1) binds to a SSB generated ahead of a replication fork and forms a complex with DNA polymerase-β (pol-β), XRCC1 and DNA ligase III (Lig3α), as well as other DNA end-processing enzymes including aprataxin (APTX). Unable to bind DNA immediately, Lig3α synthesises $Ap_4A$, which is then mono-ADP-ribosylated, either by PARP-1 or by another protein such as PARP-2 which is recruited during the later stages of SSB repair. The mono-ADP-ribosylated $Ap_4A$ then binds to the $Ap_4A$-binding site on the pol-α-associated protein and inhibits it, possibly by reducing its interaction with DNA. ADP-ribosylated $Ap_4A$ also diffuses throughout the nucleus and inhibits other replication forks in the same way. (B) Auto-poly(ADP-ribosylation) of PARP-1 reduces its affinity for DNA and allows pol-β and Lig3α to bind to the DNA and carry out the repair process. Following repair, APTX may hydrolyse the excess $Ap_4A$ thus allowing DNA replication to continue. Diagram and model adapted and updated from McLennan, 2000.

The mechanism by which $Ap_4A$ and/or ADP-ribosylated $Ap_4A$ may contribute to replication fork stalling is not yet clear, although it still remains a likely possibility that it acts through the pol-α binding protein that has previously been shown to bind $Ap_4A$ (Grummt *et al.*, 1979; Baril *et al.*, 1983; Rapaport & Feldman, 1984; Baxi *et al.*, 1994). The identity of this protein remains unknown but it is notable that its two subunits appear to be of similar sizes to two of the known isoforms of APTX (Moreira *et al.*, 2001). While it seems an unlikely scenario, it is interesting to speculate that APTX may actually be this pol-α associated $Ap_4A$ binding protein. If this were the case, $Ap_4A$ may bind to pol-α associated APTX, causing dissociation of the polymerase from DNA and therefore the stalling of DNA replication. Such a situation would be reminiscent of the role of $Ap_4A$ in binding to Hint-1 and disrupting its protein-protein interaction with the transcription factor MITF (Lee *et al.*, 2004). Both Hint-1 and APTX are related HIT superfamily proteins and share considerable sequence homology in their HIT domains (Brenner, 2002). In this model, APTX could also subsequently hydrolyse $Ap_4A$ (Kijas *et al.*, 2004), causing a decrease in its levels and thus allowing subsequent re-starting of DNA replication following damage repair.

Aside from the potential mode of action through pol-α, there are alternative possibilities for the mechanism by which $Ap_4A$ may induce the delay of S-phase progression which could also be considered. DNA replication begins only at defined sites of initiation, called origins of replication. These are not all activated simultaneously and the primary means for slowing down DNA replication during S-phase is by inhibiting late firing origins of replication (Tercero & Diffley, 2001). The two primary checkpoint-specific DNA damage sensing proteins are ataxia telangiectasia mutated (ATM) and ATM and Rad3-related (ATR), both members of the phosphatidyl inositol 3-kinase-like kinase (PIKK) family of protein kinases (Savitsky *et al.*, 1995; Cimprich *et al.*, 1996). These proteins recognise various types of DNA

damage which activates them to phosphorylate target proteins and induce multiple signalling pathways. ATM and ATR phosphorylate the Chk2 and Chk1 proteins respectively (Zhou *et al.*, 2000; Guo *et al.*, 2000), which in turn phosphorylate the transcription factor p53, thus blocking its binding to MDM2 which normally targets it for degradation (Shieh *et al.*, 2000; Hirao *et al.*, 2000). The increased levels of p53 activate transcription of p21 which then inhibits Cdk2/cyclin E. Cdk2 has an important role in phosphorylating the pre-replication complex (pre-RC), which facilitates loading of the replicative helicase cofactor Cdc45 onto the origin of replication, thus activating it (Liu *et al.*, 2006). Inhibition of Cdk2 therefore prevents the initiation of replication. Activated Chk1 can also phosphorylate Cdc25A which leads to its ubiquitination and subsequent degradation. The result of this is that Cdc25A is no longer able to carry out its usual function, which is to dephosphorylate Cdk2, thus activating the Cdk2/cyclin E or Cdk2/cyclin A complexes, which are required for the G1/S transition and S-phase progression respectively (Zhao *et al.*, 2002). Although these mechanisms primarily act to slow DNA replication by preventing initiation of late firing origins, it has also been found that active replication fork progression can be slowed down in response to DNA damage (Seiler *et al.*, 2007; Unsal-Kacmaz *et al.*, 2007). The mechanism by which this occurs is less well understood although it is notable that a requirement for Chk1 in maintaining normal replication fork progression has been reported (Petermann *et al.*, 2006).

Since $Ap_4A$ has been reported to inhibit various protein kinases (Levy *et al.*, 1983) this raises the interesting possibility that this function may be employed as part of a mechanism to slow down S-phase progression in response to DNA damage. For example, since Chk1 is required for normal replication fork progression and fork slowing occurs in its absence (Petermann *et al.*, 2006), this could be a potential target for $Ap_4A$ as a kinase inhibitor. Similarly, a number of other proteins involved in the complex DNA damage checkpoint signalling cascade

discussed above could also be potential targets for $Ap_4A$ to inhibit specific phosphorylation events in order to slow S-phase progression, either by preventing the initiation of late firing origins or by slowing fork progression. Such a role for $Ap_4A$ would be a novel aspect of the intra S-phase checkpoint to slow DNA replication in response to DNA damage.

Although some of the checkpoint pathways for the inhibition of DNA replication are already fairly well characterised, this does not rule out a role for $Ap_4A$. Given the importance of maintaining the fidelity of DNA replication and control of cell division, it is not uncommon for there to be multiple mechanisms of carrying out the same function in order to provide a failsafe system. This is also seen in a number of other places such as the multiple mechanisms for preventing more than one initiation of each replication origin in a single cell cycle (DePamphilis *et al.*, 2006).

Possibly the clearest indication of a functional involvement for $Ap_4A$ in the DNA damage response is the finding that $Ap_4A$-deficient cells generated by inducible overexpression of NUDT2 $Ap_4A$ hydrolase were more sensitive to EMS than wild-type cells. This provides the first evidence of a direct importance for $Ap_4A$ in surviving DNA damage. It is unfortunate that time constraints prevented further work on the cell line within the project, since it is likely to be a valuable tool for examining the exact function of $Ap_4A$ and probing the molecular details of this. One technique that is likely to be particularly informative is the replication fork progression assay (used in Henry-Mowatt *et al.*, 2003; Petermann *et al.*, 2006). This involves pulse labelling active replication forks for 20 minutes with bromodeoxyuridine (BrdU), which is incorporated into the length of DNA strands synthesised during that time. Following this treatment, the cells are washed to remove unincorporated BrdU and the replication forks are pulse labelled with iododeoxyuridine (IdU)

for a further 20 minutes while simultaneously subjected to a DNA damaging agent. The cells are then fixed on a slide and both BrdU and IdU are detected by different labelled antibodies. For a number of different replication forks, the length of BrdU-incorporated DNA is measured and used to calculate the fork progression rate during the initial 20 minutes before DNA damage was induced. The length of DNA with IdU incorporated is also measured for each fork and used to calculate the fork progression rate for the 20 minutes following DNA damage induction. These two values are then compared to assess what effect the DNA damage has on fork progression rate. If the $Ap_4A$-deficient cell line shows a reduced ability to slow down replication fork progression in response to DNA SSBs, this would indicate an involvement for $Ap_4A$ in the process.

The possible role of $Ap_4A$ proposed here to slow S-phase progression in response the detection of DNA damage is not incompatible with other suggested roles, such as an inducer of apoptosis under certain conditions. It is certainly conceivable that increased intracellular $Ap_4A$ may have quite different effects depending on the magnitude of the increase. Where there are relatively low levels of DNA damage, a moderate increase in the level of $Ap_4A$ occurs, such as the 2.1-fold increase reported here following EMS treatment, which may act to stall DNA replication to allow time for repair. However, it is clear that much larger increases in $Ap_4A$ can also occur such as the 13-fold increase following treatment with EMS and araC which presumably results in a very high level of strand breaks. Such a large or persistent accumulation of $Ap_4A$ in the cell could have the different effect of inducing apoptosis (Vartanian *et al.*, 1999). Therefore $Ap_4A$ may act as an important signalling molecule integrating both DNA checkpoint control and apoptosis. Such a role would in some ways be analogous to that of the well-known tumour suppressor gene p53, which has a

function in signalling pathways to induce cell cycle arrest or to initiate apoptosis dependent on various factors.

The proposed role of $Ap_4A$ as a signalling molecule in the DNA damage response is also not incompatible with its reported role as an activator of transcription under certain other conditions. It has already been suggested that the accumulation of $Ap_4A$ produced in response to different stimuli could arise from difference sources based on the differing dynamics of accumulation over time (Gilson *et al.*, 1988) and the fact that $Ap_4A$ is known to be synthesised by a wide range of different enzymes. The $Ap_4A$ produced during mast cell activation appears to be produced by LysRS (Yannay-Cohen *et al.*, 2009) and is believed to activate MITF-dependent transcription of various genes by binding to the repressor protein Hint-1 (Lee *et al.*, 2004). However, the activation of transcription appears to require a very high concentration of $Ap_4A$ and importantly, LysRS directly binds to its target protein complex to synthesise this $Ap_4A$ (Lee *et al.*, 2004). This is likely to produce very high levels of $Ap_4A$ in the vicinity of these molecules, which may be required for its effect on Hint-1. There is no indication that LysRS is activated in response to DNA damage and it seems far more plausible that Lig3α is responsible for $Ap_4A$ accumulation in this case. As part of a different protein complex, this could have an entirely different effect. Indeed, the XRCC1-Lig3α complex directly interacts with PARP-1, which may be important for the ADP-ribosylation of $Ap_4A$ and therefore its proposed function in replication fork stalling.

An interesting additional possibility for the function of $Ap_4A$ could be to act as an 'adenylate sink' to allow the re-generation of free Lig3α from Lig3α-AMP. The majority of cellular Lig3α is thought to exist as Lig3-AMP and this is the form that is required for ligation of conventional single strand nicks. However, non-adenylated Lig3 may specifically be required

to join prematurely 5' adenylated ends that have been found to occur during the attempted ligation of non-conventional DNA ends (Reynolds *et al.*, 2009). If this were the case, ATP would be a better AMP acceptor from Lig3α-AMP than $PP_i$ because of its much higher intracellular concentration, thus resulting in the production of $Ap_4A$. This proposed function for free Lig3α would complement that of APTX, which is already known to de-adenylate AMP-linked 5' ends to produce a conventional terminus which is a substrate for Lig3α-AMP (Ahel *et al.*, 2006). In XRCC1-deficient cells, the increased level of $Ap_4A$ could be due to the uncoupling of Lig3 from its multiprotein repair complex and DNA which may lead to rapid turnover of Lig3-AMP. This additional potential function for $Ap_4A$ does not preclude the other functions discussed above.

In summary, this study has made a significant contribution to our understanding of the role of intracellular $Ap_4A$ and has gathered considerable evidence supporting its involvement in the DNA damage response. Although significant progress has been made in elucidating the exact role of $Ap_4A$, there are still aspects of this that remain unclear. This project has opened up an interesting new area of study and has provided new insights into the possible role for $Ap_4A$ in cell signalling that has so far remained unknown. It is clear that there are many interesting possibilities for future investigation in this area and that the findings will add to our already detailed molecular understanding of an essential biological process, the DNA damage response.

# REFERENCES


Ahel, I., Rass, U., El-Khamisy, S.F., Katyal, S., Clements, P.M., McKinnon, P.J., Caldecott, K.W., West, S.C. (2006) The neurodegenerative disease protein aprataxin resolves abortive DNA ligation intermediates. *Nature* **443**, 713-716.

Amé, J.C., Rolli, V., Schreiber, V., Niedergang, C., Apiou, F., Decker, P., Muller, S., Höger, T., Ménissier-de Murcia, J., de Murcia, G. (1999) PARP-2, a novel mammalian DNA damage-dependent poly(ADP-ribose) polymerase. *J. Biol. Chem.* **274**,17860-17883.

Baker, J.C., Jacobson, M.K. (1986) Alteration of adenyl dinucleotide metabolism by environmental stress. *Proc. Natl. Acad. Sci. USA* **83**, 2350-2352.

Baker, J.C., Smale, S.T., Tjian, R., Ames, B.N. (1987) Inhibition of simian virus 40 DNA replication *in vitro* by poly(ADP-ribosyl)ated diadenosine tetraphosphate. *J. Biol. Chem.* **262**, 14855-14858.

Baker, J.C., Ames, B.N. (1988) Alterations in levels of 5′-adenyl dinucleotides following DNA damage in normal human fibroblasts and fibroblasts derived from patients with xeroderma pigmentosum. *Mutat. Res.* **208**, 87-93.

Baril, E., Bonin, P., Burstein, D., Mara, K., Zamecnik, P. (1983) Resolution of the diadenosine 5′,5‴-$P^1$,$P^4$-tetraphosphate binding subunit from a multiprotein form of HeLa cell DNA polymerase a. *Proc. Natl. Acad. Sci. USA.* **80**, 4931-4935.

Baxi, M.D., McLennan, A.G., Vishwanatha, J.K. (1994) Characterization of the HeLa cell DNA polymerase alpha-associated $Ap_4A$ binding protein by photoaffinity labeling. *Biochemistry* **33**, 14601-14607.

Baxi, M.D., Vishwanatha, J.K. (1995) Uracil DNA-glycosylase/glyceraldehyde-3-phosphate dehydrogenase is an $Ap_4A$ binding protein. *Biochemistry* **34**, 9700-9707.

Beranek, D.T. (1990) Distribution of methyl and ethyl adducts following alkylation with monofunctional alkylating agents. *Mutat. Res.* **231**, 11-30.

Brenner, C. (2002) Hint, Fhit, and GalT: function, structure, evolution, and mechanism of three branches of the histidine triad superfamily of nucleotide hydrolases and transferases. *Biochemistry* **41**, 9003-9014.

Bryans, M., Valenzano, M.C., Stamato, T.D. (1999) Absence of DNA ligase IV protein in XR-1 cells: evidence for stabilization by XRCC4. *Mutat. Res.* **433**, 53-58.

Caldecott, K.W., McKeown, C.K., Tucker, J.D., Ljungquist, S., Thompson, L.H. (1994) An interaction between the mammalian DNA repair protein XRCC1 and DNA ligase III. *Mol. Cell Biol.* **14**, 68-76.

Caldecott, K.W., Tucker, J.D., Stanker, L.H., Thompson, L.H. (1995) Characterization of the XRCC1-DNA ligase III complex in vitro and its absence from mutant hamster cells. *Nucleic Acids Res.* **23**, 4836-4843.

Caldecott, K.W., Aoufouchi, S., Johnson, P., Shall, S. (1996) XRCC1 polypeptide interacts with DNA polymerase beta and possibly poly (ADP-ribose) polymerase, and DNA ligase III is a novel molecular 'nick-sensor' in vitro. *Nucleic Acids Res.* **24**, 4387-4394.

Caldecott, K.W. (2003) XRCC1 and DNA strand break repair. *DNA Repair (Amst.)* **2**, 955-69.

Cappelli, E., Taylor, R., Cevasco, M., Abbondandolo, A., Caldecott, K., Frosina, G. (1997) Involvement of XRCC1 and DNA ligase III gene products in DNA base excision repair. *J. Biol. Chem.* **272**, 23970-23975.

Chan, S.W., Gallo, S.J., Kim, B.K., Guo, M.J., Blackburn, G.M., Zamecnik, P.C. (1997) $P^1$,$P^4$-dithio-$P^2$,$P^3$-monochloromethylene diadenosine 5',5'''-$P^1$,$P^4$-tetraphosphate: a novel antiplatelet agent. *Proc. Natl. Acad. Sci. USA* **94**, 4034-4039.

Chen, D.S., Herman, T., Demple, B. (1991) Two distinct human DNA diesterases that hydrolyze 3'-blocking deoxyribose fragments from oxidized DNA. *Nucleic Acids Res.* **19**, 5907-5914.

Chen, X., Zhong, S., Zhu, X., Dziegielewska, B., Ellenberger, T., Wilson, G.M., MacKerell, A.D. Jr., Tomkinson, A.E. (2008) Rational design of human DNA ligase inhibitors that target cellular DNA replication and repair. *Cancer Res.* **68**, 3169-3177.

Cimprich, K.A., Shin, T.B., Keith, C.T., Schreiber, S.L. (1996) cDNA cloning and gene mapping of a candidate human cell cycle checkpoint protein. *Proc. Natl. Acad. Sci. USA* **93**, 2850-2855.

Clements, P.M., Breslin, C., Deeks, E.D., Byrd, P.J., Ju, L., Bieganowski, P., Brenner, C., Moreira, M.C., Taylor, A.M., Caldecott, K.W. (2004) The ataxia-oculomotor apraxia 1 gene product has a role distinct from ATM and interacts with the DNA strand break repair proteins XRCC1 and XRCC4. *DNA Repair (Amst.)* **3**, 1493-1502.

Constantinou, A., Davies, A.A., West, S.C. (2001) Branch migration and Holliday junction resolution catalyzed by activities from mammalian cells. *Cell* **104**, 259-268.

Cuneo, M.J., London, R.E. (2010) Oxidation state of the XRCC1 N-terminal domain regulates DNA polymerase beta binding affinity. *Proc. Natl. Acad. Sci. USA* **107**, 6805-6810.

Dantzer, F., de La Rubia, G., Ménissier-De Murcia, J., Hostomsky, Z., de Murcia, G., Schreiber, V. (2000) Base excision repair is impaired in mammalian cells lacking Poly(ADP-ribose) polymerase-1. *Biochemistry* **39**, 7559-7569.

Date, H., Onodera, O., Tanaka, H., Iwabuchi, K., Uekawa, K., Igarashi, S., Koike, R., Hiroi, T., Yuasa, T., Awaya, Y., Sakai, T., Takahashi, T., Nagatomo, H., Sekijima, Y., Kawachi, I., Takiyama, Y., Nishizawa, M., Fukuhara, N., Saito, K., Sugano, S., Tsuji, S. (2001) Early-onset ataxia with ocular motor apraxia and hypoalbuminemia is caused by mutations in a new HIT superfamily gene. *Nat. Genet.* **29**, 184-188.

Date, H., Igarashi, S., Sano, Y., Takahashi, T., Takahashi, T., Takano, H., Tsuji, S., Nishizawa, M., Onodera, O. (2004) The FHA domain of aprataxin interacts with the C-terminal region of XRCC1. *Biochem. Biophys. Res. Commun.* **325**, 1279-1285.

Davidovic, L., Vodenicharov, M., Affar, E.B., Poirier, G.G. (2001) Importance of poly(ADP-ribose) glycohydrolase in the control of poly(ADP-ribose) metabolism. *Exp. Cell Res.* **268**, 7-13.

de Murcia, G., Schreiber, V., Molinete, M., Saulier, B., Poch, O., Masson, M., Niedergang, C., Ménissier-de Murcia, J. (1994) Structure and function of poly(ADP-ribose) polymerase. *Mol. Cell Biochem.* **138**, 15-24.

DePamphilis, M.L., Blow J.J., Ghosh S., Saha, T., Noguchi K., Vassilev A. (2006) Regulating the licensing of DNA replication origins in metazoa. *Curr. Opin. Cell Biol.* **18**, 231-239.

Dunn, W.C., Regan, J.D. (1979) Inhibition of DNA excision repair in human cells by arabinofuranosyl cytosine: effect on normal and xeroderma pigmentosum cells. *Mol. Pharmacol.* **15**, 367-374.

El-Khamisy, S.F., Katyal, S., Patel, P., Ju, L., McKinnon, P.J., Caldecott, K.W. (2009) Synergistic decrease of DNA single-strand break repair rates in mouse neural cells lacking both Tdp1 and aprataxin. *DNA Repair (Amst.)* **8**, 760-766.

El-Khamisy, S.F., Masutani, M., Suzuki, H., Caldecott, K.W. (2003) A requirement for PARP-1 for the assembly or stability of XRCC1 nuclear foci at sites of oxidative DNA damage. *Nucleic Acids Res.* **31**, 5526-5533.

Evans, E., Fellows, J., Coffer, A., Wood, R.D. (1997) Open complex formation around a lesion during nucleotide excision repair provides a structure for cleavage by human XPG protein. *EMBO J.* **16**, 625-638.

Fan, J., Otterlei, M., Wong, H.K., Tomkinson, A.E., Wilson, D.M. (2004) XRCC1 co-localizes and physically interacts with PCNA. *Nucleic Acids Res.* **32**, 2193-2201.

Fan, J., Wilson, P.F., Wong, H.K., Urbin, S.S., Thompson, L.H., Wilson, D.M. (2007) XRCC1 down-regulation in human cells leads to DNA-damaging agent hypersensitivity, elevated sister chromatid exchange, and reduced survival of BRCA2 mutant cells. *Environ. Mol. Mutagen.* **48**, 491-500.

Fishel, R., Lescoe, M.K., Rao, M.R., Copeland, N.G., Jenkins, N.A., Garber, J., Kane, M., Kolodner, R. (1993) The human mutator gene homolog MSH2 and its association with hereditary nonpolyposis colon cancer. *Cell* **75**, 1027-1038.

Fisher, D.I., McLennan, A.G. (2008) Correlation of intracellular diadenosine triphosphate ($Ap_3A$) with apoptosis in Fhit-positive HEK293 cells. *Cancer Lett.* **259**, 186-191.

Fontes, R., Günther Sillero, M.A., Sillero, A. (1998) Acyl coenzyme A synthetase from *Pseudomonas fragi* catalyzes the synthesis of adenosine 5'-polyphosphates and dinucleoside polyphosphates. *J. Bacteriol.* **180**, 3152-3158.

Frosina, G., Fortini, P., Rossi, O., Carrozzino, F., Raspaglio, G., Cox, L.S., Lane, D.P., Abbondandolo, A., Dogliotti, E. (1996) Two pathways for base excision repair in mammalian cells. *J. Biol. Chem.* **271**, 9573-9578.

Garrison, P.N., Barnes, L.D. (1992) Determination of dinucleoside polyphosphates. In A. G. McLennan (Ed.), *$Ap_4A$ and Other Dinucleoside Polyphosphates* (pp. 29-61). Boca Raton: CRC Press.

Genschel, J., Bazemore, L.R., Modrich, P. (2002) Human exonuclease I is required for 5′ and 3′ mismatch repair. *J. Biol. Chem.* **277**, 13302-13311.

Gilson, G., Ebel, J.P., Remy, P. (1988) Is $Ap_4A$ involved in DNA repair processes? *Exp. Cell Res.* **177**, 143-153.

Gottlieb, T.M., Jackson, S.P. (1993) The DNA-dependent protein kinase: requirement for DNA ends and association with Ku antigen. *Cell* **72**, 131-142.

Gradwohl, G., Ménissier de Murcia, J.M., Molinete, M., Simonin, F., Koken, M., Hoeijmakers, J.H., de Murcia, G. (1990) The second zinc-finger domain of poly(ADP-ribose) polymerase determines specificity for single-stranded breaks in DNA. *Proc. Natl. Acad. Sci. USA* **87**, 2990-2994.

Graham, F.L., Smiley, J., Russell, W.C., Nairn, R. (1977) Characteristics of a human cell line transformed by DNA from human adenovirus type 5. *J. Gen. Virol.* **36**, 59-74.

Griffin, R.J., Pemberton, L.C., Rhodes, D., Bleasdale, C., Bowman, K., Calvert, A.H., Curtin, N.J., Durkacz, B.W., Newell, D.R., Porteous, J.K., *et al.* (1995) Novel potent inhibitors of the DNA repair enzyme poly(ADP-ribose)polymerase (PARP). *Anticancer Drug Des.* **10**, 507-514.

Grummt, F., Waltl, G., Jantzen, H.M., Hamprecht, K., Huebscher, U. and Kuenzle, C.C. (1979) Diadenosine 5',5'''-$P^1$,$P^4$- tetraphosphate, a ligand of the 57-kilodalton subunit of DNA polymerase-α. *Proc. Natl. Acad. Sci. USA* **76**, 6081-6085.

Gueven, N., Becherel, O.J., Kijas, A.W., Chen, P., Howe, O., Rudolph, J.H., Gatti, R., Date, H., Onodera, O., Taucher-Scholz, G., Lavin, M.F. (2004) Aprataxin, a novel protein that protects against genotoxic stress. *Hum. Mol. Genet.* **13**, 1081-1093.

Guo, Z., Kumagai, A., Wang, S.X., Dunphy, W.G. (2000) Requirement for ATR in phosphorylation of Chk1 and cell cycle regulation in response to DNA replication blocks and UV-damaged DNA in Xenopus egg extracts. *Genes Dev.* **14**, 2745-2756.

Guranowski, A., Sillero, M.A., Sillero, A. (1990) Firefly luciferase synthesizes $P^1$,$P^4$-bis(5'-adenosyl)tetraphosphate ($Ap_4A$) and other dinucleoside polyphosphates. *FEBS Lett.* **271**, 215-218.

Guranowski, A. (2000) Specific and nonspecific enzymes involved in the catabolism of mono- and dinucleoside polyphosphates. *Pharmacol. Ther* **87**, 117-139.

Gupta, R.C., Golub, E.I., Wold, M.S., Radding, C.M. (1998) Polarity of DNA strand exchange promoted by recombination proteins of the RecA family. *Proc. Natl. Acad. Sci. USA* **95**, 9843-9848.

Habraken, Y., Sung, P., Prakash, L., Prakash, S. (1994) A conserved 5′ to 3′ exonuclease activity in the yeast and human nucleotide excision repair proteins RAD2 and XPG. *J. Biol. Chem.* **269**, 31342-31345.

Hashiguchi, K., Matsumoto, Y., Yasui, A. (2007) Recruitment of DNA repair synthesis machinery to sites of DNA damage/repair in living human cells. *Nucleic Acids Res.* **35**, 2913-2923.

Hankin, S., Thorne, N.M.H. and McLennan, A.G. (1995) Diadenosine 5',5'''-$P^1$,$P^4$-tetraphosphate hydrolase is present in human erythrocytes, leukocytes and platelets. *Int. J. Biochem. Cell Biol.* 27, 201-206.

Henry-Mowatt, J., Jackson, D., Masson, J.Y., Johnson, P.A., Clements, P.M., Benson, F.E., Thompson, L.H., Takeda, S., West, S.C., Caldecott, K.W. (2003) XRCC3 and Rad51 modulate replication fork progression on damaged vertebrate chromosomes. *Mol. Cell* **11**, 1109-1117.

Hirano, M., Yamamoto, A., Mori, T., Lan, L., Iwamoto, T.A., Aoki, M., Shimada, K., Furiya, Y., Kariya, S., Asai, H., Yasui, A., Nishiwaki, T., Imoto, K., Kobayashi, N., Kiriyama, T., Nagata, T., Konishi, N., Itoyama, Y., Ueno, S. (2007) DNA single-strand break repair is impaired in aprataxin-related ataxia. *Ann. Neurol.* **61**, 162-174.

Hirao, A., Kong, Y.Y., Matsuoka, S., Wakeham, A., Ruland, J., Yoshida, H., Liu, D., Elledge, S.J., Mak, T.W. (2000) DNA damage-induced activation of p53 by the checkpoint kinase Chk2. *Science* **287**, 1824-1827.

Hiss, E.A., Preston, R.J. (1977) The effect of cytosine arabinoside on the frequency of single-strand breaks in DNA of mammalian cells following irradiation or chemical treatment. *Biochim. Biophys. Acta.* **478**, 1-8

Holliday, R. (1964) A mechanism for gene conversion in fungi. *Genet. Res.* **5**, 282-304.

Hsiang, Y.H., Hertzberg, R., Hecht, S., Liu, L.F. (1985) Camptothecin induces protein-linked DNA breaks via mammalian DNA topoisomerase I. *J Biol. Chem.* **260**, 14873-14878.

Huebner, K., Croce, C.M. (2003) Cancer and the FRA3B/FHIT fragile locus: it's a HIT, *Br. J. Cancer* **88,** 1501-1506.

Iles, N., Rulten, S., El-Khamisy, S.F., Caldecott, K.W. (2007) APLF (C2orf13) is a novel human protein involved in the cellular response to chromosomal DNA strand breaks. *Mol. Cell Biol.* **27**, 3793-3803.

Izumi, T., Hazra, T.K., Boldogh, I., Tomkinson, A.E., Park, M.S., Ikeda, S., Mitra, S. (2000) Requirement for human AP endonuclease 1 for repair of 3′-blocking damage at DNA single-strand breaks induced by reactive oxygen species. *Carcinogenesis* **21**, 1329-1334.

Jeggo, P.A., Hafezparast, M., Thompson, A.F., Broughton, B.C., Kaur, G.P., Zdzienicka, M.Z., Athwal, R.S. (1992) Localization of a DNA repair gene (XRCC5) involved in double-strand-break rejoining to human chromosome 2. *Proc. Natl. Acad. Sci. U.S.A.* **89**, 6423-6427.

Johnson, R.D., Jasin, M. (2000) Sister chromatid gene conversion is a prominent double-strand break repair pathway in mammalian cells. *EMBO J.* **19**, 3398-3407.

Kadyrov, F.A., Dzantiev, L., Constantin, N., Modrich, P. (2006) Endonucleolytic function of MutLalpha in human mismatch repair. *Cell* **126**, 297-308.

Kameshita, I., Matsuda, Z., Taniguchi, T., Shizuta, Y. (1984) Poly (ADP-Ribose) synthetase. Separation and identification of three proteolytic fragments as the substrate-binding domain, the DNA-binding domain, and the automodification domain. *J. Biol. Chem.* **259**, 4770-4776.

Kao, F.T., Puck, T.T. (1968) Genetics of somatic mammalian cells, VII. Induction and isolation of nutritional mutants in Chinese hamster cells. *Proc. Natl. Acad. Sci. USA*. **60**, 1275-1281.

Karimi-Busheri, F., Daly, G., Robins, P., Canas, B., Pappin, D.J., Sgouros, J., Miller, G.G., Fakhrai, H., Davis, E.M., Le Beau, M.M., Weinfeld, M. (1999) Molecular characterization of a human DNA kinase. *J. Biol. Chem.* **274**, 24187-24194.

Kijas, A.W., Harris, J.L., Harris, J.M., Lavin, M.F. (2006) Aprataxin forms a discrete branch in the HIT (histidine triad) superfamily of proteins with both DNA/RNA binding and nucleotide hydrolase activities. *J. Biol. Chem.* **281**, 13939-13948.

Klungland, A., Lindahl, T. (1997) Second pathway for completion of human DNA base excision-repair: reconstitution with purified proteins and requirement for DNase IV (FEN1). *EMBO J.* **16**, 3341-3348.

Krauspe, R., Parthier, B., Wasternack, C. (1988) Synthesis of diadenosine 5',5'''-$P^1$,$P^4$-tetraphosphate by organellar and cytoplasmic phenylalanyl-tRNA synthetases of Euglena gracilis. *FEBS Lett.* **235**, 275-277.

Kubota, Y., Horiuchi, S. (2003) Independent roles of XRCC1's two BRCT motifs in recovery from methylation damage. *DNA Repair* **2**, 407-415.

Kuzminov, A. (2001) Single-strand interruptions in replicating chromosomes cause double-strand breaks. *Proc. Natl. Acad. Sci. USA* **98**, 8241-8246.

Lazewska, D., Starzynska, E., Guranowski, A. (1993) Human placental (asymmetrical) diadenosine 5',5'''-$P^1$,$P^4$-tetraphosphate hydrolase-purification to homogeneity and some properties. *Protein Expr. Purif.* **4**, 45-51.

Lee, J.W., Yannone, S.M., Chen, D.J., Povirk, L.F. (2003) Requirement for XRCC4 and DNA ligase IV in alignment-based gap filling for nonhomologous DNA end joining in vitro. *Cancer Res.* **63**, 22-24.

Lee, Y.N., Nechushtan, H., Figov, N., Razin, E. (2004) The function of lysyl-tRNA synthetase and $Ap_4A$ as signaling regulators of MITF activity in FcεRI-activated mast cells. *Immunity* **20**, 145-151.

Lee, Y.N., Razin, E. (2005) Nonconventional involvement of LysRS in the molecular mechanism of USF2 transcriptional activity in FcεRI-activated mast cells. *Mol. Cell Biol.* **25**, 8904-8912.

Leppard, J.B., Dong, Z., Mackey, Z.B., Tomkinson, A.E. (2003) Physical and functional interaction between DNA ligase IIIα and poly(ADP-Ribose) polymerase 1 in DNA single-strand break repair. *Mol. Cell Biol.* **23**, 5919-5927.

Leslie, N.R., McLennan, A.G., Safrany, S.T. (2002) Cloning and characterisation of hAps1 and hAps2, human diadenosine polyphosphate-metabolising Nudix hydrolases. *BMC Biochem.* **3**, 20.

Levin, D.S., Bai, W., Yao, N., O'Donnell, M., Tomkinson, A.E. (1997) An interaction between DNA ligase I and proliferating cell nuclear antigen: implications for Okazaki fragment synthesis and joining. *Proc. Natl. Acad. Sci. USA*, **94** 12863-12868.

Levy, B.T., Sorge, L.K., Drum, C.C., Maness, P.F. (1983) Differential inhibition of cellular and viral pp60*src* kinase by $P^1,P^4$-di(adenosine- 5′)tetraphosphate. *Mol. Cell Biol.* **3**, 1718-1723.

Li, G.M., Modrich, P. (1995) Restoration of mismatch repair to nuclear extracts of H6 colorectal tumor cells by a heterodimer of human MutL homologs. *Proc. Natl. Acad. Sci. USA* **92**, 1950-1954.

Li, Z., Otevrel, T., Gao, Y., Cheng, H.L., Seed, B., Stamato, T.D., Taccioli, G.E., Alt, F.W. (1995) The XRCC4 gene encodes a novel protein involved in DNA double-strand break repair and V(D)J recombination. *Cell* **83**, 1079-1089.

Lindahl, T. (1993) Instability and decay of the primary structure of DNA. Nature **362**, 709-15.

Lindahl, T., Satoh, M.S., Poirier, G.G., Klungland, A. (1995) Post-translational modification of poly(ADP-ribose) polymerase induced by DNA strand breaks. *Trends Biochem. Sci.* **20**, 405-411.

Liu, N., Schild, D., Thelen, M.P., Thompson, L.H. (2002) Involvement of Rad51C in two distinct protein complexes of Rad51 paralogs in human cells. *Nucleic Acids Res.* **30**, 1009-1015.

Liu, P., Barkley, L.R., Day, T., Bi, X., Slater, D.M., Alexandrow, M.G., Nasheuer, H.P., Vaziri, C. (2006) The Chk1-mediated S-phase checkpoint targets initiation factor Cdc45 via a Cdc25A/Cdk2-independent mechanism. *J. Biol. Chem.* **281**, 30631-30644.

Loeb, L.A., Liu, P.K., Fry, M. (1986) DNA polymerase-alpha: enzymology, function, fidelity, and mutagenesis. *Prog. Nucleic Acid Res. Mol. Biol.* **33**, 57-110.

Longley, M.J., Pierce, A.J., Modrich, P. (1997) DNA polymerase delta is required for human mismatch repair in vitro. *J. Biol. Chem.* **272**, 10917-10921.

Luo, H., Chan, D.W., Yang, T., Rodriguez, M., Chen, B.P., Leng, M., Mu, J., Chen, D., Songyang, Z., Wang, Y., Qin, J. (2004) A new XRCC1-containing complex and its role in cellular survival of methyl methanesulfonate treatment. *Mol. Cell Biol.* **24**, 8356-8365.

Lüthje, J., Baringer, J., Ogilvie, A. (1985) Effects of diadenosine triphosphate ($Ap_3A$) and diadenosine tetraphosphate ($Ap_4A$) on platelet aggregation in unfractionated human blood. *Blut.* **51**, 405-413.

Mackey, Z.B., Niedergang, C., Ménissier-de Murcia, J., Leppard, J., Au, K., Chen, J.W.Q., de Murcia, G., Tomkinson, A.E. (1999) DNA ligase III is recruited to DNA strand breaks by a zinc finger motif homologous to that of poly(ADP-ribose) polymerase-identification of two functionally distinct DNA binding regions within DNA ligase III. *J. Biol. Chem.* **274**, 21679-21687.

Madrid, O., Martin, D., Atencia, E. A., Sillero, A., Günther Sillero, M.A. (1998) T4 DNA ligase synthesizes dinucleoside polyphosphates. *FEBS Lett.* **433**, 283-286.

Maser, R.S., Monsen, K.J., Nelms, B.E., Petrini, J.H. (1997) hMre11 and hRad50 nuclear foci are induced during the normal cellular response to DNA double-strand breaks. *Mol. Cell Biol.* **17**, 6087-6096.

Masson, M., Niedergang, C., Schreiber, V., Muller, S., Ménissier-de Murcia, J., de Murcia, G. (1998) XRCC1 is specifically associated with poly(ADP-ribose) polymerase and negatively regulates its activity following DNA damage. *Mol. Cell Biol.* **18**, 3563-3571.

Masson, J.Y., Tarsounas, M.C., Stasiak, A.Z., Stasiak, A., Shah, R., McIlwraith, M.J., Benson, F.E., West, S.C. (2001) Identification and purification of two distinct complexes containing the five RAD51 paralogs. *Genes Dev.* **15**, 3296-3307.

Mazen, A., Ménissier-de Murcia, J., Molinete, M., Simonin, F., Gradwohl, G., Poirier, G., de Murcia, G. (1989) Poly(ADP-ribose) polymerase: a novel finger protein. *Nucleic Acids Res.* **17**, 4689-4698.

McLennan, A.G. (1999) The MutT motif family of nucleotide phosphohydrolases in man and human pathogens. *Int. J. Mol. Med.* **4**, 79-89.

McLennan, A.G., Murphy, G.A. (1999). The intracellular level of diadenosine 5′,5‴-$P^1$,$P^3$-triphosphate ($Ap_3A$) depends on the expression of the fragile histidine triad gene. *Proc. Am. Assoc. Cancer Res.* **40**, 4609.

McLennan A.G. (2000) Dinucleoside polyphosphates-friend or foe? *Pharmacol. Ther.* **87**, 73-89.

McLennan, A.G. (2006) The Nudix hydrolase superfamily. *Cell. Mol. Life Sci.* **63**, 123-143.

Ménissier-de Murcia, J., Molinete, M., Gradwohl, G., Simonin, F., de Murcia G. (1989) Zinc-binding domain of poly(ADP-ribose)polymerase participates in the recognition of single strand breaks on DNA. *J. Mol. Biol.* **210**, 229-233.

Mol, C.D., Izumi, T., Mitra, S., Tainer, J.A. (2000) DNA-bound structures and mutants reveal abasic DNA binding by APE1 and DNA repair coordination. *Nature* **403**, 451-456.

Molinete, M., Vermeulen, W., Burkle, A., Ménissier-de Murcia, J., Kupper, J.H., Hoeijmakers, J.H., de Murcia G. (1993) Overproduction of the poly(ADP-ribose) polymerase DNA-binding domain blocks alkylation-induced DNA repair synthesis in mammalian cells. *EMBO J.* **12**, 2109-2117.

Moore, D.J., Taylor, R.M., Clements, P., Caldecott, K.W. (2000) Mutation of a BRCT domain selectively disrupts DNA single-strand break repair in noncycling Chinese hamster ovary cells. *Proc. Natl. Acad. Sci. USA.* **97**, 13649-13654.

Moreira, M., Barbot, C., Tachi, N., Kozuka, N., Uchida, E., Gibson, T., Mendonca, P., Costa, M., Barros, J., Yanagisawa, T., Watanabe, M., Ikeda, Y., Aoki, M., Nagata, T., Coutinho, P., Sequeiros, J., and Koenig, M. (2001) The gene mutated in ataxia-oculomotor apraxia 1 encodes the new HIT/Zn-finger protein aprataxin. *Nat. Genet.* **29**, 189-193.

Mori, S., Shibayama, K., Wachino, J., Arakawa, Y. (2010) Purification and molecular characterization of a novel diadenosine 5',5'''-P(1),P(4)-tetraphosphate phosphorylase from Mycobacterium tuberculosis H37Rv. *Protein Expr. Purif.* **69**, 99-105.

Morioka, M., Shimada, H. (1985) Change in the cellular level of $Ap_4A$ is correlated with the initiation of DNA replication in sea urchin embryos. *Dev. Biol. 112*, 261-263.

Moris, G., Meyer, D., Orfanoudakis, G., Befort, N., Ebel, J.P., Remy, P. (1987) Dinucleoside tetraphosphate variations in cultured tumor cells during their cell cycle and growth. *Biochimie* **69**, 1217-1225.

Mortusewicz, O., Amé, J.C., Schreiber, V., Leonhardt, H. (2007) Feedback-regulated poly(ADP-ribosyl)ation by PARP-1 is required for rapid response to DNA damage in living cells. *Nucleic Acids Res.* **35**, 7665-7675.

Mosesso, P., Piane, M., Palitti, F., Pepe, G., Penna, S., Chessa, L. (2005) The novel human gene aprataxin is directly involved in DNA single-strand-break repair. *Cell Mol. Life Sci.* **62**, 485-491.

Mu, D., Park, C.H., Matsunaga, T., Hsu, D.S., Reardon, J.T., Sancar, A. (1995) Reconstitution of human DNA repair excision nuclease in a highly defined system. *J. Biol. Chem.* **270**, 2415-2418.

Murphy, G.A., Halliday, D., McLennan, A.G. (2000) The Fhit tumor suppressor protein regulates the intracellular concentration of diadenosine triphosphate but not diadenosine tetraphosphate. *Cancer Res.* **60**, 2342-2344.

Murphy, G.A., McLennan, A.G. (2004) Synthesis of dinucleoside tetraphosphates in transfected cells by a firefly luciferase reporter gene. *Cell Mol. Life Sci.* **61**, 497-501.

Nash, R.A., Caldecott, K.W., Barnes, D.E., Lindahl, T. (1997) XRCC1 protein interacts with one of two distinct forms of DNA ligase III. *Biochemistry* **36**, 5207-5211.

Okano, S., Lan, L., Caldecott, K.W., Mori, T., Yasui, A. (2003) Spatial and temporal cellular responses to single-strand breaks in human cells. *Mol. Cell Biol.* **23**, 3974-3981.

Palombo, F., Gallinari, P., Iaccarino, I., Lettieri, T., Hughes, M., D'Arrigo, A., Truong, O., Hsuan, J.J., Jiricny, J. (1995) GTBP, a 160-kilodalton protein essential for mismatch-binding activity in human cells. *Science* **268**, 1912-1914.

Parsons, J.L., Dianova, I.I., Allinson, S.L., Dianov, G.L. (2005) DNA polymerase beta promotes recruitment of DNA ligase III alpha-XRCC1 to sites of base excision repair. *Biochemistry* **44**, 10613-10619.

Pegg, A.E., Dolan, M.E., Moschel, R.C. (1995) Structure, function and inhibition of $O^6$-alkylguanine-DNA alkyltransferase. *Prog. Nucleic Acid Res. Mol. Biol.* **51**, 167-223.

Pegg A.E. (2000) Repair of O(6)-alkylguanine by alkyltransferases. *Mutat. Res.* **462**, 83-100.

Petermann, E., Maya-Mendoza, A., Zachos, G., Gillespie, D.A., Jackson, D.A., Caldecott, K.W. Chk1 requirement for high global rates of replication fork progression during normal vertebrate S phase. (2006) *Mol. Cell Biol.* **26**, 3319-3326.

Perret, J., Hepburn, A., Cochaux, P., van Sande, J., Dumont, J.E. (1990) Diadenosine 5′, 5‴-$P^1$,$P^4$-tetraphosphate ($Ap_4A$) levels under various proliferative and cytotoxic conditions in several mammalian cell types. *Cell Signal.* **2**, 57-65.

Pintor, J., Díaz-Hernández, M., Gualix, J., Gómez-Villafuertes, R., Hernando, F., Miras-Portugal, M.T. (2000) Diadenosine polyphosphate receptors. from rat and guinea-pig brain to human nervous system. *Pharmacol. Ther.* **87**, 103-115.

Plateau, P., Blanquet, S. (1992) Synthesis of $Np_nN`$ (n = 3 or 4) *In Vitro* and *In Vivo*. In A.G. McLennan (Ed.), *$Ap_4A$ and Other Dinucleoside Polyphosphates* (pp. 63-80). Boca Raton: CRC Press.

Pouliot, J.J., Yao, K.C., Robertson, C.A., Nash, H.A. (1999) Yeast gene for a Tyr-DNA phosphodiesterase that repairs topoisomerase I complexes. *Science* **286**, 552-555.

Prasad, R., Dianov, G.L., Bohr, V.A., Wilson, S.H. (2000) FEN1 stimulation of DNA polymerase beta mediates an excision step in mammalian long patch base excision repair. *J. Biol. Chem.* **275**, 4460-4466.

Purich, D.L., Fromm, H.J. (1972) Inhibition of rabbit skeletal muscle adenylate kinase by the transition state analogue, $P^1$,$P^4$-di(adenosine-5′) tetraphosphate. *Biochim. Biophys. Acta.* **276,** 563-567.

Randerath, K., Janeway, C.M., Stephenson, M.L., Zamecnik, P.C. (1966) Isolation and characterization of dinucleoside tetra- and tri-phosphates formed in the presence of lysyl-sRNA synthetase. *Biochem. Biophys. Res. Commun.* **24**, 98-105.

Rapaport, E., Feldman, L. (1984) Adenosine(5')tetraphospho (5')adenosine-binding protein of calf thymus. *Eur. J. Biochem.* **138**, 111-115.

Rapić-Otrin, V., Navazza, V., Nardo, T., Botta, E., McLenigan, M., Bisi, D.C., Levine, A.S., Stefanini, M. (2003) True XP group E patients have a defective UV-damaged DNA binding protein complex and mutations in DDB2 which reveal the functional domains of its p48 product. *Hum. Mol. Genet.* **12**, 1507-1522.

Rass, U., Ahel, I., West, S.C. (2007) Actions of aprataxin in multiple DNA repair pathways. *J. Biol. Chem.* **282**, 9469-9474.

Reynolds, J.J., El-Khamisy, S.F., Katyal, S., Clements, P., McKinnon, P.J. Caldecott, K.W. (2009) *Mol. Cell. Biol.* **29**, 1354-1362.

Ripoll, C., Martin, F., Rovira, J.M., Pintor, J., Miras-Portugal, M.T., Soria, B. (1996) Diadenosine polyphosphates: a novel class of glucose-induced intracellular messengers in the pancreatic b-cell. *Diabetes* **45**, 1431-1434.

Ruf, A., de Murcia, G., Schulz, G.E. (1998) Inhibitor and NAD+ binding to poly(ADP-ribose) polymerase as derived from crystal structures and homology modeling. *Biochemistry* **37**, 3893-3900.

Rulten, S.L., Cortes-Ledesma, F., Guo, L., Iles, N.J., Caldecott, K.W. (2008) APLF (C2orf13) is a novel component of poly(ADP-ribose) signaling in mammalian cells. *Mol. Cell Biol.* **28**, 4620-4628.

Safrany, S.T., Ingram, S.W., Cartwright, J.L., Falck, J.R., McLennan, A.G., Barnes, L.D., Shears, S.B. (1999) The diadenosine hexaphosphate hydrolases from *Schizosaccharomyces pombe* and *Saccharomyces cerevisiae* are homologues of the human diphosphoinositol polyphosphate phosphohydrolase: overlapping substrate specificities in a MutT motif. *J. Biol. Chem.* **274**, 21735-21740.

Sancar, A. (1994) Structure and function of DNA photolyase. *Biochemistry* **33**, 2-9.

Savitsky, K., Bar-Shira, A., Gilad, S., Rotman, G., Ziv, Y., Vanagaite, L., Tagle, D.A., Smith, S., Uziel, T., Sfez, S. (1995) A single ataxia telangiectasia gene with a product similar to PI-3 kinase. *Science* **268**, 1749-1753.

Sawa, A., Khan, A.A., Hester, L.D., Snyder, S.H. (1997) Glyceraldehyde-3-phosphate dehydrogenase: nuclear translocation participates in neuronal and nonneuronal cell death. *Proc. Natl. Acad. Sci. USA* **94**, 11669-11674.

Scherer, W.F., Syverton, J.T., Gey, G.O. (1953) Studies on the propagation in vitro of poliomyelitis viruses. IV. Viral multiplication in a stable strain of human malignant epithelial cells (strain HeLa) derived from an epidermoid carcinoma of the cervix. *J. Exp. Med.* **97**, 695-710.

Schild, D., Lio, Y.C., Collins, D.W., Tsomondo, T., Chen, D.J. (2000) Evidence for simultaneous protein interactions between human Rad51 paralogs. *J. Biol. Chem.* **275**, 16443-16449.

Schreiber, V., Amé, J.C., Dollé, P., Schultz, I., Rinaldi, B., Fraulob, V., Ménissier-de Murcia, J., de Murcia, G. (2002) Poly(ADP-ribose) polymerase-2 (PARP-2) is required for efficient base excision DNA repair in association with PARP-1 and XRCC1. *J. Biol. Chem.* **277**, 23028-23036.

Seiler, J.A., Conti, C., Syed, A., Aladjem, M.I., Pommier, Y. (2007) The intra-S-phase checkpoint affects both DNA replication initiation and elongation: single-cell and -DNA fiber analyses. *Mol. Cell Biol.* **27**, 5806-5818.

Sen, N., Hara, M.R., Kornberg, M.D., Cascio, M.B., Bae, B.I., Shahani, N., Thomas, B., Dawson, T.M., Dawson, V.L., Snyder, S.H., Sawa, A. (2008) Nitric oxide-induced nuclear GAPDH activates p300/CBP and mediates apoptosis. *Nat. Cell Biol.* **10**, 866-873.

Shen, M.R., Zdzienicka, M.Z., Mohrenweiser, H., Thompson, L.H., Thelen, M.P. (1998) Mutations in hamster single-strand break repair gene XRCC1 causing defective DNA repair. *Nucleic Acids Res.* **26**, 1032-1037.

Shen, Z., Cloud, K.G., Chen, D.J., Park, M.S. (1996) Specific interactions between the human RAD51 and RAD52 proteins. *J. Biol. Chem.* **271**, 148-152.

Shieh, S.Y., Ahn, J., Tamai, K., Taya, Y., Prives, C. (2000) The human homologs of checkpoint kinases Chk1 and Cds1 (Chk2) phosphorylate p53 at multiple DNA damage-inducible sites. *Genes Dev.* **14**, 289-300.

Sijbers, A.M., de Laat, W.L., Ariza, R.R., Biggerstaff, M., Wei, Y.F., Moggs, J.G., Carter, K.C., Shell, B.K., Evans, E., de Jong, M.C., Rademakers, S., de Rooij, J., Jaspers, N.G., Hoeijmakers, J.H., Wood, R.D. (1996) Xeroderma pigmentosum group F caused by a defect in a structure-specific DNA repair endonuclease. *Cell* **86**, 811-822.

Sillero, A., Günther Sillero, M.A. (2000) Synthesis of dinucleoside polyphosphates catalyzed by firefly luciferase and several ligases. *Pharmacol. Ther.* **87**, 91-102.

Simonin, F., Ménissier-de Murcia, J., Poch, O., Muller, S., Gradwohl, G., Molinete, M., Penning, C., Keith, G., de Murcia, G. (1990) Expression and site-directed mutagenesis of the catalytic domain of human poly(ADP-ribose)polymerase in *Escherichia coli*. Lysine 893 is critical for activity. *J. Biol. Chem.* **265**, 19249-19256.

Sobol, R.W., Prasad, R., Evenski, A., Baker, A., Yang, X.P., Horton, J.K., Wilson, S.H. (2000) The lyase activity of the DNA repair protein beta-polymerase protects from DNA-damage-induced cytotoxicity. *Nature* **405**, 807-810.

Stamato, T.D., Weinstein, R., Giaccia, A., Mackenzie, L. (1983) Isolation of cell cycle-dependent gamma ray-sensitive Chinese hamster ovary cell. *Somatic Cell Genet.* **9**, 165-173.

Stasiak, A.Z., Larquet, E., Stasiak, A., Muller, S., Engel, A., Van Dyck, E., West, S.C., Egelman, E.H. (2000) The human Rad52 protein exists as a heptameric ring. *Curr. Biol.* **10**, 337-340.

Swarbrick, J.D., Buyya, S., Gunawardana, D., Gayler, K.R., McLennan, A.G., Gooley, P.R. (2005) Structure and substrate binding mechanism of human $Ap_4A$ hydrolase. *J. Biol. Chem.* 280, 8471-8481.

Sugasawa, K., Okamoto, T., Shimizu, Y., Masutani, C., Iwai, S., Hanaoka, F. (2001) A multistep damage recognition mechanism for global genomic nucleotide excision repair. *Genes Dev.* **15**, 507-521.

Sugimura, K., Takebayashi, S., Taguchi, H., Takeda, S. and Okumura, K. (2008) PARP-1 ensures regulation of replication fork progression by homologous recombination on damaged DNA. *J. Cell Biol.* **183**, 1203-1212.

Tajima, H., Tsuchiya, K., Yamada, M., Kondo, K., Katsube, N., Ishitani, R. (1999) Over-expression of GAPDH induces apoptosis in COS-7 cells transfected with cloned GAPDH cDNAs. *Neuroreport* **10**, 2029-2033.

Takahashi, T., Tada, M., Igarashi, S., Koyama, A., Date, H., Yokoseki, A., Shiga, A., Yoshida, Y., Tsuji, S., Nishizawa, M., Onodera, O. (2007) Aprataxin, causative gene product for EAOH/AOA1, repairs DNA single-strand breaks with damaged 3'-phosphate and 3'-phosphoglycolate ends. *Nucleic Acids Res.* **35**, 3797-3809.

Tanaka, Y., Matsunami, N., Itaya, A., Yoshihara, K. (1981) Histone-dependent ADP-ribosylation of low molecular nucleotide by poly(ADP-ribose) polymerase. *J. Biochem.* **90**, 1131-1139.

Tano, K., Shiota, S., Collier, J., Foote, R.S., Mitra, S. (1990) Isolation and structural characterization of a cDNA clone encoding the human DNA repair protein for *O*6-alkylguanine. *Proc. Natl. Acad. Sci. USA.* **87**, 686-690.

Tebbs, R.S., Flannery, M.L., Meneses, J.J., Hartmann, A., Tucker, J.D., Thompson, L.H., Cleaver, J.E., Pedersen, R.A. (1999) Requirement for the Xrcc1 DNA base excision repair gene during early mouse development. *Dev. Biol.* **208**, 513-529.

Tercero, J.A., Diffley, J.F. (2001) Regulation of DNA replication fork progression through damaged DNA by the Mec1/Rad53 checkpoint. *Nature* **412**, 553-557.

Thompson, L.H., Fong, S., Brookman, K. (1980a) Validation of conditions for efficient detection of HPRT and APRT mutations in suspension-cultured Chinese hamster ovary cells. *Mutat. Res.* **74**, 21-36.

Thompson, L.H., Rubin, J.S., Cleaver, J.E., Whitmore, G.F., Brookman. K. (1980b) A screening method for isolating DNA repair-deficient mutants of CHO cells. *Somatic Cell Genet.* **6**, 391-405.

Thompson, L.H., Brookman, K.W., Dillehay, L.E., Carrano, A.V., Mazrimas, J.A., Mooney, C.L., Minkler, J.L. (1982) A CHO-cell strain having hypersensitivity to mutagens, a defect in DNA strand-break repair, and an extraordinary baseline frequency of sister-chromatid exchange. *Mutat. Res.* **95**, 427-440.

Thompson, L.H., Brookman, K.W., Jones, N.J., Allen, S.A., Carrano, A.V. (1990) Molecular cloning of the human XRCC1 gene, which corrects defective DNA strand break repair and sister chromatid exchange. *Mol. Cell Biol.* **10**, 6160-6171.

Thorne, N.M.H., Hankin, S., Wilkinson, M.C., Nuñez, C., Barraclough, R., McLennan, A.G. (1995) Human diadenosine 5′,5‴-$P^1$,$P^4$-tetraphosphate pyrophosphohydrolase is a member of the MutT family of nucleotide pyrophosphatases. *Biochem. J.* **311**, 717-721.

Tomkinson, A.E., Vijayakumar, S., Pascal, J.M., Ellenberger, T. (2006) DNA ligases: structure, reaction mechanism, and function. *Chem. Rev.* **106**, 687-699.

Trujillo, K.M., Yuan, S.S., L.H., Takeda, S. (2000) The Rad51 paralog Rad51B promotes homologous recombinational repair. *Mol. Cell. Biol.* **20**, 6476-6482.

Uchiyama, Y., Suzuki, Y., Sakaguchi, K. (2008) Characterization of plant XRCC1 and its interaction with proliferating cell nuclear antigen. *Planta* **227**, 1233-1241.

Unsal-Kaçmaz, K., Chastain, P.D., Qu, P.P., Minoo, P., Cordeiro-Stone, M., Sancar, A., Kaufmann, W.K. (2007) The human Tim/Tipin complex coordinates an Intra-S checkpoint response to UV that slows replication fork displacement. *Mol. Cell Biol.* **27**, 3131-3142.

Vartanian, A., Prudovsky, I., Suzuki, H., DalPra, I., Kisselev, L. (1997) Opposite effects of cell differentiation and apoptosis on $Ap_3A/Ap_4A$ ratio in human cell cultures. *FEBS Lett.* **415**, 160-162.

Vartanian, A., Alexandrov, I., Prudowski, I., McLennan, A., Kisselev, L. (1999) $Ap_4A$ induces apoptosis in cultured human cells. *FEBS Lett.* **456**, 175-180.

Vidal, A.E., Boiteux, S., Hickson, I.D., Radicella, J.P. (2001) XRCC1 coordinates the initial and late stages of DNA abasic site repair through protein-protein interactions. *EMBO J.* **20**, 6530-6539.

Ward, J.E. (1998) Nature of Lesions Formed by Ionizing Radiation. In J.A. Nickoloff, M.F. Hoekstra (Eds.), *DNA repair in higher eukaryotes* (pp. 65-84). Totawa NJ: Human Press Inc.

Wei, Y.F., Robins, P., Carter, K., Caldecott, K., Pappin, D.J., Yu, G.L., Wang, R.P., Shell, B.K., Nash, R.A., Schar, P., Barnes, D.E., Haseltine, W.A., Lindahl, T. (1995) Molecular cloning and expression of human cDNAs encoding a novel DNA ligase IV and DNA ligase III, an enzyme active in DNA repair and recombination. *Mol. Cell Biol.* **15**, 3206-3216.

Weinmann-Dorsch, C., Hedl, A., Grummt, I., Albert, W., Ferdinand, F.J., Friis, R.R., Pierron, G., Moll, W., Grummt, F. (1984) Drastic rise of intracellular adenosine (5′) tetraphospho (5′) adenosine correlates with onset of DNA synthesis in eukaryotic cells. *Eur. J. Biochem.* **138**, 179-185.

Whitehouse, C.J., Taylor, R.M., Thistlethwaite, A., Zhang, H., Karimi-Busheri, F., Lasko, D.D., Weinfeld, M., Caldecott, K.W. (2001) XRCC1 stimulates human polynucleotide kinase activity at damaged DNA termini and accelerates DNA single-strand break repair. *Cell* **104**, 107-117.

Wiederhold, L., Leppard, J.B., Kedar, P., Karimi-Busheri, F., Rasouli-Nia, A., Weinfeld, M., Tomkinson, A.E., Izumi, T., Prasad, R., Wilson, S.H., Mitra, S., Hazra, T.K. (2004) AP endonuclease-independent DNA base excision repair in human cells. *Mol. Cell* **15**, 209-220.

Wiese, C., Collins, D.W., Albala, J.S., Thompson, L.H., Kronenberg, A., Schild, D. (2002) Interactions involving the Rad51 paralogs Rad51C and XRCC3 in human cells. *Nucleic Acids Res.* **30**, 1001-1008.

Wilson, S.H. (1998) Mammalian base excision repair and DNA polymerase beta. *Mutat. Res.* **407**, 203-215.

Winters, T.A., Weinfeld, M., Jorgensen, T. (1992) Human HeLa cell enzymes that remove phosphoglycolate 3'-end groups from DNA. *Nucleic Acids Res.* **20**, 2573-2580.

Winters, T.A., Henner, W.D., Russell, P.S., McCullough, A., Jorgensen, T.J. (1994) Removal of 3'- phosphoglycolate from DNA strand-break damage in an oligonucleotide substrate by recombinant human apurinic/apyrimidinic endonuclease 1. *Nucleic Acids Res.* **22**, 1866-1873.

Wood, R.D., Mitchell, M., Sgouros, J., Lindahl, T. (2001) Human DNA repair genes. *Science* **291**, 1284-1289.

Yannay-Cohen, N., Carmi-Levy, I., Kay, G., Yang, C.M., Han, J.M., Kemeny, D.M., Kim, S., Nechushtan, H., Razin, E. (2009) LysRS serves as a key signaling molecule in the immune response by regulating gene expression. *Mol. Cell* **34**, 603-611.

Yoshihara, Y., Tanaka, Y. (1981) ADP-ribosylation of diadenosine 5',5'''-$P^1$,$P^4$-tetraphosphate by poly(ADP-ribose) polymerase *in vitro*. *J. Biol. Chem.* **256**, 6756-6761.

Zamecnik, P.C., Stephenson, M.L., Janeway, C.M., Randerath, K. (1966) Enzymatic synthesis of diadenosine tetraphosphate and diadenosine triphosphate with a purified lysyl-sRNA synthetase. *Biochem. Biophys. Res. Commun.* **24**, 91-97.

Zhao H., Watkins J.L., Piwnica-Worms H. (2002) Disruption of the checkpoint kinase 1/cell division cycle 25A pathway abrogates ionizing radiation-induced S and G2 checkpoints. *Proc. Natl. Acad. Sci. USA* **99**, 14795-14800.

Zharkov, D.O. (2008) Base excision DNA repair *Cell. Mol. Life Sci.* **65**, 1544-1565.

Zhou, B.B., Chaturvedi, P., Spring, K., Scott, S.P., Johanson, R.A., Mishra, R., Mattern, M.R., Winkler, J.D., Khanna, K.K. (2000) Caffeine abolishes the mammalian G(2)/M DNA damage checkpoint by inhibiting ataxia-telangiectasia-mutated kinase activity. *J. Biol. Chem.* **275**, 10342-10348.